Preparation and Characterization of Chitosan /Calcium Phosphate Based Composite Biomaterials

By

Oktay YILDIRIM

A Dissertation Submitted to the Graduate School in Partial Fulfillment of the Requirements for the Degree of

MASTER OF SCIENCE

Department: Materials Science and Engineering
Major: Materials Science and Engineering

İzmir Institute of Technology
İzmir, Turkey

August,2004

We approve the thesis of **Oktay YILDIRIM** **Date of signature**

27.08.2004

Prof Dr. Muhsin ÇİFTÇİOĞLU
Supervisor
Department of Chemical Engineering

27.08.2004

Prof.Dr. Şebnem HARSA
Co-Supervisor
Department of Food Engineering

27.08.2004

Assoc.Prof.Dr. Mustafa GÜDEN
Department of Mechanical Engineering

27.08.2004

Assoc.Prof.Dr. Metin TANOĞLU
Department of Mechanical Engineering

27.08.2004

Prof Dr. Muhsin ÇİFTÇİOĞLU
Head of Department

ACKNOWLEDGEMENTS

I would like to thank to my advisors Prof.Dr. Muhsin Çiftçioğlu and Prof.Dr.Şebnem Harsa for their supervision, valuable suggestions and comments through my study. Special thanks to Specialist Rukiye Çiftçioğlu for her contributions and help in the laboratory work.

Thanks indeed to research assistants Hasan Demir, Ulaş Atikler and Deniz Şimşek for their help and support in mechanical testing, CMR staff for their co-operation and perseverance.

I wish to thank my roommates Naz Gültekin and İlker Erdem for their understanding, kindness and friendship.

Finally I am grateful to my family members, for their encouragement and understanding throughout my study.

ABSTRACT

In this study the preparation and characterization of three-dimensional chitosan-calcium phosphate composite structures and porous hydroxyapatite bodies for biomaterial applications have been studied. The effects of chitosan calcium phosphate amount on density, porosity, microstructure, chemical composition and mechanical properties on the composites and effects of porosifier contents, hydroxyapatite content of the slurry and sintering temperature on density, porosity and microstructure of the porous ceramic samples were investigated. SEM was used for microstructural analysis, XRD and FTIR were used for chemical analysis, Archimedes method was used for investigating physical properties and compression test for investigating mechanical properties. In this study low molecular weight chitosan, β-tricalciumphosphate, hydroxyapatite and hydroxyapatite whisker have been used. For composites freeze drying technique and for the porous bodies dry pressing, polymer sponge method and dough method have been used.

The densities of the composites prepared by using chitosan as the matrix and hydroxyapatite, hydroxyapatite whisker, and β-tricalciumphosphate as reinforcement increased and the porosities decreased with the increase in the ceramic content. The modulus of elasticity and the yield stress generally increased with the increasing ceramic content except for the chitosan/β-tricalciumphosphate composites. The densities and porosities of the composite structures varied in the range of 0.059-0.29 g/cm^3 and 96-88% respectively. The elastic moduli of the composites varied in a range of 4.45-10.09 MPa and yield stress varied in a range of 0.14-0.34 Mpa due to the change in the ceramic weight%. Changing the ceramic weight% also had influence on the microstructure. Generally with increasing ceramic content the pore sizes decreased. The pore sizes varied in a range between 100-250μ, 100-400μ and 100-200μ for chitosan/hydroxapatite, Chitosan/β-TCP/Hydroxyapatite and chitosan/HA whisker composites respectively. FTIR and XRD analysis showed that the composite structures contained original constituents, no new chemical compounds were formed the production process had not affected crystallinity of ceramic phases.

The densities of the porous ceramic bodies decreased and the porosities increased with the increasing porosifier content at the porous ceramics prepared by dough method and dry pressing method. The porosity and density values of porous hydroxyapatite samples changed in range of 34-72% and 2.03 to 0.87 g/cm^3. Pore sizes of polymeric sponge samples were found to be around 300-400μ and dry pressing and dough method samples were found to be 10μ.

ÖZ

Bu çalışma biomedikal uygulamalarda kullanılması amaçlanan kitosan/kalsiyum fosfat kompozitler ve gözenekli hidroksiapatit yapıların hazırlanması ve karakterizasyonunu içermektedir. Kompozit malzemelerin yoğunluk, gözenek yapısı, mikroyapı, kimyasal kompozisyon ve mekanik özellikleri üzerinde kitosan kalsiyum fosfat miktarının etkisi araştırılmış hazırlanan başlangıç maddelerindeki gözenek yapıcı katkı maddesinin, hidroksiapatit miktarının ve sinterlenme sıcaklığının gözenekli hidroksiapatit yapılara etkileri de incelenmiştir. Elde edilen seramik numunelerin gözenek yapıları ve mikroyapıları SEM görüntüleriyle belirlenmiştir. Kimyasal analizlerde XRD ve FTIR kullanılmıştır. Fiziksel özelliklerin belirlenmesi için Arşimed yöntemine ve mekanik özelliklerin bulgulanması için basma testine başvurulmuştur. Düşük molekül ağırlıklı kitosan, ß-trikalsiyumfosfat, hidroksiapatit ve hidroksiapatit visker hammadde olarak kullanılmıştır. Kompozitlerin üretiminde dondurmalı kurutma yöntemi ve gözenekli yapıların hazırlanmasında kuru presleme, polimer süngere emdirme ve hamur metodları kullanılmıştır.

Matris olarak kitosan ve güçlendirici olarak hidroksiapatit, hidroksiapatit visker ve ß-trikalsiyumfosfatın kullanılmasıyla oluşturulan kompozit malzemelerin seramik miktarı arttığında yoğunluklarının da arttığı ve gözenekliliklerinin azaldığı gözlenmiştir. Kitosan/ß-trikalsiyumfosfat kompozitleri dışındaki numunelerde elastik modül değerleri ve çökme stresi de seramik miktarı arttığında yükselme götermiştir. Tüm kompozit malzemelerin yoğunlukları 0.059-0.29 g/cm^3 ve gözeneklilikleri 96-88% aralıklarında değişmiştir. Kompozitlerin elastik modülleri ise seramik ağırlık yüzdesine bağlı olarak değişmiş, 4.45-10.09 MPa aralığında saptanmıştır. Çökme stres değerleri ise yine seramik ağırlık yüzdesine bağlı olarak 0.14-0.34 MPa aralığında değişim göstermiştir. Numunelerin seramik yüzdelerindeki değişim mikroyapıda da değişimlere neden olmuş,genellikle seramik miktarında artışla gözeneklerin daraldığı gözlenmiştir. Kitosan/HA, Kitosan//β-TCP/HA ve Kitosan/HA visker kompozitlerin gözenek boyutları sırasıyla 100-250 μ, 100-400 μ ve 100-200 μ aralıklarında değişmektdir. FTIR ve XRD analiz sonuçları kompozit malzemelerin yapımda kullanılan hammaddelerin orijinal yapılarını koruduğunu ve üretim sürecinin seramiklerin kristalinitesi üzerinde değişime neden olmadığını göstermiştir.

Gözenekleştirici miktarı artırıldığında hamur ve kuru pres metoduyla hazırlanan seramik yapıların yoğunlukları düşmüş, gözeneklilikleri artmıştır. Hazırlanan gözenekli hidroksiapatit numunelerin yoğunlukları 34-72% gözenek değerlerine ulaşacak şekilde 2.03 ve 0.87g/cm^3 yoğunluk aralığında değişmiştir. Süngere emdirme metoduyla hazırlanan örneklerin gözenek boyutları ise 300-400 μ aralığında gözlenirken kuru pres ve hamur metodlarıyla hazırlanan örneklerin gözenek boyutları 10 μ olarak belirlenmiştir.

TABLE OF CONTENTS

LIST OF FIGURES

LIST OF TABLES

CHAPTER 1

INTRODUCTION

Human beings are likely to face serious problems caused by diseases, accidents and aging during their lifetime. In the past physicians had very limited material choices on solving these medical problems with the removal of the illfunctioning parts or tissues being the most frequently applied solution. Advances in science and technology of medical materials today significantly altered the choices of physicians for the solution of the implantation problems [1].

Biomaterials are defined as materials natural or man-made origin that are used direct, supplement, or replacing the functions of living tissues of human body. Two important criteria which biomaterial must fulfill are biocompatibility and biofunctionality. According to a report published in 1995 by the Institute of Materials London, the estimated world market for biomaterials are around $12 billion per year [2]. This gives an idea of the size of the economy about this area. Biomaterials has much more importance than the economical aspect because they have vital importance for human life in many cases.

Hard tissue of the human body is very important. The skeletal system provides support and gives shape to the body and provides a network where all soft tissues attach to. The most common problems that are faced to at hard tissues are bone fractures, in addition to other various problems which needed to be cured. The developments in artificial bone area seem to solve most of the hard tissue problems. On the other hand artificial bones themselves may cause other problems and in many cases they do not have sufficient mechanical properties.

Ceramics, polymers, metals and composite materials, with all advantages and drawbacks they have, are developed to be used for bone problems. Polymers have very low mechanical strength compared to bone, metals have superior mechanical properties but they are very corrosive, and despite their other desired properties such as wear resistance, biocompatibility and hardness, ceramics are brittle and have low fracture toughness. When all these properties of polymers, ceramics and metals are considered producing composite materials is a reasonable approach.

Bone consists of 69 wt% calcium phosphate (mainly hydroxyapatite), 21% collagen, 9%water and 1% other constituents. It has a composite nature which is composed of mainly ceramic (hydroxyapatite) and polymer (collagen), with a complex hierarchical microstructure impossible to imitate which gives most of the superior mechanical properties to bone. There are many researchs done for bone substitute composite materials composed of mainly hydroxyapatite and a polymer. Hydroxyapatite has very good properties such as bioactivity, biocompatibility, non-toxicity and osteoconductivity but also has low toughness. Chitosan, deacetylated form of chitin which is a natural polymer found in vast amounts in crustaceans. It has very good properties such as biocompatibility and bioresorbability. It is non-toxic and easily soluble in dilute weak organic acids. Some of the studies are on chitosan/hydroxyapatite composites which are partially biodegradable which may be an advantage. When the polymer matrix is reabsorbed new bone may intergrow around the hydroxyapatite particles. Extensive research on relatively new chitosan/hydroxyapatite composites has been conducted through [3-11].

The objective of this study is to prepare and characterize polymer/calcium phosphate composite biomaterials by using chitosan as polymer and hydroxyapatite, β-tricalciumphosphate and hydroxyapatite whisker as ceramics. The effects of parameters such as calcium phosphate types and calcium phosphate/polymer ratios on mechanical, microstructural and physical properties have been studied. Porous hydroxyapatite have also been produced to be used for further studies.

CHAPTER 2

BIOMATERIALS AND THEIR APPLICATIONS

2.1 Biomaterials

In the treatment of a disease or an injury, various materials can be used. Common examples are sutures and tooth fillings. A biomaterial is a synthetic material used to replace part of a living system or to function in close contact with living tissue. The Clemson University Advisory Board for Biomaterials has formally defined a biomaterial to be "a systematically and pharmacologically inert substance designed for implantation within or incorporation with living systems" [14]. The last definition is insufficient with ignoring some biomaterials which have bioactive and biodegradable properties. The uses of biomaterials include replacement of a body part that has lost function due to disease or trauma, to assist in healing, or to improve function, and to correct abnormalities. Performance of materials in the body can be viewed from several perspectives. Biomaterials can be classified as metals, polymers, ceramics and composites as shown in Table 2.1.

Metals have been used in various forms as implants. They have very good mechanical durability, high strength and ductility. Most important drawback of metals is their corrosive nature. The consequence of corrosion is loss of material, which will weaken the implant, and probably more important, the corrosion products escape into the tissue resulting in undesirable effects [14]. They have also other drawbacks such as low biocompatibility, too high stiffness compared to tissues and high density.

Stainless steel (316 and 316L) is the first material used to produce artificial bone and easily cast into different shapes. 316L has a better corrosion resistance than 316 with its lower carbon content. However it may corrode inside the body under certain circumstances such as in a highly stressed oxygen-depleted region. Both 316 and 316L are suitable to use in temporary devices such as fracture plates, screws, and hip nails. They are cheaper and easily cast into different shapes but not durable [14].

Table 2.1 Types and properties of biomaterials.

Materials	**Advantages**	**Disadvantages**	**Examples**
Polymers Nylon Silicones	Resilient Easy to fabricate Bioresorbable, bioinert	Insufficient properties for load bearing applications, Deform with time May degrade	Sutures, blood vessels, hip socket, ear, nose
Metals Titanium Co-Cr alloys Gold Stainless steel	High strength, tough, ductile	corrosive, dense	Joint replacement, bone plates and screws, dental root implants
Ceramics Alumina Carbon Hydroxyapatite	Biocompatible, inert, strong in compression,wear resistant, bioactive	Brittle, difficult to produce, not resilient, high modulus	Dental, hip socket
Composites	High strength, controllable mechanical properties and microstructure	Difficult to produce	Joint implants, heart valves

Cobalt based alloys, usually referred as cobalt-chromium alloys, have better corrosion resistance and higher elastic modulus. Some wear resistant types are suitable for the applications that require long service life without fracture or stress fatigue. Ti alloys are expensive and difficult to process but are used mainly for prostheses to replace large joints such as hip and knee [14].

Ti and Ti based alloys are lighter than the other metals and have good mechanochemical properties. Ti has poor shear strength, making it less desirable for bone screws, plates and similar applications. Ti alloy has an excellent biocompatibility and currently the most widely used [14].

Although they have superior mechanical properties, metals may cause several problems such as elastic modulus mismatch with host tissue, no active bonding to the tissue, low biocompatibility, causing inflammatory and allergic reactions which usually limits the time of implant and makes surgical removal of the implant necessary.

Ceramics are refractory, polycrystalline compounds, usually inorganic, including silicates, metallic oxides, carbides, and various refractory hybrides, sulfides and selenides. Oxides such as Al_2O_3, MgO and SiO_2 contain metallic and nonmetallic elements, whereas others such as NaCl, CsCl and ZnS are ionic salts. Exceptions are diamond and carbonaceous structures like graphite and pyrolized carbons, which are covalently bonded [14]. Specially designed ceramics for the repair, reconstruction and replacement of diseased or damaged parts of the body are termed "bioceramics" [15]. Ceramics have been used for some time in dentistry for dental crowns owing to their inertness to the body fluids, high compressive strength, and good esthetic appearance [14]. Ceramics may be bioinert (e.g. alumina and zirconia), resorbable (e.g. tricalciumphosphate), bioactive (e.g. hydroxyapatite, bioactive glasses, and glass ceramics), or porous for tissue ingrowth (e.g. hydroxyapatite-coated metals). Different phases of calcium phosphate ceramics are used depending upon whether a resorbable or bioactive material is desired. Applications include replacements for hips, knees, teeth, tendom and ligaments and repair for peridontal disease, maxillofacial reconstruction, augmentation and stabilization of the jaw bone, spinal fusion and bone repair after tumor surgery. By using bioactive ceramics tissue bonding between ceramic and soft tissues can be achieved [15].

There are many types of bioceramics available at present, oxide ceramics, calcium phosphate ceramics, glass and glass ceramics.

1-Oxide ceramics are alumina and zirconia. Although there exist precious stones of natural single crystals of alumina, the alumina used in artificial bones and joints is polycrystalline. Alumina (Al_2O_3) ceramics are used for the heads of bones in artificial joints and as a filling for bony defects left after the excision of lesions. Both alumina and zirconia are bioinert ceramics.

2-Calcium phosphate ceramic is hydroxyapatite (HAP). The structural formula of HAP is the same as that for the inorganic component of bone, and synthetic HAP can be regarded as equivalent to bone itself. Its affinity for bone is far higher than that of alumina. Consequently this material is ideal as a filling for bony defects left after the excision or curettage of lesions. Because it is vulnerable to mechanical stress it is

inappropriate to use HAP in the weight-bearing portions of a bone and joint. In order to overcome this major disadvantage a number of attempts have been made to increase durability of HAP ceramic materials [15]. One of the most important property of HAP is its biocompatibility.

3-Glass ceramics are silica (SiO_2) based ceramics. Bioceramics of this type are used in the repair and regenaration of hard tissues. There is a chemical bonding between tissue and implant.

Comparison of mechanical properties of typical metallic and ceramic biomaterials can be seen at Table 2.2 [2].

Table 2.2 Mechanical properties of some metallic and ceramic materials [2].

Material	Modulus (Gpa)	Tensile Strength (Mpa)
Stainless Steel	190	586
Co-Cr Alloy	210	1085
Ti Alloy	116	965
Amalgam	30	58
Alumina	380	300
Zirconia	220	820
Bioglass	35	42
Hydroxyapatite	95	50

Ceramics are known for their good biocompatibility, corrosion resistance, and high compression resistance. Drawbacks of ceramics are brittleness, low fracture strength, difficulty of fabrication, low mechanical reliability, lack of resilience, and high density [2].

A polymer is a substance composed of molecules characterized by the multiple repetition of one or more species of atoms (constitutional repeating units) linked to each other in amounts sufficient to provide a set of properties that do not vary markedly with the addition of one or a few of the constitutional repeating units. There are either covalent bonds through the cross links between chains or secondary bonding forces such as Van der Waals or hydrogen bonds through the long chains. Polymeric materials have a wide variety of applications for implantation since they are available in a wide variety of compositions, properties and they can be easily fabricated into many forms,

fibers, textiles, films, rods, and viscous liquids. Polymers have a close resemblance to natural polymeric tissue components such as collagen. In some cases it is possible to achieve a bond between synthetic polymers and natural tissue polymers [14]. However, polymers tend to be too flexible and too weak to meet the mechanical demands in orthopedic surgery and they may absorb liquids and swell, leach undesirable products (e.g. monomers, fillers, plasticizers, antioxidants), depending on the application and usage. Moreover, the sterilization processes (autoclave, ethylene oxide, and Co irradiation) may affect the polymer properties [2].

Synthetic polymeric materials have been used in dental materials, implant, dressing, encapsulate, polymeric delivery system, orthopedic devices and medical disposable supplies. Polymers can be classified as non resorbable and resorbable polymers. Some examples to non-resorbable polymers are polypropylene, polyethylene and polymethylmetacrylate. Polyglycolic acid, polylactic acid and chitosan are resorbable polymers, which means they degrade in body. A polymer to be used as a biomaterial must be biocompatible, non-toxic, must have sufficient mechanical properties and sterilizable. Mechanical properties of typical polymeric materials are given in Table2.3.

Considering the structural or mechanical compatibility with tissues polymers are for the soft tissue applications unlike metals and ceramics which are chosen for hard tissue applications. Polymer composite materials provide alternative choice to overcome many shortcomings of polymeric materials mentioned above [2].

Composite materials are those that contain two or more distinct constituent materials or phases, on a microscopic or macroscopic size scale. The term composite is usually used for those materials in which the distinct phases are separated on a scale larger than the atomic, and in which properties such as the elastic modulus are significantly altered in comparison with those of a homogeneous material. The properties of the composite materials depend very much on the structure as they do in homogeneous materials. Composites differ from homogeneous materials because considerable control can be eachieved over the larger scale structure to have the desired properties. In particular the properties of a composite material depend on the shape of the inhomogeneties, on the fraction of constituents, and on the interface among the constituents [14].

Table 2.3 Mechanical properties of typical polymeric biomaterials [2].

Material	Modulus (Gpa)	Tensile Strength (Mpa)
Polyethylene (PE)	0.88	35
Polyurethane (PU)	0.02	35
Polytetrafluoroethylene (PTFE)	0.5	27.5
Polyacetal (PA)	2.1	67
Polymethylmethacrylate (PMMA)	2.55	59
Polyethylene terephtalate (PET)	2.85	61
Polyethereethereketone (PEEK)	8.3	139
Silicone rubber (SR)	0.008	7.6
Polysulfone (PS)	2.65	75

There are several types of composites. Examples of typical microstructures for the three main classes, grouped according to the nature of the matrix are : metal matrix composites (MMCs), polymer matrix composites (PMCs), ceramic matrix composites (CMCs). Some important properties are the stiffness (Young's modulus), strength and toughness, compressive and tensile yield stresses, density and thermal properties.

A large number of polymers such as polyethylene (PE), polyurethane (PU), polyetrafluoroethylene (PTFE), polyacetal (PA), polymethylmethacrylate (PMMA), polyethylene terephtalate (PET), silicone rubber (SR), polysulfone (PS), polyethereethereketone (PEEK), poly(lactic acid) (PLA), and poly(glycolic acid) (PGA) are also used in various biomedical appplications, HA/PE, silica/SR, carbon fiber/ultra high molecular weight polyethylene (CF/UHMWPE), carbon fiber/epoxy (CF/epoxy), and CF/PEEK are few examples of polymer composite biomaterials. Each type of material has its own positive properties which make them suitable for specific applications [2].

Polymer composite materials provide alternative choice to overcome many shortcomings of homogeneous materials with several specific advantages they have. Generally tissues are grouped into hard and soft tissues. Bone and tooth are examples

of hard tissues, and skin, blood vessels, cartilage and ligaments are a few examples of soft tissues. As can be understood from their names, the hard tissues are stiffer (elastic modulus) and stronger (tensile strength) than the soft tissues in general. Considering the structural or mechanical compatibility with tissues, metals or ceramics are chosen for hard tissue applications and polymers for the soft tissue applications [2]. The elastic moduli of metals and ceramics are at least 10-20 times higher than those of hard tissues. One of the major problems in orthopedic surgery is the mismatch of stiffness between the bone and metallic or ceramic implants. In the load sharing between the bone and the implant, the amount of stress carried by each of them is directly related to their stiffness. When bone is insufficiently loaded compared to the implant, this phenomenon is called 'stress shielding ' or stress protection. Many investigators have shown that the degree of stress protection is proportional to the degree of stiffness mismatch. The stress-shielding affects the bone remodeling and healing process leading to increased bone porosity (also known as bone atropy). It has been recognized that by matching the stiffness of the implant with that of the host tissues limits the stress shielding effect and produces desired tissue remodeling. In this respect the use of low-modulus materials such as polymers appears interesting; however low strength associated with low modulus usually decreases their potential use. Polymer composite materials have low elastic modulus and high strength, they are suitable for several orthopedic applications. Additionally, by controlling the volume fractions of the local and general arrangement of the reinforcement phase, the design of the composite implant can be varied and suited to the mechanical and physiological conditions of the host tissues. Moreover the human tissues are essentially composite materials with anisotropic properties, which depend on the roles and structural arrangements of various components such as collagen, elastin and hydroxyapatite of the tissues. For example the longitudonal mechanical properties of cortical bone are higher than the properties of the transverse direction. These similarities also led to the development of composite biomaterials. Composite biomaterials have several other advantages such as absence of corrosion and fatigue failure of metal alloys and release of metal ions such as Nickel or Chromium which may cause loosening of the implant, patient discomfort, and allergic skin reactions [2].

Metals alloys and ceramics are radio opaque and in some cases they result in undesirable artifacts in X-ray radiography. In the case of polymer composite materials the radio transparency can be adjusted by adding contrast medium to the polymer. Moreover the polymer composite materials are fully compatible with the modern

diagnostic methods such as computed tomography (CT) and magnetic resonance imaging (MRI) as they are non-magnetic [2].

Polymer composite materials offer desired high strength and bone like elastic properties. Several investigators proposed a variety of polymer composite materials for bone plate applications. They may be grouped into non-resorbable, partially resorbable and fully resorbable bone plates. Ramakrishna et al. [2] grouped composites as shown in Figure 2.1 such as vital/avital composites, avital/avital composites and their subgroups.

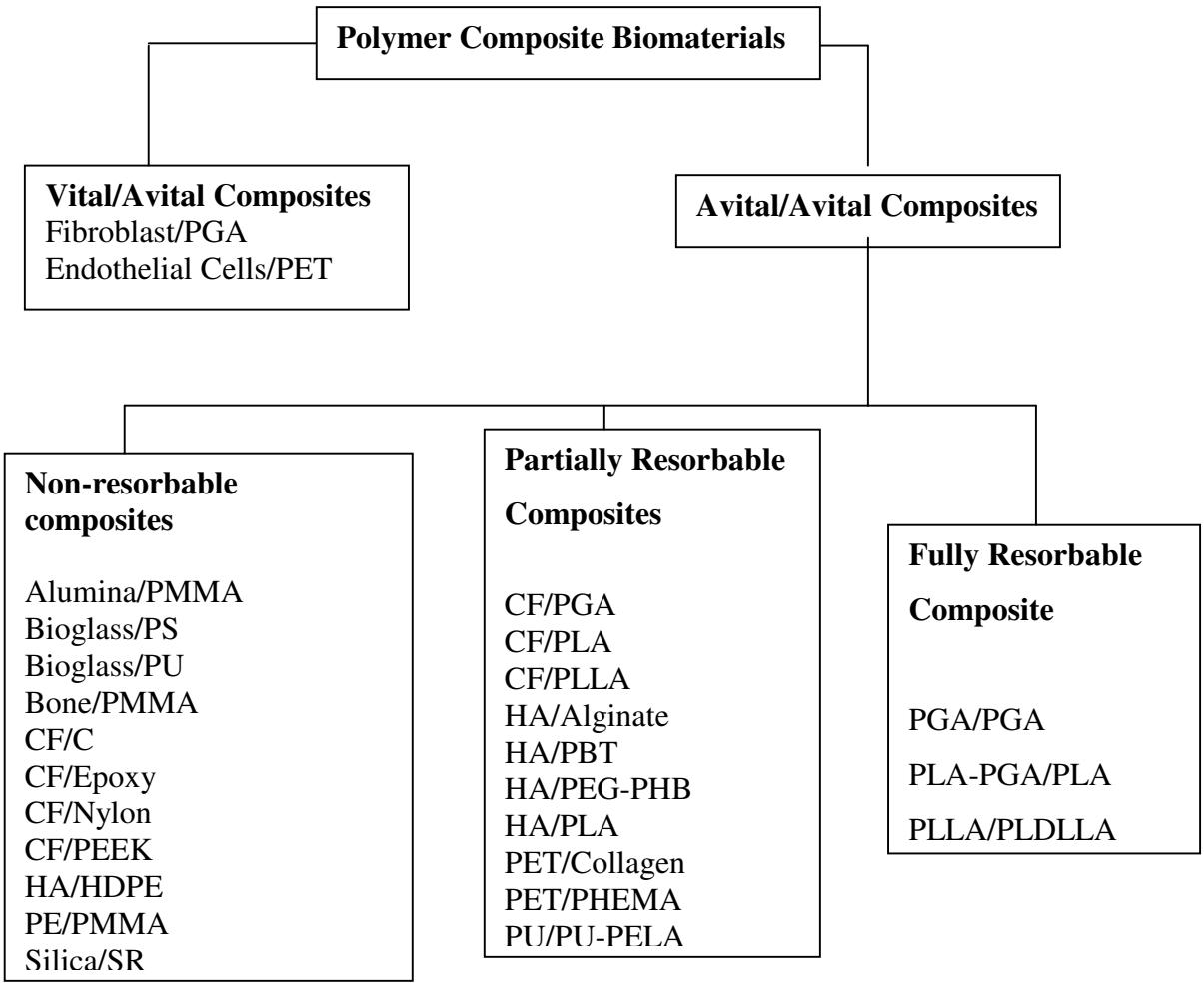

Figure 2.1 Classification of polymer composite biomaterials.

As can be seen in Figure 2.2 the only materials that exhibit a range of properties, namely tensile strength, and elastic modulus, equivalent to bone are composites. The approach used to achieve properties analogous to bone is to stiffen biocompatible synthetic polymer, such as polyethylene, with a higher-modulus ceramic second phase, such as HA powder. Bonfield et al. [16] have developed HA/HDPE composites since the early 1980s. They increased Young's modulus from 1 to 8 GPa and decreased strain

to failure from >90% to 3% as the volume fraction HA increases to 0.5. In this range the Young's modulus of the composite is in the lower band of values for bone and has a comparable fracture toughness. The transition from ductile to brittle behaviour occurs between 0.4 and 0.45 volume fraction HA. The mechanical properties of the polyethylene- HA composites are similar to bone. PE-0.4 volume fraction HA composite is less stiff (E ≅ 5GPa) but has a superior fracture toughness compared to bone. The main disadvantage of the composite is; it is not biodegradable. PE is bioinert and this decreases the ability to bond to bone. Various applications of different polymer composite biomaterials are shown in Figure 2.3 [2].

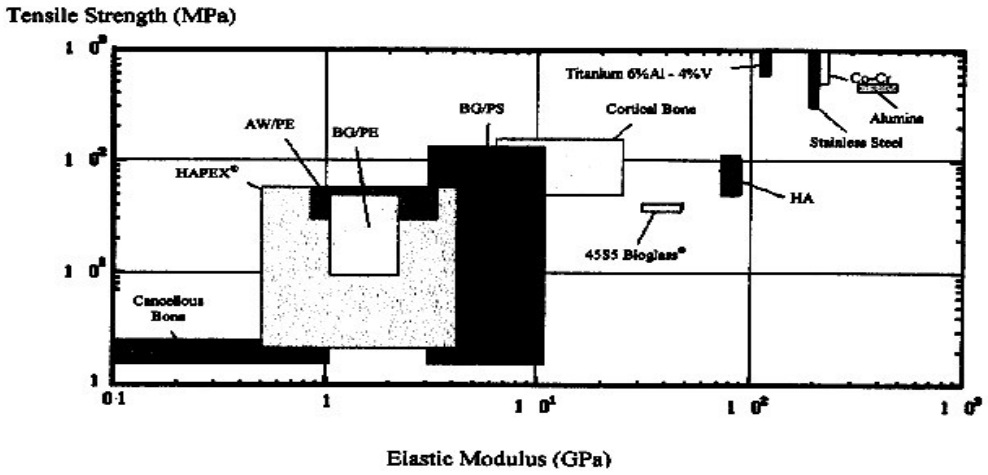

Figure 2.2 Range of Mechanical Properties of Some Biomaterials, Cancellous and Trabecular bone [15].

There are several examples to HA- polymer composites with biodegradable polymers such as PLA, PLLA or chitosan.

Shikinami et al. [17] worked on HA/poly L-Lactide (PLLA) composites. HA microparticles were uniformly distributed within PLA matrix and precipitation was made by dropping ethanol into dichloromethane polymer solution. The precipitate was extruded to produce a thick billet. Extrusion was followed by compression molding

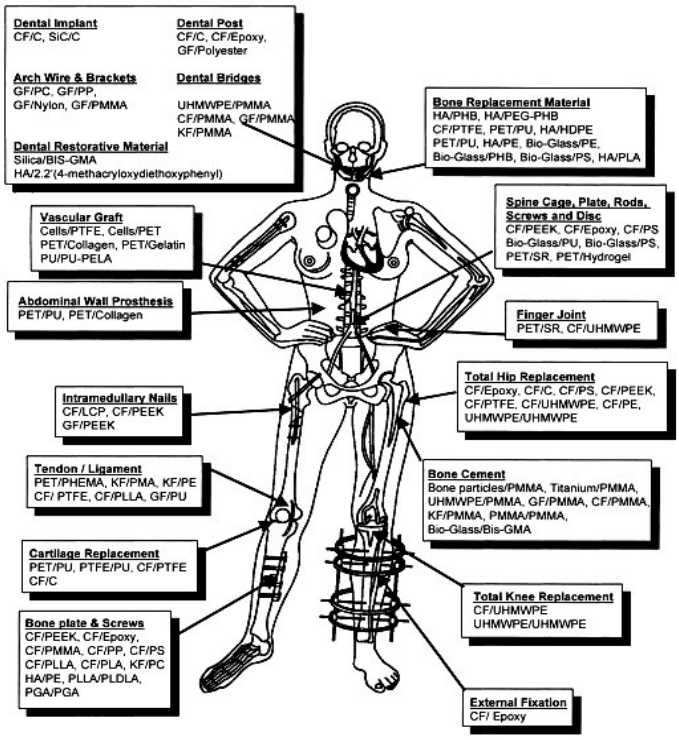

Figure2.3 Various Applications of Different Polymer Composites [2].

handled at 103 ^{o}C. 20, 30, 40 and 50 wt % of HA composites were produced. Effect of HA/PLA ratio on mechanical properties were investigated. Increasing HA percent caused gradual decrease in tensile strength. A value of 100Mpa tensile strength was reached. Mechanical interlocking between HA particles and PLA matrix caused high mechanical strength, bending, impact and shear strengths and high bending modulus.

Zhang et al. [18] studied on porous Poly (L-lactic acid)/ HAp and Poly(D,L-lactic acid co-glycolic acid)/HAp composite foams produced by solid-liquid phase separation of polymer solutions and subsequent sublimation of solvent by using freeze drying. This process resulted hard and tough foams with continuous structure of interconnected pores and a polymer/HAP composite skeleton. The microstructure of the pores and the walls was controlled by varying the polymer concentration, HAP content, quenching temperature, polymer and solvent used. Pore sizes ranging from several microns to a few hundred microns were obtained. Foams with porosity as high as 95 % were achieved. The compressive modulus and yield strength of PLLA/HAP composite foam were found to be higher than pure PLLA foam's.

Using biodegradable polymer such as PLA or chitosan has several advantages. Bone growth may be achieved through the pores meanwhile the polymer is resorbed and the bone tissue gradually replaces polymer, which will result a better bonding compared to composites which has bioinert polymer matrix constituent such as PE.

2.2 Bone

There is a necessity for replacing bone substance which has been lost due to traumatic or nontraumatic events [19]. At the case of implantation of hard tissue to achieve a good result and to have a appropriate host response, the implanted biomaterial must have properties in certain ranges. To have similar structure to the bone, firstly the microstructural and mechanical properties of the bone must be thoroughly understood.

Main function of the bone is load carrying. Bone is an anisotropic, heterogeneous, inhomogeneous, nonlinear, thermorheologically complex viscoelastic material. The complexity of bone's properties arises from th complexity in its structure.

2.2.1 Structure and Composition of the Bone

The extracellular matrices (ECMs) of hard tissues are composed of organic and inorgaic phases, the inorganic phase consisting primarily of HA crystals, and the organic phase consisting mainly of type I collagen and small amounts of other substance including glycosaminoglycans (GAGs), proteoglycans and glycoproteins [3].

Bone is difficult to analyze because it has so many levels of organization. The main constituents of bone are collagen (21wt.%), calcium phosphate (69 wt.%), Table 2.4. Additionally, water and other organic materials such as proteins, polysaccharides and lipids are also present in small quantities. Collagen which can be considered as the matrix, is in the form of small microfibers. It is difficult to observe distinct collagen fibers because of its net-like mass appearence. The diameter of collagen microfiber varies from 100 to 2000nm [19]. The hydroxyapatite crystals are present in the form of plates or needles which are about 40-60 nm long, 20 nm wide and 1.5-5 nm thick. They are arranged parallel to the collagen fibers, such that the larger dimension of crystals axis along the axis of fiber.There is a hierarchical structure which can be seen in Figure 2.4 [14].

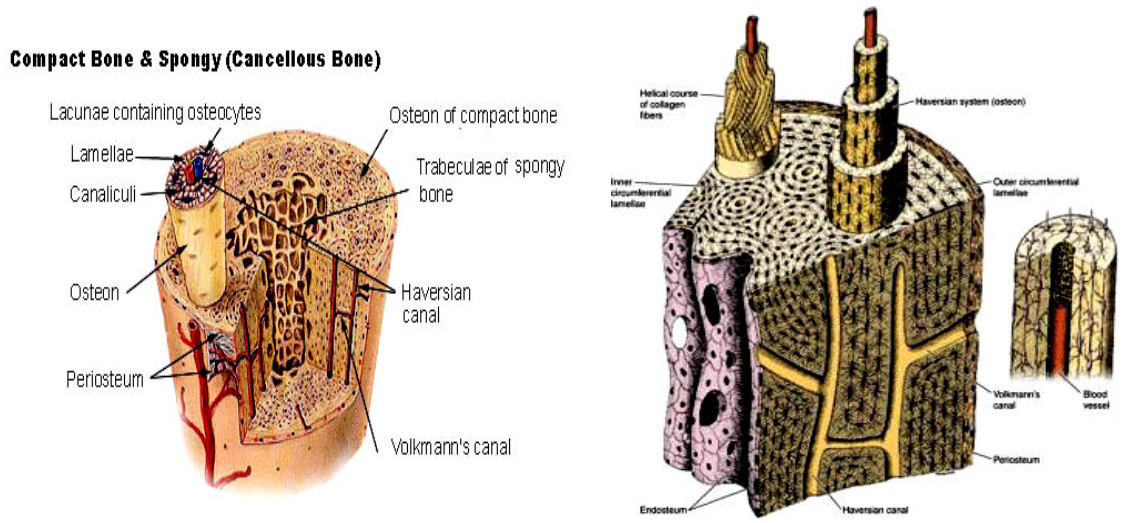

Figure 2.4 Organisation of Bone (a) Compact and Cancellous (b) Compact.

Bone consisits of two main parts, compact bone, also known as cortical bone, and the cancellous bone, also known as trabecular or spongy bone. Compact bone is the outer surface of the human bone. It is harder and denser compared to the spongy bone. Cancellous bone is softer and has lower density compared to the compact bone. The mineral-containing fibers are arranged into lamellar sheets (3-7 μm thick) 4-20 lamelae, which are arranged in concentric rings around the Harversian Canal, form an osteon [19].

The metabolic substances can be transported by the intercommunicating systems of canaliculi, lacunae, and Volkman's canals, which are connected with the narrow cavity. The various interconnecting systems are filled with body fluids and their volume can be as high as 19% [19].

Due to the properties mentioned, there is not a homogeneous composition, all the properties and composition are directionally and regionally dependent.

Table 2.4 Composition of Bone.

Component	Amount (wt %)
Hydroxyapatite	69%
Organic matrix Collagen Others	22% 90-96% of organic matrix 4-10% of organic matrix
Water	9%

2.2.2 Mechanical Properties of Bone

Bones of the skeletal system provide the supporting structure for the body. The low elastic modulus collagen fibers are aligned in bone along the main stress direction. The high elastic modulus hydroxyapatite mineral includes approximately 70 % of the dry bone mass and contributes significantly to the bone stiffness. Bone can remodel and adapt itself to the applied mechanical environment, which is generally known as Wolff's Law which is the principle relating the internal structure and architecture of the bone to external mechanical stimuli. Remodeling of bone takes place in response to mechanical stimulation so that the new structure becomes suitably adapted to the load. Density of living bone is influenced by the stress condition applied to the bone. Higher applied stress leads to the denser bone, conversely if the applied stress is lower than the normal physological load, the bone mass decreases and leads to bone weakening. Bone is an anisotropic material as longitudonal mechanical properties of cortical bone are higher than the transverse direction properties, Table 2.5. Bone is generally weak in tension and shear, particularly along the longitudonal plane [2].

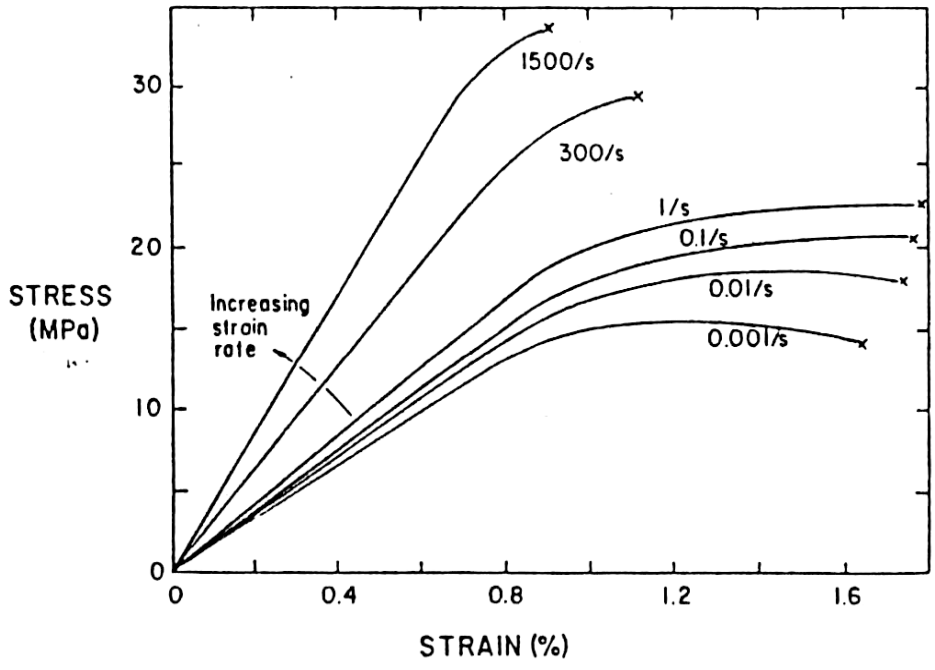

Figure 2.5 Stress as a function of strain and strain rate for human compact bone [14].

Bone exhibits excellent toughness (at low strain rates) mostly due to its hierarchical structure, which stops cracks after a little propagation. The main toughening mechanism seem to be microcracks, which appear in the plastic region of the stress-strain curve. The stress strain curves of bone due to changing strain rates are given in Figure2.5.

Young's Modulus (compressive) and compressive strength are in the range of 1-20 GPa and 1-200 MPa, respectively. With increasing bone density both Young's Modulus and compressive strength significantly increase. The mechanical properties of bone is shown in Table 2.5.

The mechanical properties of bone depend largely on the humidity, mode of applied load, direction of the applied load, and the kind of bone. With increasing level of bone mineralization, strength increases. Moreover, strength and other mechanical properties of bone depend on orientation of the collagen fibers, bone density, and porosity, molecular structure and arrangement of its constituent apatite crystals within their collagen matrix [19]. Both strength and volume of human bone decrease dramatically with age.

Table 2.5 The Mechanical Properties of Human Compact Bone [15].

Properties	**Test Direction**	
	Parallel	Normal
Tensile Strength (MPa)	124-174	49
Compressive Strength (MPa)	170-193	133
Bending Strength (MPa)	160	-
Shear Strength (MPa)	54	-
Young's Modulus (GPa)	17.0-18.9	11.5
Work of Fracture (J/m^2)	6000 (low strain rate)	-
	98 (high strain rate)	
Ultimate Tensile Strain	0.014-0.031	0.007
Ultimate Compressive Strain	0.0185-0.026	0.028
Yield Tensile Strain	0.007	0.004
Yield Compressive Strain	0.010	0.011

CHAPTER 3

CHITOSAN HYDROXYAPATITE COMPOSITES

As the consequence of tumors, infections, trauma, or other causes, bone defects need to be repaired. An ideal clinical bone substitute material should be nontoxic, biocompatible with all the tissues, including bone and blood, around it, and osteoconductive to form a good environment in the interface of mature bone and the implant, and maintain good mechanical properties in the wet state [6].

The observations on chitosan/HA composite biomaterials for hard tissue applications have been done for about 4-5 years but if bioresorbable composite devices other than chitosan are considered they have been in clinical use for about 16 years and even this is not a very long time. This is a promising area beause use of bioresorbable polymer ceramic composites have many advantages. The main drawback of such material is insufficient mechanical properties compared to bone.

To obtain such a composite with the desired mechanical, physical, chemical and biological properties as a potential bone substitute, extensive research has been undertaken into polymeric substrates designed to enhance the bioactivities and mechanical properties of inorganic calcium phosphate (e.g. HA). Yokogawa et.al. have introduced some biomimetic methods to grow calcium phosphate on chitin scaffolds, phosphorylated chitin fibers or chitosan films. However no expected mechanical strength improvement has been achieved ownig to poor affinity of these organic materials and heterogeneous distribution in inorganic components [20].

It has been known for a long time that various biocomposites exist in nature. They are made from organic matrix and inorganic fraction and fulfill the mechanical properties required in their function as the skeleton, teeth or shells of organisms. For example, organic collagen is combined with inorganic hydroxyapatite [HA: $Ca_{10}(PO_4)_6(OH)_2$] in bone and chitin is associated with calcium carbonate in crab shell. These constitutions have very good mechanical properties and they withstand tremendous pressures [20].

Hydroxyapatite which has been proved to have good properties of hardness, biocompatibility, osteoconductivity, a certain degree of bioactivity, and high resistance to moisture, has been used in a variety of oral and maxillofacial applications. It is

available in dense blocks, porous blocks, and granules. However each of these forms has its own drawbacks: Dense HA is difficult to machine without causing large-scale fracture, granules tend to migrate, and the macroporous material leaves a ragged surface finish. Therefore in recent years, HA-reinforced degradable polymers, such as collagen, gelatin, chitosan, chitin. When the polymer matrix is reabsorbed, new bone may intergrow around the HA particles [6].

3.1 Hydroxyapatite and β-Tricalciumphosphate

Pure HA, $Ca_{10}(PO_4)_6(OH)_2$, has the theoretical composition of: 39.68 wt% Ca, 18.45 wt% P, Ca/P ratio, 2.151 and Ca/P molar ratio of 1.67 [21].

The term apatite describes a family of compounds having similar structures but not necessarily having identical compositions. Apatite is a description not a composition. Hydroxyapatite also named as calcium hydroxyapatite has a definite composition and a crystallographic structure. Hydroxyapatite belongs to the hexagonal system, with a space group, $P6_3/m$. this space group is characterized by a six-fold c-axis perpendicular to three equivalent a-axes (a_1,a_2,a_3) at angles 120^o to each other. Unit cell consists of Ca, PO_4, and OH groups closely packed together [21]. Figure 3.1 represents the crystal structure of hydroxyapatite.

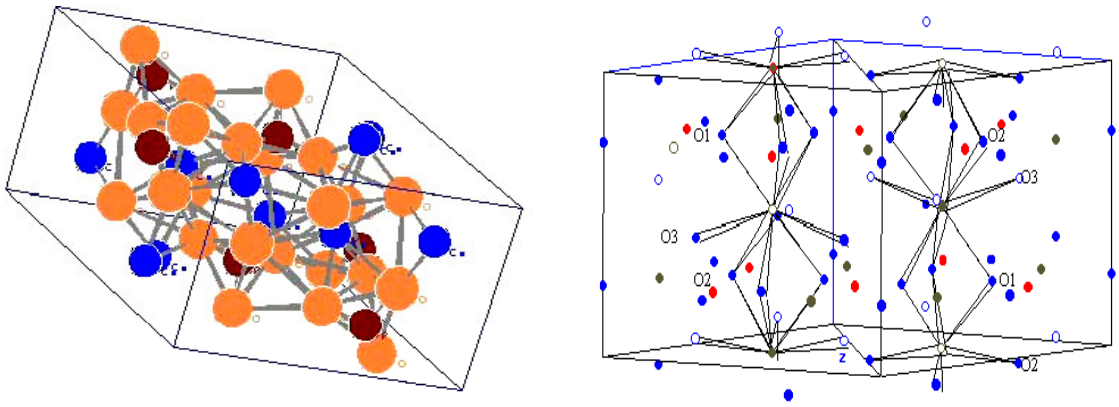

Figure 3.1 Schematic of crystal structure of hydroxyapatite (hexagonal).

The ten calcium atoms belong to either Ca(I) or Ca(II) subsets depending on their environment. Four calcium atoms occupy the Ca(I) positions: two at levels z=0 and two at z=0.5. six calcium atoms occupy the Ca(II) positions: one group of three calcium atoms describing a triangle located at z=0.25, the other group of three at z=0.75, surrounding the OH groups located at the corners of the unit cell at z= 0.25 and

0.75 respectively . The six phosphate (PO_4) tetrahedra are in a helical arrangement from levels z=0.25 to z=0.75. The network of PO_4 groups provide the skeletal framework which gives the apatite structure its stability [21].

From the point of view of biocompatibility, hydroxyapatite seems to be the most suitable ceramic material for the hard tissue replacement implants since hydroxyapatite is the main mineral constituent of teeth and bones. Hydroxyapatite ceramics do not have any toxic effects. They show excellent biocompatibility with hard tissues and also with skin and muscle tissues. Moreover HAp can directly bond to bone. Unfortunately due to the low reliability, especially in wet environments the HAP ceramics cannot presently be used for heavy load bearing appications, like artificial teeth or bones. There has been a lot of research aiming to increase mechanical reliability of HA [21].

Many reports are available dealing with clinical uses of HA for jaw augmentation, tooth replacement, bone replacement and middle ear reconstruction [22].

β-TCP is a biodegradable calcium phosphate with the chemical formula $Ca_3(PO_4)_2$. β-TCP particles slowly dissolve in physiological media and increase the concentration of Ca and P ions. The deposition of Ca and P ions on the material surface favor the formation of an apatite layer. Apatite layer increases bioactivity since bioactive materials bond to living bone through this apatite layer [23].

3.2 Production of Porous Hydroxyapatite

In recent years attention was particularly placed on the fabrication of bioceramics with “porous” configuration because the porous network allows the tissue infiltration, which further enhances the implant tissue attachment [24].

Cellular ceramics can be classified into two main groups, honeycombs and foams. The honeycomb cells form a two dimensional array of hollow polygons. Foams can be classified into two categories depending on whether or not the cells have solid faces. If the solid of which the foam is made is contained only in the cell edges, the material is termed open-cell. If the cell faces are present the foam is termed closed-cell and the individual cells are isolated from each other. It is clear that foams can be partly open and partly closed.

These porous network structures have relatively low mass, low density and different permeation properties. By using proper methods and materials porous ceramics which have relatively high strength can be produced [25].

The three important parameters in porous bioceramics are porosity, pore size distribution and the open pore content. If the foam has interconnected open pores rather than closed ones, this enables to apply further processes on the foam such as soaking it in a solution. The open pores also enable bone ingrowth when a porous ceramic biomaterial is implanted in a body. On the other hand porosity must be set within a suitable range because increasing porosity and pore size causes a decrease in strength.

Two of the several methods to produce porous ceramic materials will be mentioned:

The first one, polymeric sponge method, patented in 1963 consists in the impregnation of a polymeric sponge with a ceramic slurry followed by a thermal treatment which leads to the burning out of the organic portion and to the sintering of the ceramic skeleton.

The steps must be optimized carefully to develop a foam product having the desired performances. The choice of polymeric sponge, preparation and solid percent in the slurry, the impregnation, the thermal cycle including drying, burning out of the volatile components and sintering of the ceramic portion must be considered in this method.

The choice of sponge is very important. The residual stress and disruption of unsintered ceramic network should be avoided. The sponge should volatilize at low temperature without yielding harmful by products. Its resiliency, hydrophobic behavior and ability to be uniformly covered by slurry are other important properties. There are many polymeric sponge materials satisfying these requirements such as poly(urethane), cellulose, poly(vinyl chloride), latex [25].

The ceramic type is determined depending on the application and the desired properties of the final product. The ceramic slurry must be able to uniformly cover the polymeric walls, easily sinter in a dense ceramic network and be able to bear in-use constraints. A fine ceramic powder having a narrow size distribution is generally recommended with a mean particle size of a few microns. The quantity of the particles penetrating the polymeric sponge changes according to the structure of the sponge which is the suction force optimized by increasing the open porosity of the sponge and also according to the concentration of the slurry. The slurries may contain very variable solid weight percent but usually ranges between 50 and 70 wt % of solid. Higher the solid concentration more and more viscous the slurry and this makes the particles difficult to penetrate the sponge that will cause loading decrease [25].

Many additives can be used for improving coating performances. A binder provides strength to ceramic structure after drying and prevent collapse during volatilization of the organic part. During the impregnation the slurry must be fluid enough to enter, fill and uniformly cover the sponge walls and then regain enough viscosity under static conditions to remain in the sponge. Impregnation is usually done by compression of the sponge in the slurry to remove air followed by free expansion of polymer in the slurry. The ceramic suspension should not be too viscous which will slow the sponge while trying to expand to its original shape.

A typical cycle of polymeric sponge method is the preparation of the ceramic slurry, immersion of sponge in the slurry, impregnation and then drying, thermal cycle applied to the impregnated foam which consists of two stages first of which is slowly decomposing and burning out of polymer support without collapsing and the second is sintering and densification of the ceramic powder, summarized in Figure 3.2.

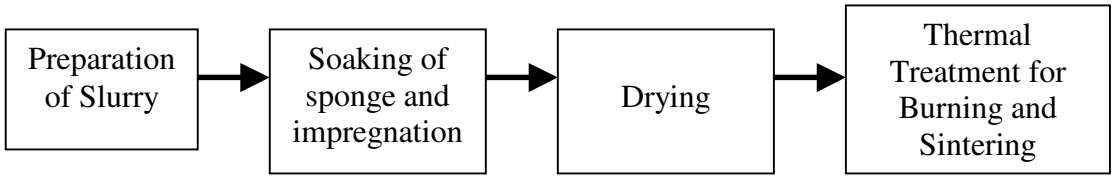

Figure 3.2 Polymeric Sponge Method for porous ceramic production.

There are several studies in the literature about the production of ceramic foams with this method. Callcut et al. [26] prepared glass-reinforced hydroxyapatite foams by immersion of polyurethane foam into glass-reinforced hydroxyapatite suspension in water. After ceramic coated foam was dried, it was heat treated to 600 ^{o}C a heating rate of 1^{o}C min^{-1} to slowly burn off the polyurethane foam followed by an increase to 1250 ^{o}C for 8h with a heating rate of 5^{o}C min^{-1} to to fully sinter the ceramic. At the end of the process porous GR-HA ceramic has the identical macrostructure with polyurethane. The characterization was made by using mechanical testing, X-Ray diffraction, SEM and density measurements. All the samples tested showed the classic three regions characteristic of an elastic brittle foam as shown in Figure 3.3. The ceramic foams were found to exhibit mechanical properties of typical isotropic open cellular foams.

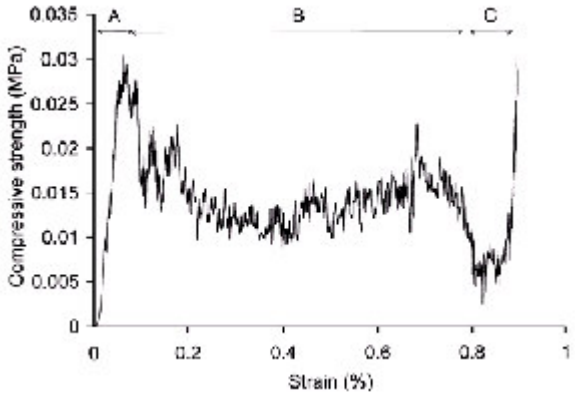

Figure 3.3 Compressive test of a GR-HA foam [26].

In another study Tampieri et. al [27] produced porous HA bodies. By varying the characteristics of starting HA powders and impregnation strategy of cellulose sponges, a wide range of physico-chemical and mechanical properties of the porous ceramics were obtained. HA powders with different degrees of crystallinity were prepared by a precipitation technique. Two types of porous bodies were prepared by soaking cellulose sponges into the HA slurries. The HA/water ratio were 1:1 and 1:1.6 respectively. Finally ultrasonic treatment was applied. After air drying of wet sponges for 72h sintering was done at 1250 ^{o}C for 1h.

Dry pressing is another common method to produce porous ceramic structures. In this method a polymer powder and ceramic powder mixture is die pressed uniaxially at several pressures. These compacts blocks are then heat treated with a similar path described in the polymeric sponge method.

Dean-Mo Liu [28] produced porous HA ceramic using poly vinyl butyral (PVB) as a porosifier. PVB particles with varying sizes were mixed with HA powder. Five gram of the mixed powder was die-pressed uniaxially under pressures of 27 MPa and 55 MPa to form rectangular compacts. These compacts were then heat-treated to 500^{o}C at a heating rate of 0.5 ^{o}C min^{-1} to burn off PVB particles followed by an increase to 1200^{o}C for 2 to 48h for densification. According to the measurements the pores are interconnected, the pore shape is nearly spherical and similar to the shape of PVB particles. A porosity value of 71% was obtained.

In another study Dean-Mo Liu [29] investigated the compressive strength of Porous HA in terms of porosity and pore size. The porosity increase caused a decrease in compressive strength as shown in Figure 3.4. The porous HA consisting of smaller

macropores exhibits higher strength in comparison with those with larger macropores as shown in Figure 3.5.

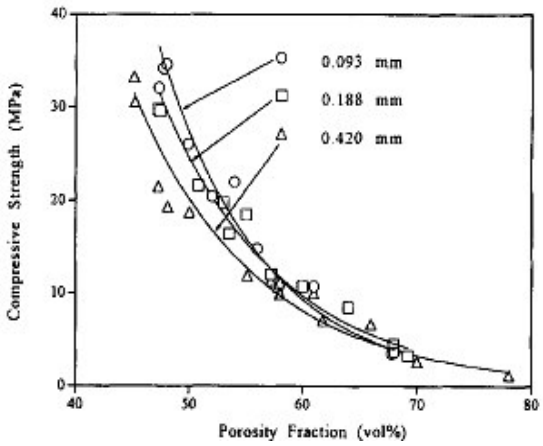

Figure 3.4 Porosity-compressive strength behaviour of porous HA ceramics in terms of different sizes of starting PVB particles [29].

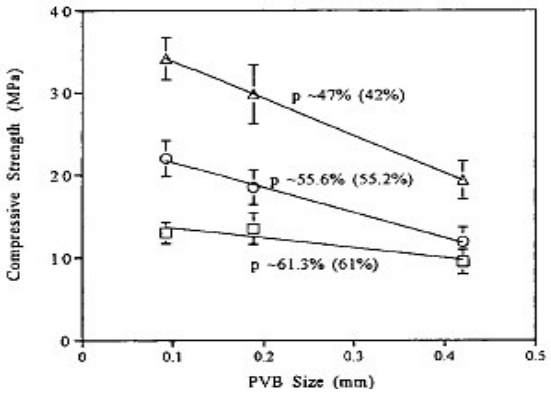

Figure 3.5 Pore size-compressive strength behavior for given porosity [29].

3.3 Chitin and Chitosan

Chitin is the most abundant natural amino polysaccharide and is estimated to be produced annually almost as much as cellulose. Chitin is the supporting material of crusteceans, insects, etc., and is well known to consist of 2-acetamido-2-deoxy-β-D-glucose through a β (1→4)linkage. Chitin is highly insoluble like cellulose and has low chemical reactivity.

Chitosan is the *N*-deacetylated derivative of chitin, although this *N*-deacetylation is almost never complete. Formation of chitosan from chitin is shown in Figure 3.6 and the structures of chitin and chitosan are shown in Figure 3.7 [30].

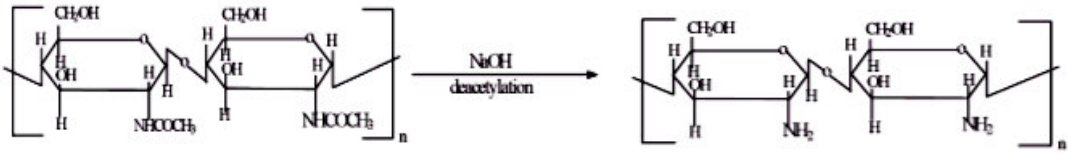

Figure 3.6 Formation of chitosan from chitin

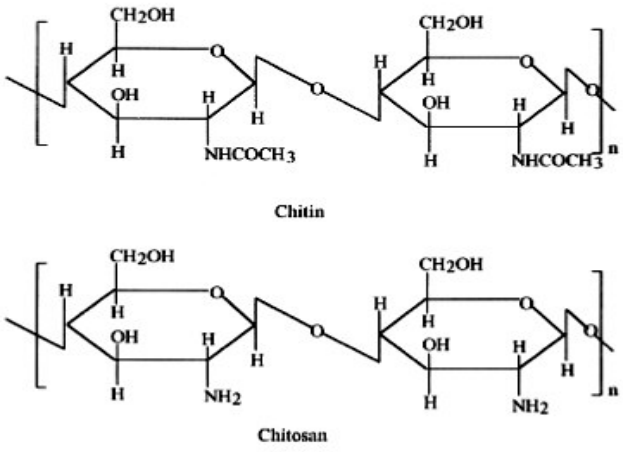

Figure 3.7 Structures of Chitin and Chitosan [30].

As most of the present day polymers are synthetic materials, their biocompatibility and biodegradability are much more limited than those of natural polymers such as cellulose, chitin, chitosan and their derivatives. However these naturally abundant materials also have a limitation in their reactivity and processability. In this respect, chitosan is recommended as suitable functional material, because this natural polymer has excellent properties such as biocompatibility, biodegradability, non-toxicity, adsorption properties etc.

Chitin and chitosan are now produced commercially in India, Japan, Poland, Norway and Australia.

Most of the naturally occuring polysaccharides such as cellulose, dextran, pectin, alginic acid or agar are neutral or acidic in nature but chitin and chitosan are highly basic polysaccharides. They have film forming property. Chitosan is soluble in dilute organic acids such as acetic acid, formic acid.

Converting chitin into chitosan lowers the molecular weight and changes the charge distribution, which in turn effects the agglomeration. The weight-average molecular weight of chitosan is $1X10^5$ to $5X10^5$. Chitosan degrade before melting which is typical for polysaccharides with extensive hydrogen bonding [30].

It has been suggested that chitosan may be used to inhibit fibroplasia in wound healing and promote tissue growth and differentiation in tissue culture. For cosmetic applications organic acids are good solvents and chitosan has fungicidial property. There are many other applications of chitosan but more related ones to the body applications are artificial skin, wound dressing, food and nutrition, opthalmology (contact lenses), chitosan tablets for controlled release, blood anticoagulants, chitosan-polyethylene oxide nanoparticles as protein carriers. Figure 3.8 shows two of the biomaterial applications which are contact lens and wound dressing.

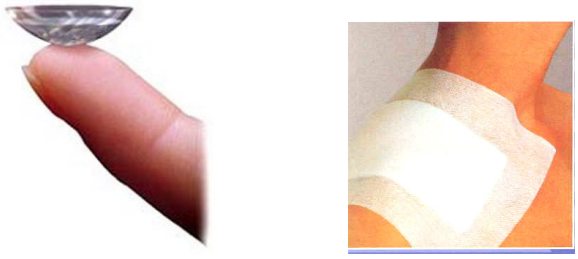

a) b)

Figure 3.8 Biomaterial application of chitosan, a)contact lens, b)wound dressing.

3.4 Processing of Calcium Phosphate and Hydroxyapatite Reinforced Chitosan Composites

Preparation and characterization of HA/chitosan composites to be used as hard tissue implants have been studied in the literature. There are several preparation techniques for chitosan/HA composites. Main methods are phase separation (freeze drying) [3,4], precipitation [8], sol-gel [5,31] and cement [20,32].

Zhao et al. [3] investigated the preparation of three dimensional hydroxyapatite/chitosan-gelatin network composite scaffolds produced by phase separation method. A suspension was prepared by using pulverized hydroxyapatite and deionized distilled water. After 0.5 h stirring at room temperature the suspension was treated ultrasonically until the HA powder was thoroughly dispersed in the water. Chitosan and acetic acid were added under agitation. After stirring overnight gelatin was added to this suspension held in 40^{o}C water bath. After addition of a glutaraldehyde solution the mixture was put into plastic petri dishes at 4^{o}C half an hour then rapidly transferred to a freezer at –40^{o}C to solidify the solvent and induce solid-liquid phase

separation. Solidified mixture was maintained at that temperature for 2 hours and placed in a freeze-drier. The sample was finally freeze-dried for at least 30h resulting in a foam which were cut into disks. Changing the HA content and the compositional variables of the original suspension allowed control of the porosities and densities of the scaffold as tabulated in Table 3.1.

Table 3.1 Porosity and density of CS-Gel/HA scaffolds [3].

CS-Gel concentration (w/v)%	CS-Gel/HA Ratio (w/w)%	Quenching Temperature (^oC)	Density (kg/m^3)	Porosity (%)
1.0	50/50	-20	0.042±0.017	95.8±8.3
2.5	50/50	-20	0.083±0.09	93.4±11.5
5.0	50/50	-20	0.156±0.011	90.6±6.8
7.5	50/50	-20	0.237±0.05	85.2±3.9
2.5	70/30	-20	0.078±0.010	94.7±8.7
2.5	30/70	-20	0.091±0.013	91.0±7.2
2.5	50/50	-80	0.092±0.011	91.8±5.9

In another study Ang et al. [4] prepared three dimensional chitosan-hydroxyapatite scaffolds using a robotic dispensing system. The dispensing material was prepared by dissolving chitosan in acetic acid and adding HA to obtain different HA/chitosan ratios to form a hydrogel. The mixture was stirred for 2h and transferred to a vacuum oven (preset at 37^oC) to remove air bubbles. By using the robotic dispensing machine the dispensing materials were extruded into a dispensing medium. The extruded 3D scaffolds were immersed in ethanol for 5 min and washed 3 times with distilled water. The scaffolds were then rapidly transferred to a freezer at –20 ^oC to solidify solvent so as to induce a solid liquid phase separation. The frozen scaffolds were maintained at –20 ^oC for at least 8h and then freeze dried at –56 ^oC for 2 days to remove solvent. In vitro cell culture study was performed for biocompatibility characterization.

Zhang et al. [23] prepared chitosan scaffolds reinforced by calcium phosphates by phase separation method. Chitosan solutions with concentration of 2 wt% were

prepared by dissolution of chitosan in acetic acid solution. The mixture was stirred at 50 ^{o}C for 2h to obtain a homogeneous polymer solution. Calcium phosphate invert glass and β-TCP powders were added into the solution. The final composition of the composite foam was determined by the concentration of the chitosan solution and calcium phosphate content in the mixture. The mixture was then rapidly transferred into a freezer (–20 ^{o}C) to solidify the solvent and induce solid liquid phase separation. The solidified mixture was maintained at that temperature for 8h and the frozen mixture was then transferred into a freeze-drier at –5 ^{o}C preset temperature. The samples were freeze dried at 0.5 mmHg for at least 4 days to completely remove the solvent. In their study the effect of the chitosan content on mechanical properties, physical properties and in vitro observation was investigated. Figure 3.9 shows a series of compression stress-strain curves of pure chitosan and composite scaffolds. Physical properties of composites can be seen in Table 3.2 and mechanical properties of composites as a function of composition can be seen in Figure 3.10.

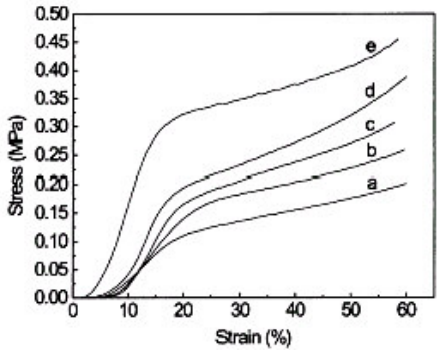

Figure 3.9 Stress-strain curves of pure chitosan scaffolds (a) and composites weight chitosan/ ß-TCP ratio of (b)90/10 (c)70/30,(d) 50/50, (e)30/70 [23].

Yamaguchi et al. [10] prepared hydroxyapatite chitosan composites using a co-precipitation method. A chitosan aqueous solution of 1.5 wt% prepared by dissolving chitosan powder into distilled water containing 0.6 wt% of acetic acid and subsequently the chitosan solution was adding into 8.5 wt % of H_3PO_4 solution. The obtained chitosan/ H_3PO_4 solution was gradually dropped into 3.7 wt% $Ca(OH)_2$ suspension upon vigorous stirring until pH 9±0.2. At this time chitosan became insoluble and precipitated with small hydroxyapatite crystals forming chitosan/HA composite. The

Table.3.2 Densities and Properties of Chitosan/Calcium Phosphate Composite Scaffolds [23].

Chitosan/ß-TCP/Glass Composition	Density (g/cm^3)	Porosity
100/0/0	0.046	88.89%
90/10/0	0.054	89.47%
70/30/0	0.067	87.50%
50/50/0	0.071	87.26%
30/70/0	0.105	85.71%
90/5/5	0.062	75.95%
90/0/10	0.054	84.27%

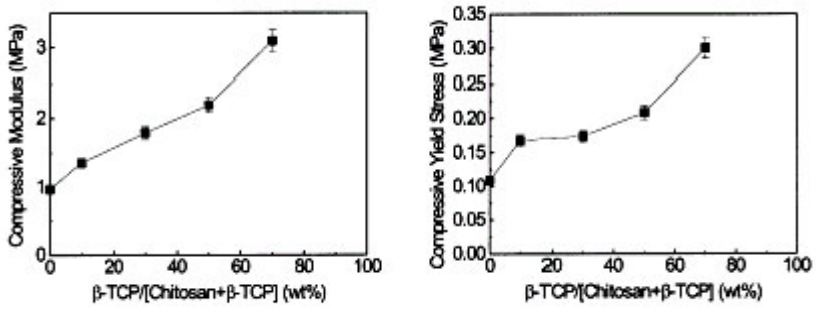

Figure 3.10 Compressive Modulus and Yield Stress of chitosan/ß-TCP composites as a function of composition [23].

reaction temperature was at 25 ^{o}C and dropping speed was 3.2 ml/min. the resulting solution was aged for 24 h upon continuous stirring. The preparation of chitosan/HA composite using citric acid was as follows: an aqueous solution of 50wt% citric acid was added into a suspension of chitosan /HA (20/80) composite upon stirring. The slurry obtained was then aged for 24h. the precipitate was filtered and washed with distilled water. The effect of citric acid on mechanical properties of the composite were investigated as shown in Figure 3.11.

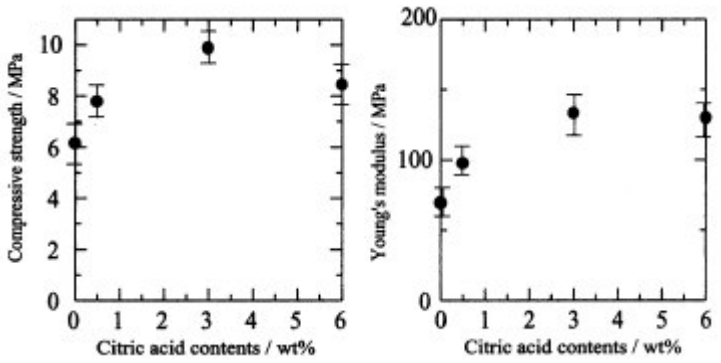

Figure 3.11 Compressive Strength and Young's Modulus of Chitosan/HA composite as a function of citric acid content [10].

Yin et al. [6] prepared a composite composed of HA and a network formed by crosslinking of chitosan and gelatin with glutaraldehyde was developed by sol-gel method. Chitosan sol was prepared by dissolving chitosan in aqueous acetic acid solution by stirring 24 h at room temperature. A glutaraldehyde solution was prepared by dissolving it in water. HA powder was added in deionized distilled water and ultrasonicated until the HA powder was thoroughly dispersed in water. The slurry was held for 5h to let HA powder deposit. The deposited paste mixed with a chitosan solution under agitation then gelatin was added to the mixture. After dissolving of gelatin glutaraldehyde aqueous solution was added. At last the resulting mixture with homogeneously dispersed HA powder was cut into a mold and air dried to obtain composite plate. HA content is changed to handle composites with different HA %wt.

Ito et al. [5] investigated the effect on certain physical properties of adding various amounts of HAP to chitosan sol and also investigated connective tissue reactions to a composite membrane. Chitosan sol was prepared by mixing chitosan with malonic acid dissolved in physiologic salt solution. Varying amounts of HA were added to the sol. The mixtures were mixed manually with a spatula to make a paste. The paste was neutralized with polyphosphate solution. For evaluation of shrinkage and for measuring tensile strength and elongation the paste was spread into petri dishes and dried at room temperature for 2h to form membranes.

There are also calcium phosphate chitosan bone cements in some of which calcium phosphate transform in to hydroxyapatite.

Wang et al. [20] worked on phosphorylated chitosan as additive of calcium phosphate cements. Chitosan was phosphorylated by P_2O_5 in methanosulfonic acid

solution. The reaction mixture was filtrated and the filtrate was dialyzed thoroughly against distilled water to remove small molecular substances. After concentration by vacuum evaporation and freeze-drying, solid phosphorylated chitosan was obtained. The solid DCPD, MCPM, $Ca(OH)_2$ and CaO were milled for 8h in a rotating micromill to give the corresponding particles with average sizes around 6.88, 74.3, 3.32 and 1.95 μm respectively. Cement powders were prepared by mixing a calcium phosphate (DCPD or MCPM) with a basic calcium compound $Ca(OH)_2$ or CaO. The liquid phase was 1M Na_2HPO_4 aqueous solution or 1M phosphate buffer (pH 7.4) prepared from Na_2HPO_4 and $NaHPO_4$. Different amounts of P-chitosan were dissolved into the liquid phases. Cement was prepared by mixing powder phase with liquid phase containing P-chitosan. It was found that in certain amounts p-chitosan enhanced mechanical properties which are shown in Table 3.3.

Table 3.3 The effect of p-chitosan on mechanical properties of MCPM cement [20].

P-chitosan (wt)%	CS (MPa)	Young's Modulus (MPa)
0.0	1.32	27.8
0.5	6.42	302.09
1.0	8.41	266.92
1.5	4.45	170.54
2.0	4.56	215.53
2.5	2.99	117.15
3.0	3.68	120.14

Yokoyama et al. [32] studied on calcium phosphate cement using chitosan at citric acid for bone substitute materials. The cement developed consisted of both powder and liquid components. Powder component was a mixture of α-TCP and TeTCP at a molecular ratio of 2:1. The liquid component was a solution of citric acid, chitosan and glucose. In this study two types of liquid components were used. Both types contained citric acid, glucose and chitosan. The mechanical properties due to the citric acid concentration change and biocompatibility were investigated. In physiological salt solution cement transformed to HAP.

In another study Xu et al. [33] prepared strong and non rigid calcium phosphate cement. Tetracalciumphosphate (TTCP) powder was synthesized from a solid state reaction between equimolar amounts of $CaHPO_4$ (dicalciumphosphate anyhydrous or DCPA) and $CaCO_3$ which were mixed and heated at 1500^oC for 6h in a furnace. The heated mixture was quenched to room temperature, ground in a ball mill and sieved so that TTCP particles could be obtained with sizes ranging from 1μm to 80 μm. The DCPA powder was ground for 24 h and sieved, yielding particles with sizes ranging from 0.4μm to 3μm then the TTCP and DCPA powders were mixed in a micromill in equimolar amounts to form CPC powder. Chitosan lactate was mixed with distilled water and CPC powder was added to make paste. The paste was placed into stainless steel mold and the mold was sandwiched between two glass slides and set in a humidor with 100% relative humidity at 37^oC for 4h. Hardened specimens were demolded and immersed in a simulated physiological solution stored in an oven at 37^oC for 20h. Mechanical properties of the composite were investigated.

Takagi et al. [12] prepared calcium phosphate cement-chitosan composites. For the solid phase, CPC powder consisting of equimolar mixture of tetracalcium phosphate (TTCP) and dicalcium phosphate anyhydrous (DCPA), was prepared by thoroughly mixing ground TTCP and DCPA in a blender. For the liquid phase chitosan with mass fraction of 5 and 15 were dissolved in 1M HCl. Additionally 15%wt chitosan lactate and 15 % wt chitosan malate were dissolved in distilled water. Samples were prepared with changing powder/liquid ratios of 2 to 4. Mechanical properties of the composites were investigated.

Hockin et al. [13] prepared mesh and chitosan hardened calcium phosphate cement. CPC powder consisted of equimolar amounts of tetracalcium phosphate (TTCP) and dicalcium phosphate anyhydrous (DCPA). Chitosan lactate dissolved in distilled water at 15%. The liquid was mixed with CPC powder at a powder liquid ratio of 2 to have a flowable paste to impregnate the meshes. CPC was placed with a spatula on the mesh and slightly pressed. The specimen was set in a humidor with 100% relative humidity for 4h. The hardened specimens were demolded and immersed in a simulated physiological solution at 37 ^oC. Mechanical properties of specimens with CPC+chitosan, CPV+mesh, and CPC+chitosan+mesh were investigated.

Varma et al. [34] studied on porous calcium phosphate coating over phosphorylated chitosan film by a biomimetic method. Chitosan film was made by first dissolving chitosan powder in acetic acid solution. The viscous liquid was then poured

into glass petri dishes and kept in a vacuum oven at 700mmHg and 35 ^{o}C for 6h to clear all the entrapped gas bubbles. The dishes were then transferred into an air oven and dryed at 60^{o}C for 24h. The chitosan film was easily pealed off when saturated NaOH solution was introduced into the dishes. The wet films were then thoroughly rinsed with distilled water. For the phosphorylation reaction chitosan film H_3PO_4 , urea and dimethyl formamide were mixed together in a round bottomed flask fitted with a condenser, thermometer and nitrogen gas inlet tube. The bottle was then heated to 110^{o}C with the reactants refluxed for 1h under gentle stirring using a magnetic stirrer. After cooling, films were removed and thoroughly rinsed with distilled water. Lime soaked, phosphorylated chitosan films were vertically suspended in plastic jars with cotton threads and 50ml of solution was added. Some phosphorylated films were suspended in saturated $Ca(OH)_2$ solution. Both resulted by calium phosphate formation on the films.

Hu et al. [11] prepared biodegradable chitosan/hydroxyapatite composite rods by a new in situ hybridization method. $Ca(NO)_3.4H_2O$ and KH_2PO_4 were added into 100 ml acetic acid aqueous solution with concentration of 2%(v/v). The solution was stirred for 30 min until the calcium salt and phosphate salt were entirely dissolved. 5g of chitosan powder were added under agitation and the mixture was stirred for 4h at room temperature to obtain a homogeneous polymer solution. The resulting solution was held for 6h to remove air bubbles trapped in viscous liquid. Chitosan solution was cast on internal surface of glass mold and the mold was soaked in a solution of 5%(wt/v) NaOH aqueous solution for 2h to precipitate a chitosan membrane. The mold filled with the resulting solution was 5% (wt/v) NaOH aqueous solution for 8h to form a chitosan/HA gel rod containing 95-97% (v) water. The gel rod was washed with distilled water until the pH of washed water is about 7 and chitosan membrane was removed then air dried in oven at 60^{o}C for 24 h. A transparent, slight yellow chitosan /hydroxyapatite rod was prepared after a large shrinkage during drying process. The mechanical properties of the rods were tested.

3.5 Characterization of Calcium Phosphate Chitosan Composites

In literature there are different characterization techniques to observe physical, mechanical, morphological and microstructural properties of the composites.

The mechanical characterization of composite is done by several mechanical tests. The mechanical tests give information about strength, ductility, brittleness and

toughness of the material. The mechanical properties of the composites are affected by many factors such as the material selected, matrix/fiber wt%, homogeneous dispersion of filler, filler-matrix bonding efficiency and interface, preparation technique, direction of the applied load (anisotropy) etc. For the polymer ceramic composites to be used as bone substitute materials, especially Young's Modulus, strength (both tensile and compressive), yield stress and fracture toughness are important parametres to characterize the mechanical properties of the composites. Young's Modulus ,which is the slope the stress strain curve in the elastic region, gives information on the rigidity of the composite, which is very important as mentioned in the previous chapters. Tensile yield stress is very important because it gives information on the maximum allowable load before plastic deformation occurs. Compressive yield stress is also very important by the same reason and also taking into account that the load on bones in the body is usually compressive. Fracture toughness gives important information about the energy absorbed up to fracture. Mechanical testing machines are used for mentioned characterization.

There are other characterization techniques such as XRD, FTIR and EDX which gives important knowladge on the chemical composition of the composite, chemical bonds existing in the material also gives valuable information about what phases exist at a certain condition and what phase transformations occur.

At characterizing morphology of the composites microscopy techniques are important. Optical and scanning electron microscopy (SEM) gives information about the morphology, fracture surfaces, dispersion of reinforcement particles in polymer matrix, examining the interface region. Optical microscopy have some limitations due to its lower resolution compared to the SEM which has resolution to several nanometers and give detailed images especially on fracture surface.

Mechanical and microstructural properties of chitosan calcium phosphate based composites have been investigated in the literature.

Xu et al. [33] investigated the effect of chitosan content on strength and strain before failure in CPC-chitosan lactate composites. Flexural strength, strain-at-peak-load, elastic modulus and work-of-fracture were measured. Specimen surfaces were examined with SEM. Hydroxyapatite formation was examined with XRD. The strengths of specimens with 15% and 20% chitosan lactate were 12.4 Mpa and 15.7 Mpa respectively about 3 times higher than 4.9 Mpa for 0% chitosan lactate. Compared with CPC without chitosan lactate, the work of fracture was increased by about ten times.

The changes in the elastic modulus were relatively small, with the elastic modulus at 20% chitosan lactate significantly higher than those 10%, 5% and 2%. For the CPC-chitosan lactate specimens at a lower powder : liquid ratio of 1, CPC with 0% chitosan lactate failed in a brittle manner. CPC with 5% chitosan lactate failed noncatastrophically. The strain was increased from about 0.2% for CPC with 0% chitosan lactate to 15.8% for specimens containing 15 % chitosan lactate.The load-displacement curves for specimens with 0%, 5% and 15% chitosan lactate can be seen in Figure 3.12.

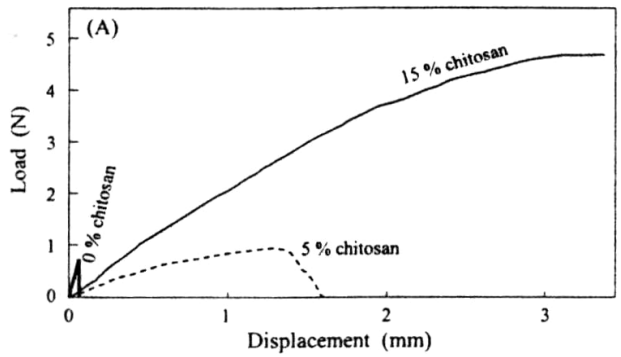

Figure 3.12 Load displacement curves of calcium phosphatecement-chitosan lactate composites [33].

The work of fracture was increased from 1.3J/m^2 to 860 J/m^2 due to chitosan lactate. The elastic moduli at 5% and 20% chitosan lactate were significantly lower than that without chitosan lactate. The SEM analysis showed that most of the surfaces were smooth and crack-free (at 10 % chitosan lactate, powder to liquid ratio:1) and rarely were microcracks observed. In more brittle specimens such microcracks would have propagated catastrophically through entire specimen. In contrast the crack observed appeared arrested. The XRD analysis showed that there was CPC conversion to HA at 0% and 2% chitosan lactate CPCs after 1 day's immersion to physiological solution.

Wang et al. [20] investigated the compressive strengths and Young's modulus of two types of calcium phosphate cement formulations after settings and the effect of phosphorylated-chitosan. CPC containing P-chitosan, DCPD, MCPM $Na(OH)_2$ and CaO were prepared. The infrared spectra of P-chitosan showed that hydroxyl groups in chitosan were phosphorylated. The characterization of P-chitosan was done by P-NMR spectra and gel permeation chromatograhy (GPC). The cements containing MCPM and

CaO were referred as CPC-I and those containing DCPD and $Ca(OH)_2$ as CPC-II. The ones with P-chitosan were P-CPC-I and P-CPC-II. Both four kinds resulted with hydroxyapatite as final product but their setting times were different and some contained intermediate products at the end of 24h. The compressive strengths and Young's moduli were obviously improved by addition of P-chitosan into the liquid phase of each CPC system while the setting time was slightly prolonged. For a P-chitosan concentration in the liquid phase (0-2% wt) for PCPC-I and 0-10% for PCPC-II, the compressive strengths and modulus of CPCs (especially) PCPC-II increased greatly with increasing P-chitosan. After a certain limit this addition caused a decline in strength and decrease in setting time but strain was not effected much. Because there were lots of phosphorylated groups on one P-chitosan chain the formed HA crystalline particles could be interlocked by polymeric chains. This was why the mechanical properties of the cements were improved by addition of P-chitosan. The highest compressive strength reached was 12.49 Mpa and Young's modulus was 436.99 Mpa. Compared with CPCs, PCPCs seemed much denser owing to their construction gathered from small crystalline particles.

Yokoyama et al. [32] studied on the effects of citric acid and chitosan content on the mechanical properties and biocompatibility of a calcium phosphate cement prepared from α-TCP, TeTCP, citric acid, chitosan and glucose. When incubated in physiological saline, cements were transferred to hydroxyapatite in 3 and 6 weeks. The compressive strengths were 15.6 and 20.7 Mpa in 45% citric acid (liquid phase), 20% citric acid (liquid phase), respectively with a powder liquid ratio of 2.0. The chewing gum property that the cement has is thought to be due to addition of chitosan to the liquid component. The researches state that citric acid added to the liquid component influences both the mechanical properties and biocompatibility of the cement.

Varma et al. [34] studied on porous calcium phosphate coating over phosphorylated chitosan films. They investigated the effect of soaking P-chitosan films in $Ca(OH)_2$ solution on calcium phosphate growth over the films upon immersion in SBF. The EDX, XRD and micro-FTIR analysis showed that there were no calcium phosphate formation over the films which were not treated with $Ca(OH)_2$. The treatment that produces calcium phosphate coating over film surface that helps in creating local supersaturation conditions for the precipitation of HAP during the SBF immersion stage.

Zhao et al. [3] studied on preparation of a biodegradable hydroxyapatite/chitosan-gelatin network composite of similar composition to that of normal human bone by phase separation method. Changing the solid content and the compositional variables of the original mixtures, the porosities and densities of the composites were controlled. By using scaffolds of 90.6% porosity, the proliferation and functions of the cells in this three dimensional microenvironment by culturing neonatal rat calderia osteoblasts, Figure 3.13. Histological staining and SEM observation indicated that the osteoblasts attached to and proliferated on the scaffolds. SEM analysis also showed that HA particles are embedded in the complex chitosan-gelatin network matrix and a compact block structure of pore wall is formed,Figure 3.14. Even 70% mass content of HA particles cannot be distinguished because they are covered by organic network.

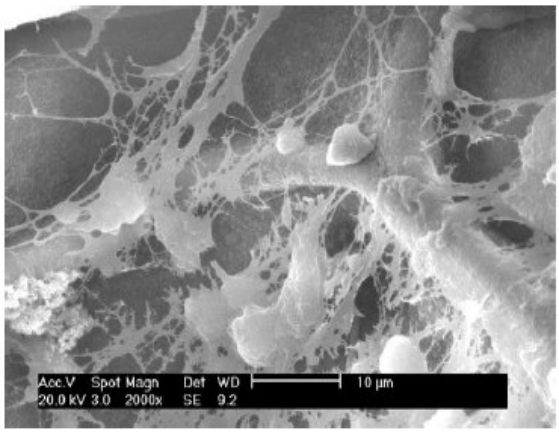

Figure 3.13 SEM micrograph of osteoblast scaffold construct [3].

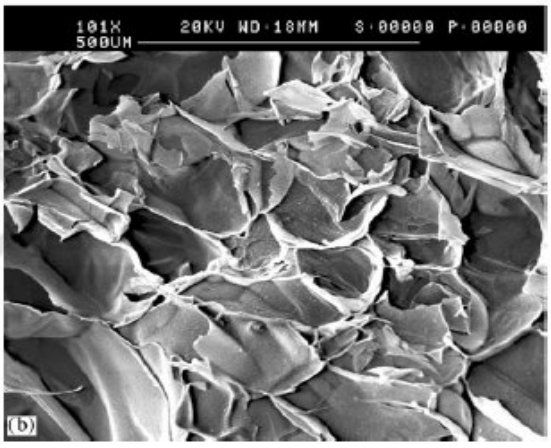

Figure 3.14 SEM micrograph of HA/CS-Gel scaffold with 30 wt% HA [3].

Ang et al. [4] prepared three dimensional chitosan-hydroxyapatite scaffolds by phase separation method and investigated the biocompatibility of the composite. SEM images showed that there was good cell attachment and proliferation in the third week of in vitro culture as shown in Figure 3.15.

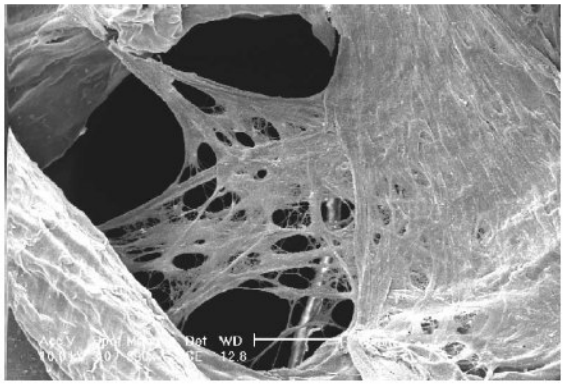

Figure 3.15. SEM image of the cells on 40%HA scaffold.

Zhang et al. [23,31] investigated microstructural and mechanical properties of β-tricalcium phosphate and calcium phosphate invert glass reinforced chitosan composites prepared by phase separation method. The pure chitosan scaffolds appeared to be macroporous and an interconnected open pore microstructure with pore size around 100μm was achieved. Pore structure of composite scaffold with low β-TCP content was similar to pure chitosan scaffold and morphology was uniform. The pore diameter decreased by increasing β-TCP content. Increasing fraction of β-TCP caused a higher density of the particles within the scaffolds and cell walls. Pure chitosan scaffolds were soft, spongy and very flexible. With the addition of β-TCP both compressive modulus and yield strength were greatly improved. The compressive modulus increased from 0.967 to 2.191Mpa and yield strength from 1.109 to 1.208 Mpa respectively with increase of β-TCP content to 50%.

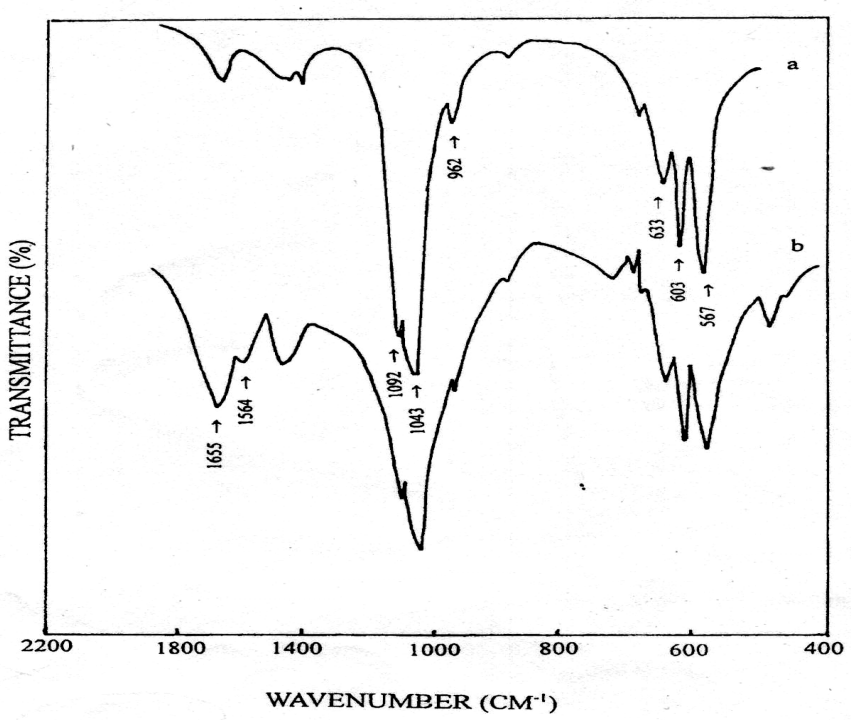

Figure 3.16 IR spectra of (a) HA and (b) HA/polymer composite [6].

Yin et al. [6] investigated the morphology, change in the component crystal, formation of the network in the presence of HA of the HA/chitosan-gelatin network composite prepared by sol-gel method. When the IR spectra of HA and HA/polymer composite is considered in the second case some new bands were observed as shown in Figure3.16. The researches claim that these new peaks suggest formation of a cross-linked chitosan/gelatin hybrid polymer network in the composite. So it was concluded that HA does not disturb the formation of the network. The observers pointed that the network not only served as a matrix to the HA powder but also binding them together to form composite. The XRD analysis showed that HA content makes the crystallinity of the polymer matrix lower than before but results indicate that organic matrix of the composite has no significant influence on the crystallinity of HA and XRD pattern of composite with 70% HA content practically is the same as that of pure HA as shown in Figure 3.17. Pulverized HA was also used and this improved the mechanical properties of the composite. The impact strength (kj/m^2) and bending strength (Mpa) of composites prepared with pure HA were 8.38 and 27 respectively and the ones prepared with pulverized HA were 11.96 and 32 respectively. When the SEM micrographs the fracture surfaces were considered, increasing HA content made surface rougher unlike the smooth surface of 0% HA content.

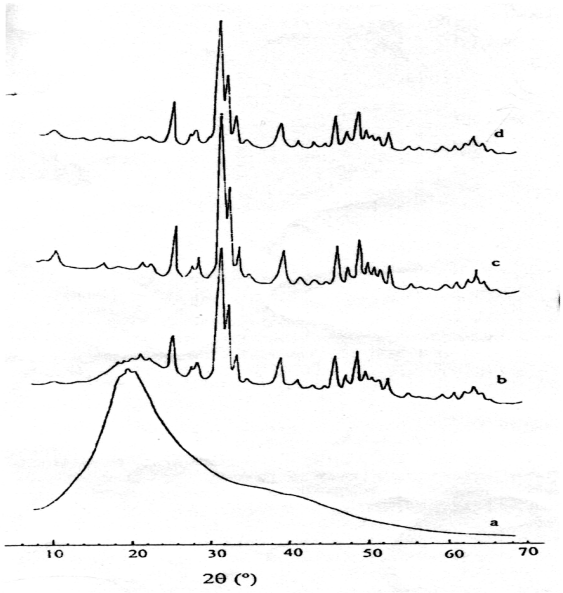

Figure 3.17 XRD patterns of composite with HA content in the range of 0-100 wt% (a) 0wt%, (b) 30wt%, (c) 70wt%, (d)100wt% [6].

Ito et al. [5] studied on the effect of HA content on physical properties and connective tissue reactions to a chitosan/HA composite membrane prepared by sol-gel method. The shrinkage of both freshly set membranes and rehydrated dry membranes decreased with an increase in amount of HA. The least shrinkage was observed at 5/11 HA/chitosan level. The tensile strength of rehydrated dry membranes was greater than that of freshly set membranes. With freshly set membranes the highest tensile strength was obtained with HA/chitosan ratio of 4/11 (20gf/mm^2). Hardness and tensile strength increased with increasing HA content. Generally rehydrated specimens had better mechanical properties.

Yamaguchi et al. [8] observed the effect of compositional variables on the microstucture of chitosan/hydroxyapatite nanocomposites prepared by a co-precipitation method. The XRD analysis showed that using acetic acid and lactic acid HAP in the composite have same crystal structure with pure HAP but when malic acid and citric acid were used no peak of HA was observed which was indicating that calcium phosphate in the composites containing malic acid and citric acid was amorphous

Yamaguchi et al. [10] investigated the effect of citric acid addition on compressive strength and Young's Modulus of chitosan/hydroxyapatite composite. The microstructure and particle size distribution of the specimens were determined using

TEM (transmission electron miccroscopy). The average molecular weight of chitosan powder is determined using gel permeation chromatography and its deacetylation is estimated from H-NMR measurements. The precipitate composed of HA/chitosan and citric acid were evaluated by measurements of precipitate size distribution and ζ-potential. The microstructure of the chitosan/hydroxyapatite composites were observed with TEM and the crystal structure of calcium phosphate in the freeze-dried precipitate was determined with X-Ray diffraction. Thermo gravimetric and differential thermal analysis (TG-DTA) were done by using Al_2O_3 powder as reference. The compressive strength of the composite was measured using a universal testing machine. Young's Modulus was determined from the initial linear elastic part in the stress-strain curves. The ζ-potential of the composite increased with increasing chitosan content. It was largely negative at low chitosan content. The isoelectric point (i.e. ζ = 0mV) was located at 25wt% chitosan. Average particle size has a maximum value at 25%wt chitosan so it was suggested that size of precipitates was affected by the surface charge with an electrostatic repulsive force being minimal around isoelectric point. According to the TEM images with increasing chitosan content HA crystallites align more orderly. At 20 wt% chitosan, composite is most homogeneous. Figure 3.18 gives the schematic relationship between particle size and ζ-potential. Citric acid enlarged the precipitate size of chitosan/HA composite and affected chitosan rather than HA. The compressive modulus of the composites were improved by adding a small amount (3wt%) of citric acid. A compressive strength value of about 10 MPa and Young's Modulus value of about 140 MPa were reached.

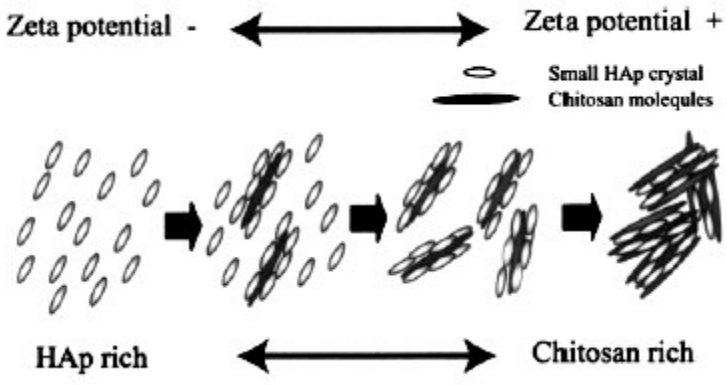

Figure 3.18 Relationship between particle size and ζ-potential [10].

Hu et al. [11] produced chitosan/hydroxyapatite nanocomposite rods by hybridization and investigated mechanical properties. The XRD analyses showed that

the composite contained hydroxyapatite. According to the TEM results nano sized hydroxyapatite particles were well dispersed in chitosan matrix homogeneously. Bending strength and modulus of the composites are 86 MPa and 3.4 GPa respectively.

Takagi et al. [12] investigated the mechanical properties of calcium phosphate cement-chitosan composites. According to the compressive strength analysis samples with powder/liquid ratio of 4 showed higher compressive strength than other specimens with a strength value of 66.1 MPa. Flexural tensile strength results showed that calcium phosphate cement composite with same powder liquid ratio of 4 had best values.

Hockin et al. [13] investigated the synergistic reinforcement effect of mesh and chitosan on calcium phosphate cement. A standard three-point flexural test was done to the specimens. Flexural strength, elastic modulus and WOF were determined. Specimen surfaces were examined by using SEM. According to the SEM images cracks on surfaces of CPC+mesh and CPC+chitosan+mesh sustained without catastrophic fracture unlike CPC control spcimen which which fractured catastrophically during tree point flexure test. Numerous cracks were seen on the SEM images of CPC+mesh although the specimens were still whole due to mesh reinforcement. CPC+chitosan+mesh composite had few cracks after extensive deformation. The mechanical test results indicated that both chitosan and mesh improved flexural strength when used separately. When they were used at the same time improvement is better with a flexural value of about 43 MPa. Using chitosan had no effect on work of fracture but mesh improved work of fracture. When both chitosan and mesh are used the improvement is about twice with a value of about 9 kJ/m^2. When used together chitosan and mesh improved E from about 2.2 GPa to 2.65 GPa.

CHAPTER 4

EXPERIMENTAL

4.1 Materials

Polymeric material used in this study was low molecular weight chitosan purchased from Sigma-Aldrich. Three different types of calcium phosphate were used; commercial hydroxyapatite, commercial beta-tricalcium phosphate and hydroxyapatite whisker prepared in the laboratory using commercial hydroxyapatite with a method previously reported [35]. The whiskers were produced by preparing a K_2SO_4 and HA mixture which contained 25 wt% of HA. The mixture were then sintered at 1100^oC for 1hr. After cooling to room temperature HA whiskers were handled by washing out of K_2SO_4 Commercial sponge, commercial starch as a porosifier and paraffin produced by Baykim Kimya Sanayi with the code of Snow-I as a binder were used. Commercial hydroxyapatite and tricalcium phosphate were purchased from Sigma-Aldrich and Fluka respectively. Acetic acid (glacial), purchased from Merck, was used as a solvent after dilution by deionised water, for the preparation of the polymer solution.

Table 4.1 Properties of Materials Used in This Study

	Hydroxyapatite	β-TCP	Acetic Acid	Chitosan
Chemical Formula	$Ca_{10}(PO_4)_6(OH)_2$	$Ca_3(PO_4)_2$	CH_3COOH	---
Molecular weight (g/mol)	1004.6	308.24	60.05	---
Density (g/cm^3)	3.14	3.04	1.05	1.51
Purity	---	---	100%	---

4.2 Methods

Experimental methods can be divided into two main groups: the production of porous hydroxyapatite and the production of chitosan/calcium phosphate composites. Three different methods were used for the production of porous ceramics.

4.2.1 Polymeric Sponge Method for Porous HA Production

First set of porous ceramic samples was prepared by polymeric sponge method and coded beginning from PP1 to PP23 where first P denoted "porous", second P denoted "polymeric sponge" and numbers from 1 to 11 denoted sample number. The information about samples are given in Table 4.2.

Table 4.2 Properties of porous ceramics prepared by polymeric sponge method.

SAMPLE	THERMAL CYCLE	SLURRY	
		%HA(vol)	%HA(wt)
PP1	1	22	47
PP2	1	23	48
PP3	2	21	46
PP4	2	22	47
PP5	2	23	48
PP6	2	24	50
PP7	3	23	48
PP8	3	24	50
PP9	5	22	47
PP10	5	23	48
PP11	5	24	50

Hydroxyapatite slurries having different powder vol% were prepared by using deionized water. The slurries were ultrasonicated using ultrasonic bath for 20 min. Commercial sponges were cut into cubic and rectangular prism shapes with desired sizes. The sponges were immersed into the slurries. Impregnation was done by using a pens. Then the ceramic coated polymeric sponges were air dried for 2-3 days. 5 different thermal cycles consisting of burning out of the polymer and sintering of the ceramic were applied to the bodies. The thermal cycles chosen similar to the previous work published in literature are given in Figure 4.1.

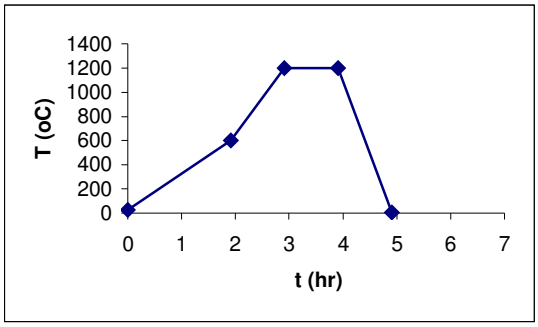

a) Thermal Cycle1.

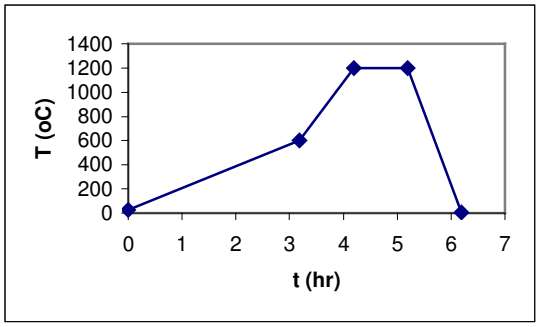

b) Thermal Cycle2.

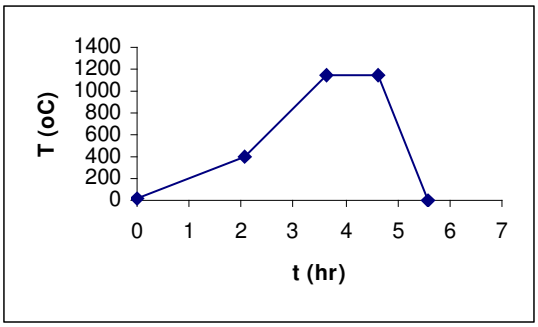

c) Thermal Cycle3

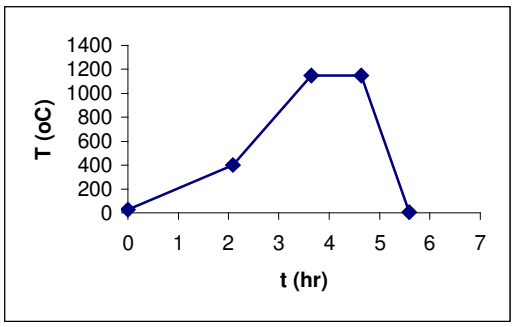

d) Thermal Cycle4

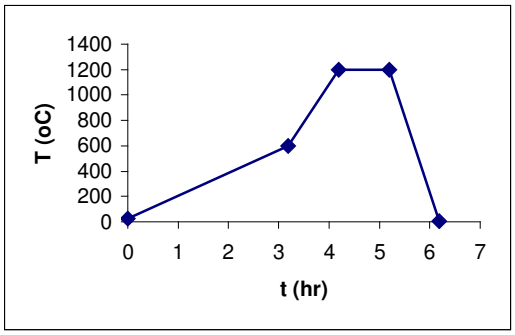

e) Thermal Cycle5

Figure4.1 Thermal Cycles Applied at Porous HA Preparation.

4.2.2 Dry Pressing Method for Porous HA Production

Second set of samples were prepared by dry pressing method and coded as PDP1 to PDP12 where P denoted “porous”, DP denoted “dry pressing” and numbers 1-5 denoted the number of samples. The information on samples are given in Table 4.3. Commercial starch were used as a porosifier. Starch and HA powder mixtures were prepared and paraffin was added as a binder. The powder mixture were die-pressed with different amounts under 26.4MPa pressure in cylindrical shape by using a 1cm diameter

die. Then same thermal cycles with the previous method except for thermal cycle 1 were applied to the bodies for burning out of paraffin and starch and sintering of hydroxyapatite.

Table 4.3 Properties of porous ceramics prepared by dry pressing method.

SAMPLE	CYCLE	WEIGHT%		
		HA	STARCH	WAX
PDP1	2	43	43	14
PDP2	3	49	36	15
PDP3	3	44	44	12
PDP4	4	49	36	15
PDP5	4	44	44	12

4.2.3 Dough Method for Porous HA Production

Third method used in the preparation of porous ceramic was the dough method. The samples were coded as PD1 to PD6 where P denoted “porous”, D denoted “dough” and numbers 1 and 2 denoted different samples. The information about the samples are given in Table 4.4. Starch, HA and water were mixed by using a spatula to prepare a dough. The dough was cut into desired shapes by using a knife. After air drying 3 days heat treatment was applied to burn off starch and to sinter HA. The fourth thermal cycles given in Figure 4.1 was used.

Table 4.4 Properties of porous ceramics prepared by dough method.

SAMPLE	CYCLE	WEIGHT %		
		HA	STARCH	WATER
PD1	4	28	44	28
PD2	4	29	42	29

Three different types of composites were prepared by freeze drying method by using hydroxyapatite, hydroxyapatite-β-tricalciumphosphate mixture (1/1 wt ratio) and hydroxyapatite whisker as ceramic and chitosan as polymer.

4.2.4 HA/Chitosan Composites

The chitosan/hydroxyapatite composites were coded as CH10 to CH100 where C denoted “composite”, H denoted “hydroxyapatite” and the numbers denoted chitosan wt%. In Table 4.5 wt% of composites are given. Acetic acid was used as the solvent to prepare polymer solution. By using 3.3 v/v % acetic acid solution, chitosan was dissolved by using magnetic stirrer for 3h and the polymer solution was left overnight in romm temperature to remove the air bubbles trapped in the viscous solution. Then suitable amount of hydroxyapatite was dispersed in deionised water by 30 min ultrasonication. Ultrasonication was necessary to avoid agglomeration of ceramic powder and to achieve proper dispersion. Hydroxyapatite in water was mixed with polymer solution under agitation. The chitosan and the deionized water amount were arranged so as to achieve 3g of chitosan in 100 ml of solution which contained 2ml acetic acid and 98ml water. In all the samples chitosan amount was fixed and hydroxyapatite amount was changed. The homogeneously mixed solution is poured in syrnge used as cylindrical moulds and immediately taken to deep freeze at –18 ^{o}C. After 48h freezing the samples were quickly taken to freeze drier and 35h freeze dried. Freeze drier is shown in Figure 4.2.

Table 4.5 wt% of hydroxyapatite and chitosan in HA/Chitosan composites.

SAMPLE	**wt %**	
	HA	**CHITOSAN**
CH100	0	100
CH80	20	80
CH60	40	60
CH50	50	50
CH40	60	40
CH35	65	35
CH30	70	30
CH20	80	20
CH10	90	10

Figure 4.2 Freeze Dryer.

The freeze dried composites were further dried at 35^{o}C for 48h. Finally the samples were cut into discs with an L/D ratio of 1 and L=D about 1cm for mechanical testing and cut in different sizes for FTIR, SEM, XRD and porosity measurements.

4.2.5 HA/ β-TCP/Chitosan Composites

The chitosan/hydroxyapatite-β-tricalciumphosphate composites were coded as CHT100 to CHT60 where C denoted “composite”, H denoted “hydroxyapatite”, T denoted "TCP" and the numbers denoted chitosan wt%. The amounts of hydroxyapatite, β-tricalciumphosphate and chitosan on wt% basis is shown in Table 4.6. The procedure was the same with chitosan hydroxyapatite composites. The only difference from the previous one was, half of the hydroxyapatite by weight was replaced by β-tricalciumphosphate.

Table 4.6 wt% of HA, β-TCP and chitosan in Chitosan/HA/ β-TCP composites.

SAMPLE	WEIGHT %		
	HA	β-TCP	CHITOSAN
CHT100	0	0	100
CHT90	5	5	90
CHT80	10	10	80
CHT70	15	15	70
CHT60	20	20	60

4.2.6 HA Whisker/Chitosan Composites

The chitosan/HA whisker composites were coded as CW30 to CW100 where C denoted "composite", W denoted "whisker" and numbers denoted chitosan wt%. The amounts of constituents of the composite can be seen in Table 4.7. Acetic acid was used as the solvent to prepare polymer solution. By using 2 v/v % acetic acid solution chitosan was dissolved by using magnetic stirrer for 3 h and the polymer solution was left overnight to remove the air bubbles trapped in the viscous solution. Then suitable amount of whisker powder was directly added to the polymer solution. These samples were similarly processed and characterized to CH samples.

Table 4.7 wt% of HA whisker and chitosan in Chitosan/HA whisker composites.

SAMPLE	WEIGHT %	
	HA WHISKER	CHITOSAN
CW100	0	100
CW80	20	80
CW60	40	60
CW50	50	50

4.3 Characterization of Composites

Particle size measurement of β-tricalciumphosphate, and hydroxyapatite which gave information on the size distribution of particles were performed in the range of 1-100μ by sedigraph (Micromeritics SediGraph 5100).

Compressive test were conducted for all the three types of calcium phosphate/chitosan composites. At least three and at most four specimens were tested for each type of sample. The test was performed with a crosshead speed of 1mm/min. The tests were handled by Testometric Universal Testing Machine. The stress strain graph, compressive modulus and collapse stress were investigated.

FTIR analysis gave information on the chemical structures of the composite, presence of chitosan and ceramic phases and gives information on the bonds of polymer composite structure also the possible bands caused by the solvent. IR spectra were taken in the range of 400 to 4000 cm^{-1} with a FTIRSchimadzu 8201 Model.

X-Ray diffraction characterization of the composites were done to gain information on the nature of the crystalline phases present in the composites. XRD spectra were taken by X-Ray Diffractometer (Philips XPERT PRO).

Scanning Electron Microscopy (SEM) was used to determine the morphology of the composites and Energy Dispersive X-Ray (EDX) analysis gave information on the elemental composition of samples (Philips XL 30S FEG).

Porosities, densities of the composites samples were determined by using Archimedes principle using SORTORIUS density measurement kit.

CHAPTER 5

RESULTS AND DISCUSSION

In this study the preparation and characterization of porous hydroxyapatite and biopolymer/bioceramic composites by using chitosan as polymer and hydroxyapatite, hydroxyapatite whisker, β-tricalciumphosphate/hydroxyapatite mixture as ceramic were investigated. The effects of processing parameters like the ceramic content in the slurry, the wax/starch/hydroxyapatite ratio, thermal cyles on the density, porosity, pore size and open pore content of porous hydroxyapatite bodies were examined and discussed. The effects of type and weight percent of calcium phosphate phases on the physical, chemical, microstructural and mechanical properties of chitosan calcium phosphate composite biomaterials were examined and discussed.

5.1 Characterization of Calcium Phosphate Powder

Commercial hydroxyapatite, hydroxyapatite whisker and β-tricalciumphosphate were characterized using different methods to examine particle size distrubution, chemical structure and crystallinity.

Particle size measurement gives information on the size distrubution of particles**.** The particle size of commercial hydroxyapatite and β-tricalciumphosphate can be seen in Figure 5.1 and Figure 5.2 respectively. As can be seen in the figures, particle size of 90% of hydroxyapatite was less than 10μ and particle size of 24% of hydroxyapatite was less then 1μ. Particle size of 90% of size of β-TCP was less than 18μ and 10% of β-TCPwas less than 1μ.

The FTIR spectra of hydroxyapatite powder is shown in Figure 5.3. Phosphate peaks can be seen at 474, 572, 601, 972 1040 and 1100 cm^{-1} [36,37]. The phosphate peaks at 572 and 601 were due to phosphate bending and the peaks at 972 1040 and 1100 were due to phosphate stretching [38]. The peaks at 633 and 3570 cm^{-1} represented OH

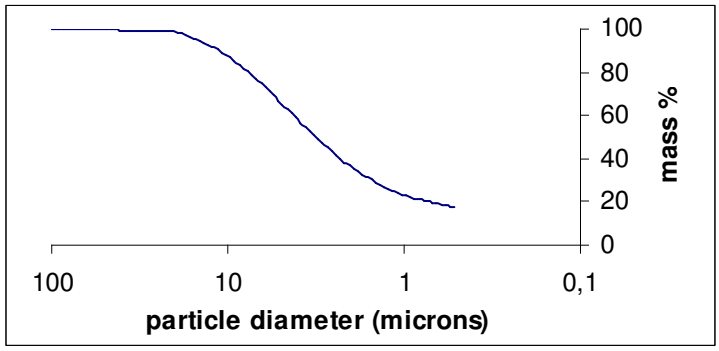

Figure 5.1 Particle Size Distribution of Hydroxyapatite.

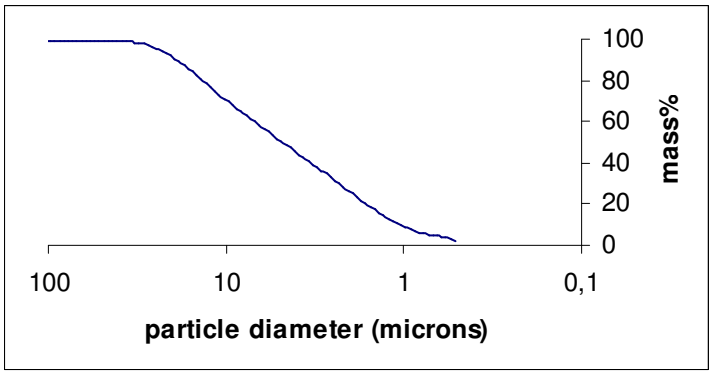

Figure 5.2. Particle Size Distribution of β-tricalciumphosphate.

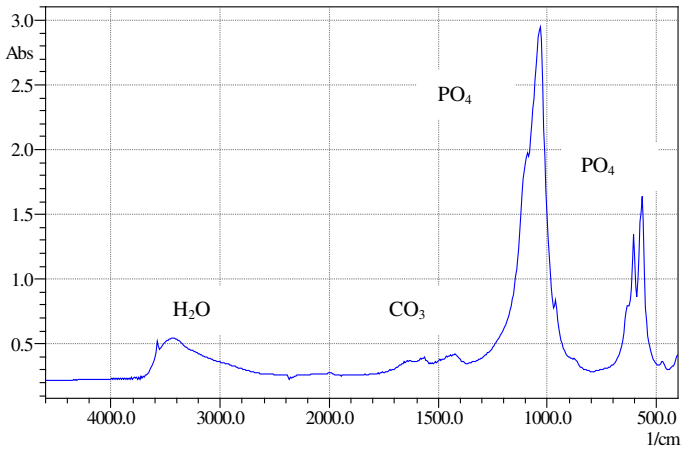

Figure 5.3 FTIR Spectra of Commercial Hydroxyapatite.

vibration. The broad peak at 3500 cm^{-1} and the peak at 1660 cm^{-1} represented the absorbed water [37,8]. Carbonate bands were observed at 870 cm^{-1} and 1430 cm^{-1} [8]. When the reported work in the literature was considered it was seen that the FTIR spectra corresponds to hydroxyapatite.

The FTIR spectra of hydroxyapatite whisker is seen in Figure 5.4. The same characteristic peaks of hydroxyapatite were seen except for the broad ones at around 3500 cm^{-1} and 1660 cm^{-1} which represented the absorbed water.

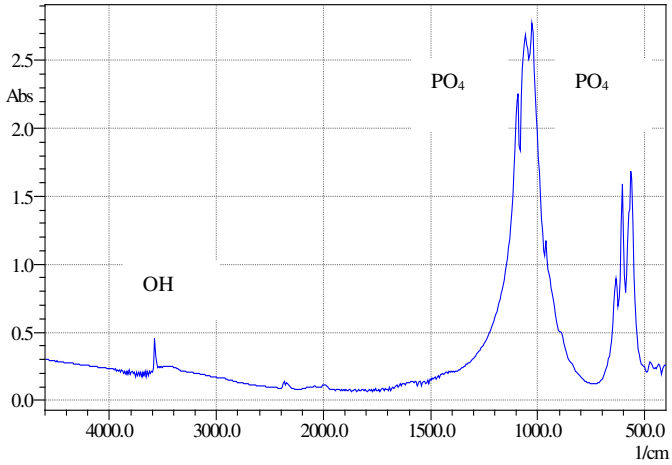

Figure 5.4 FTIR Spectra of Hydroxyapatite Whisker

The FTIR spectra of β-tricalciumphosphate is seen in Figure 5.5. The peaks seen at 540, 603, 973 and 1120 cm^{-1} were consistent with the peaks previously reported in literature [39, 40].

The XRD pattern of hydroxyapatite used in this study is seen in Figure 5.6. The peaks tabulated in Table 5.1 corresponds to characteristic peaks of hydroxyapatite previously published in literature.

Table 5.1 2θ values of XRD pattern of Hydroxyapatite and β-TCP.

Peak	2θ of HA	2θ of β-TCP
1	26	21.5
2	28	25.5
3	29	26.5
4	31	27.5
5	32.5	29.5
6	34	31
7	40	32.5
8	47	33.5
9	48	34
10	49	39
11	54	

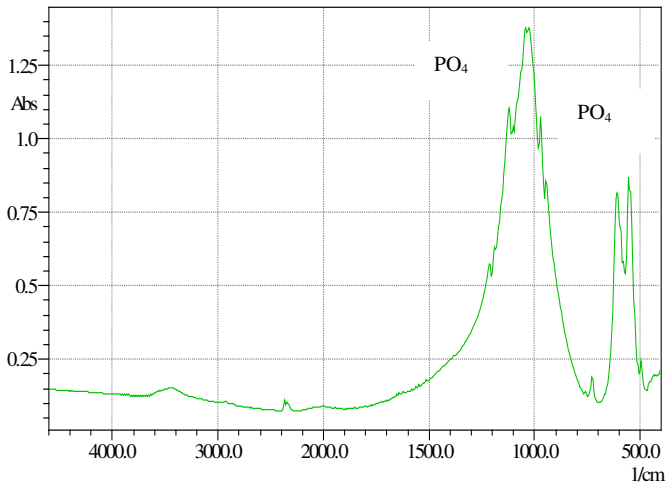

Figure 5.5 FTIR Spectra of β-tricalciumphosphate.

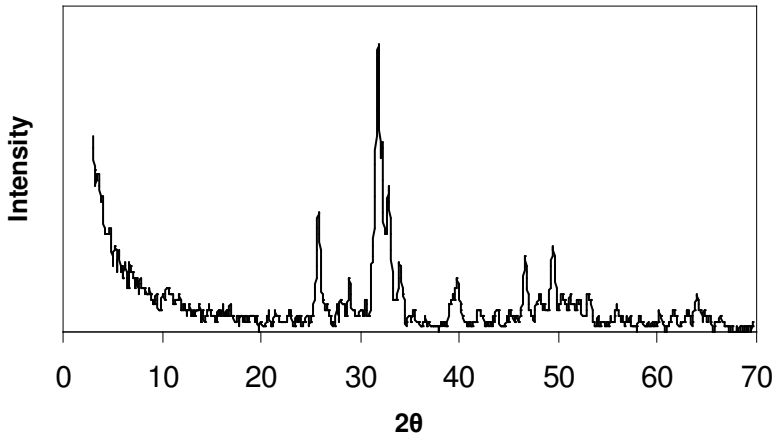

Figure 5.6 XRD Spectra of Commercial Hydroxyapatite.

XRD pattern of hydroxyapatite whisker is seen in Figure 5.7. The peaks previously mentioned for hydroxyapatite powder were also seen in HA whisker pattern. However the intensity of peak at 32.5^{o} was higher than the peak at 31^{o} unlike the same peak of hydroxyapatite powder. The intensities of peaks at 26^{o} , 40^{o} also seemed to increase when compared with the one in the XRD pattern of HA. The broadness of those peaks and many other minor peaks decreased. Regarding that the peaks at same 2θ values were observed, it can be stated that the structure is still hydroxyapatite and no

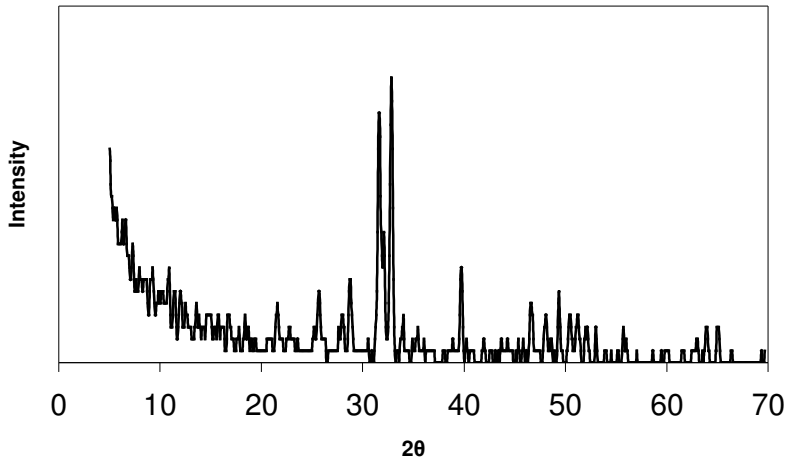

Figure 5.7 XRD Spectra of HA Whisker

new crystal phase was formed during whisker production. The increasied sharpness and intensities and decreased broadness of mentioned peaks can be explained by the increase in crystal sizes. During whisker preparation process the randomly oriented and relatively small crystals which were in the form of powders with particle size of 90% less than 10 microns formed preferentially oriented crystals with more larger sizes.

The XRD pattern of β-tricalciumphosphate used in this study is seen in Figure 5.8. The peaks Tabulated in Table 5.1corresponded to characteristic peaks previously published in literature [39,40].

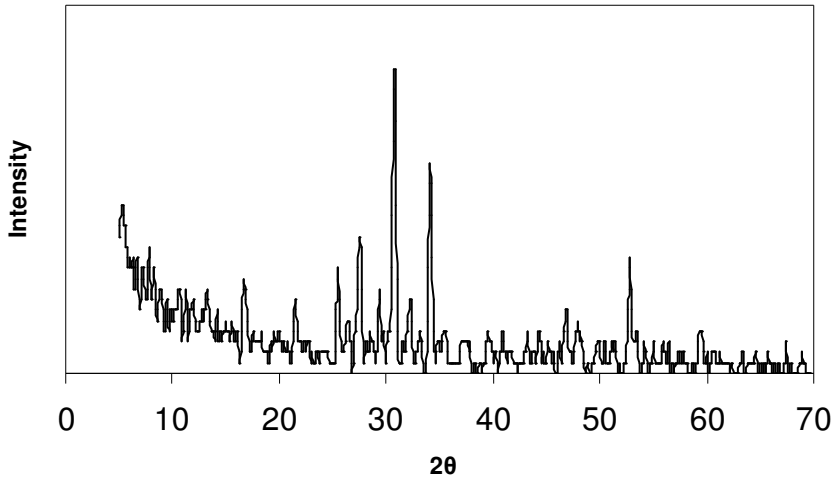

Figure 5.8 XRD Spectra of β-tricalciumphosphate.

5.2 Characterization of Porous Hydroxyapatite and Calcium phosphate/Chitosan composites

Physical properties and morphology of the porous hydroxyapatite bodies were characterized by using different methods**.** Porosity, density and open pore volume percent in total pore volume of samples prepared by polymeric sponge method are seen in Table 5.2. There was not a significant relation between %HA in slurry and porosity which was calculated by using density. Slurry containing more HA did not necessarily led to denser sponges, because some sponges were impregnated more than any other one. Two sponges soaked in the same type of slurry did not necessarily have sucked hydroxyapatite amount which would lead to same HA weight %. Some samples which

were probably less impregnated have higher porosities. The maximum porosity which meant the minimum density values were 69% and 0.95g/cm^3 respectively.

Table 5.2 Physical Properties of Porous HA prepared by polymeric sponge method.

SAMPLE	%HA(wt) in slurry	ρ (g/cm^3)	POROSITY (%)	Vop (%)
PP1	47	2,08	34	61
PP2	48	1,72	45	75
PP3	46	1,9	38	75
PP4	47	1,9	40	90
PP5	48	1,17	63	91
PP6	50	1,7	46	90
PP7	48	1,7	45	94
PP8	50	1,53	51	99
PP9	47	1,47	53	99
PP10	48	0,95	69	99
PP11	50	1,64	47	99

Physical properties of porous hydroxyapatite samples prepared by dry pressing method can be seen in Table5.3. This method enabled better control on parameters when compared with polymeric sponge method. The increase in porosity seemed to be achieved due to the decreased hydroxyapatite content and increase in starch and wax content which was an expected result. Maximum porosity reached is 65% with this method. Open pore content was significantly higher than polymeric sponge method due to employing starch as a porosifier.

Table 5.3 Physical Properties of Porous HA prepared by dry pressing method.

SAMPLE	%HA(wt)	ρ (g/cm^3)	POROSITY (%)	Vopen (%)
PDP1	43	1,17	62	98
PDP2	49	1,16	63	99
PDP3	43	1,09	65	99
PDP4	49	1,3	58	98
PDP5	43	1,11	64	99

The highest porosity values were achieved by dough method as seen in Table 5.4. This was due to employment of starch and no pressure applied on the samples during production unlike the previous method.

Table5.4 Physical Properties of Porous HA prepared by dough method.

SAMPLE	%HA(wt) in paste	ρ (g/cm^3)	POROSITY (%)	Vop (%)
PD1	28	0.87	72	95
PD2	29	0.87	72	99

The SEM images of Porous hydroxyapatite ceramics prepared by three different methods are seen through Figures 5.9 and 5.11. The homogeneously distributed interconnected pore structure which was also supported by the high porosity and high open pore content determined by Archimedes method. of polymer sponge method samples are seen in Figures 5.9a and 5.9b. The pore size distrubution seemed to be uniform due to the uniformity of the sponge used. The morphology was strongly influenced by the sponge used in the method by using other sponge types with different pore sizes it could be controlled. Pore sizes were around 300-400μ which is above the critical value of 100 μ to allow bone ingrowth [15].

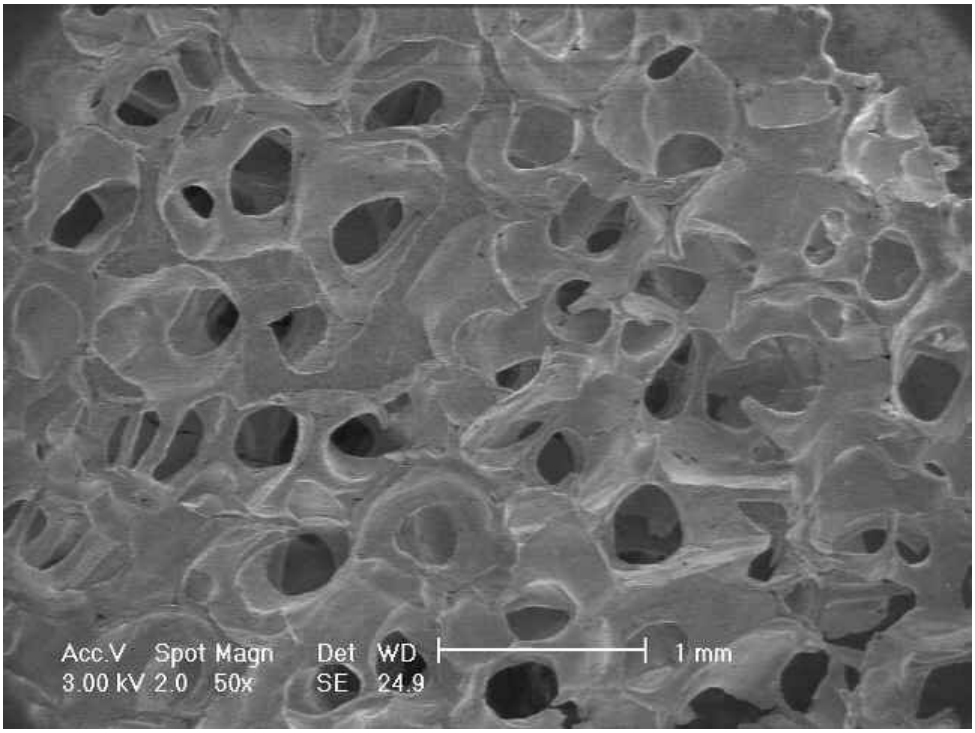

Figure 5.9 a) SEM of porous HA produced by polymeric sponge method,PP11.

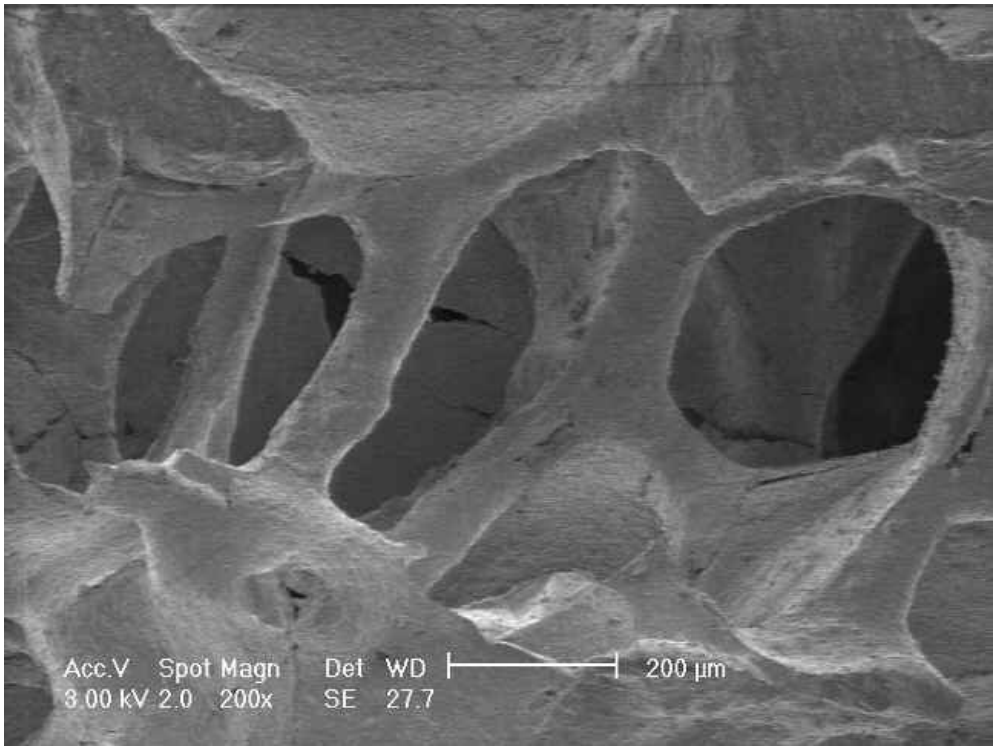

Figure 5.9 b) SEM of porous HA produced by polymeric sponge method, PP11.

In Figure 5.10a and 5.10c the homogeneous distribution of pores in the dry pressing method samples are seen. The pores seem to be interconnected and this was also supported by the high porosity and high open pore content determined by Archimedes method. The pore sizes are around 10µ due to the starch particles used as porosifier. According to Figure 5.10b hydroxyapatite seem to be sintered well and formed dense cell walls.

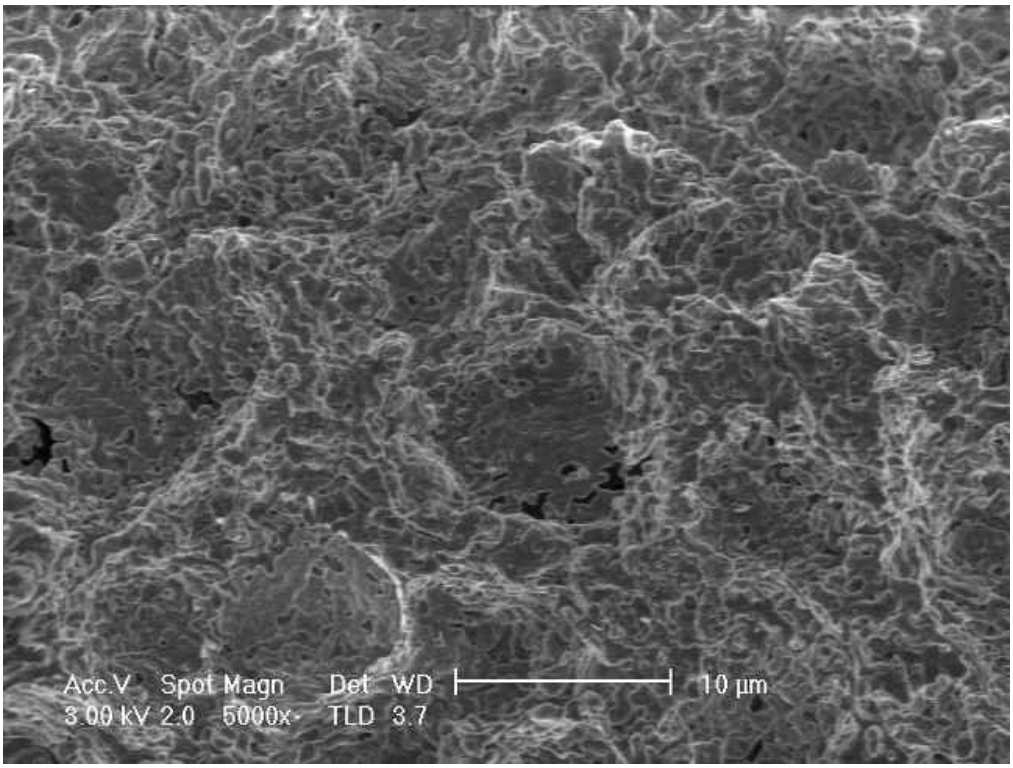

Figure 5.10 a)SEM of porous HA produced by dry pressing method, PDP5.

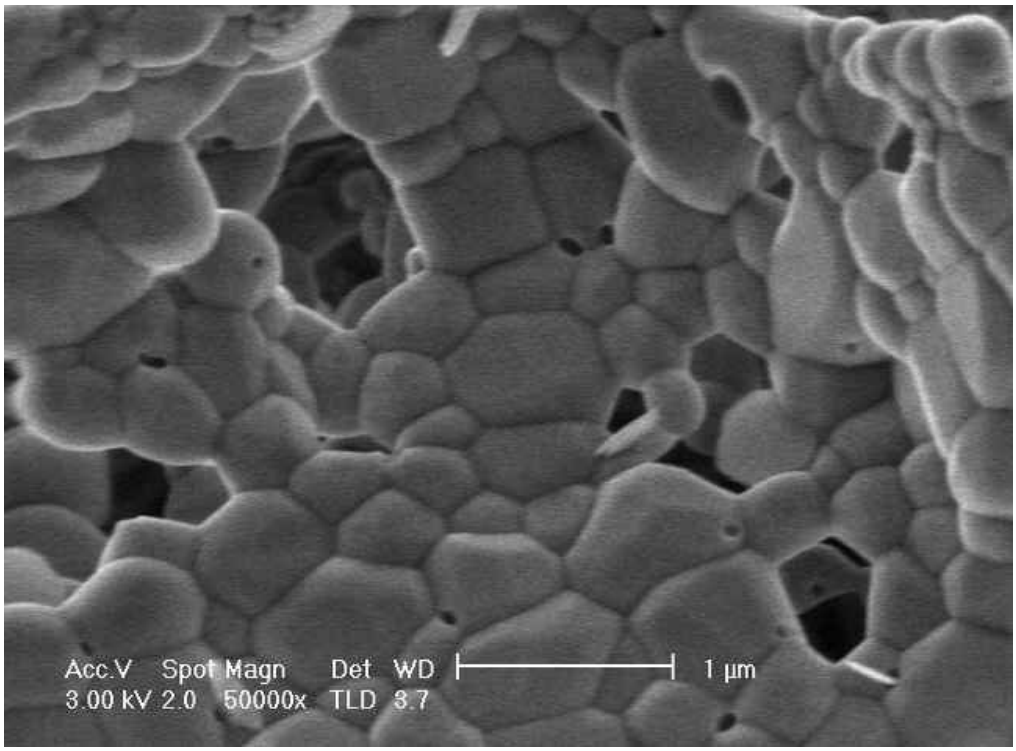

Figure 5.10 b) SEM ofporous HA produced by dry pressing method, PDP5.

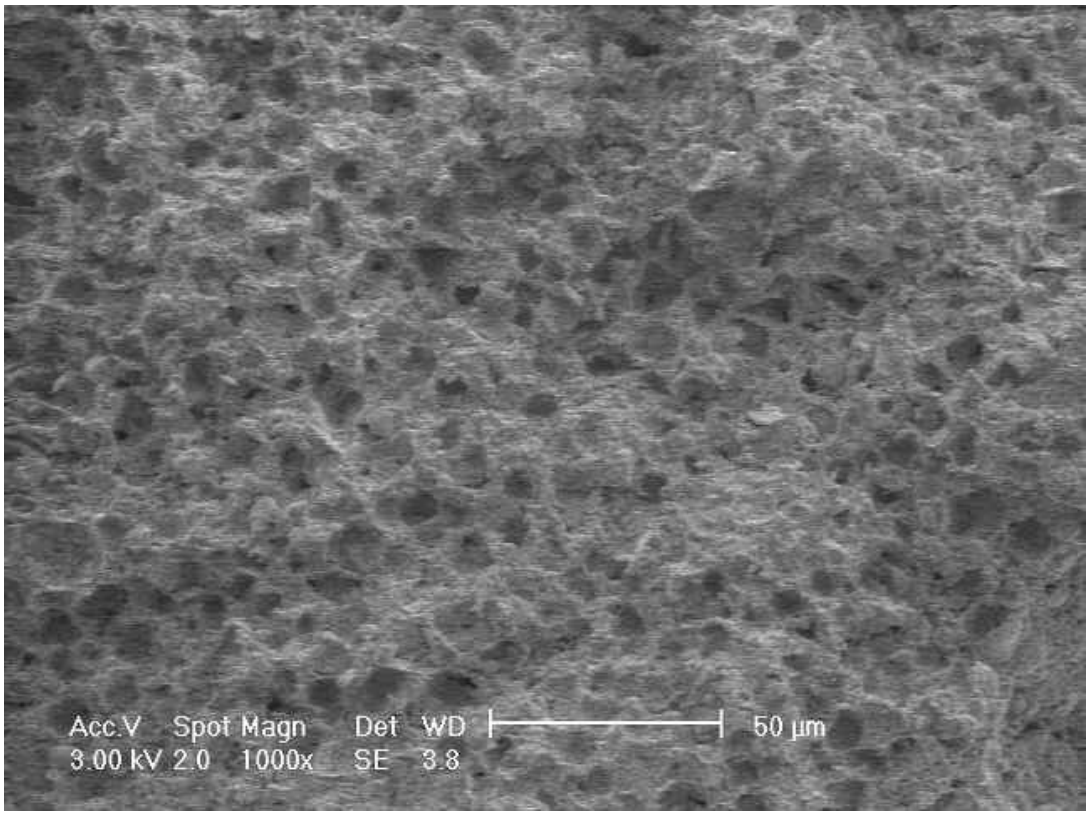

Figure5.10 c) SEM of porous HA produced by dry pressing method, PDP5

In the dough method samples, as in previous method the homogeneous distribution of pores are seen in Figure 5.11a and 5.11b. The pores seemed to be interconnected and this was also supported by the high porosity and high open pore content determined by Archimedes method. The morphology and the microstructure seemed not to change since the materials used and heat treatment applied were almost the same. The pore sizes were around 10µ due to the starch particles used as porosifier. According to Figure 5.11c hydroxyapatite seemed to be sintered well and formed dense cell walls.

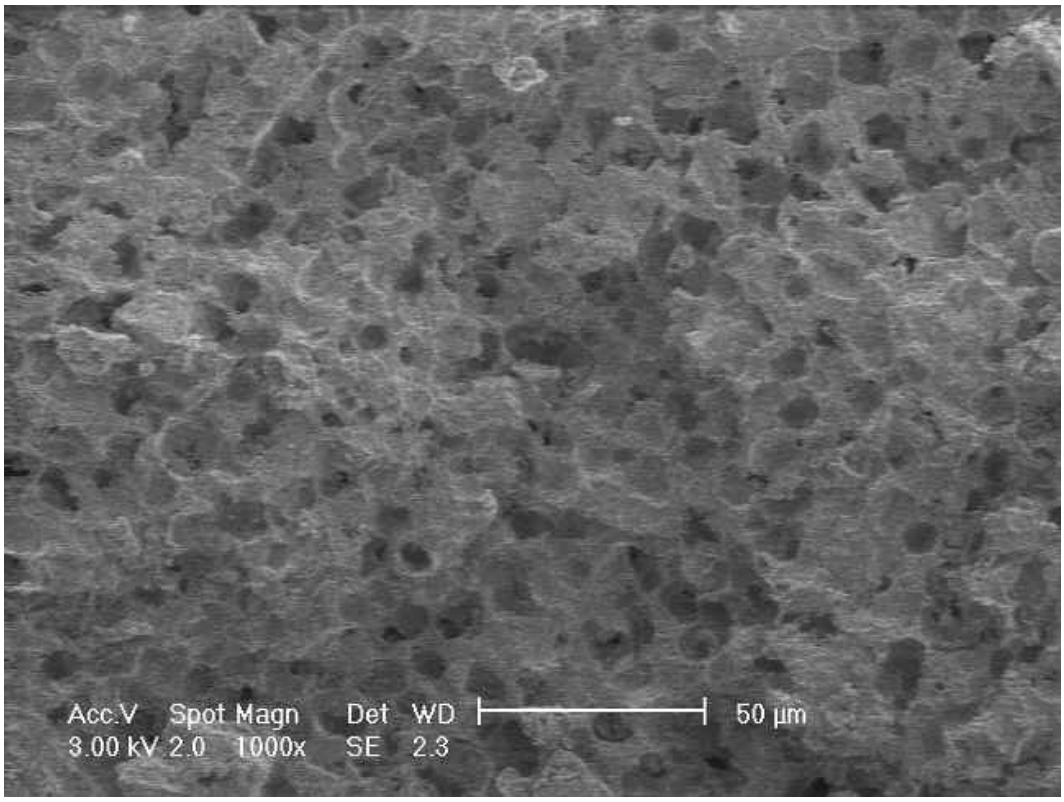

Figure5.11 a) SEM of porous HA produced by dough method, PD2.

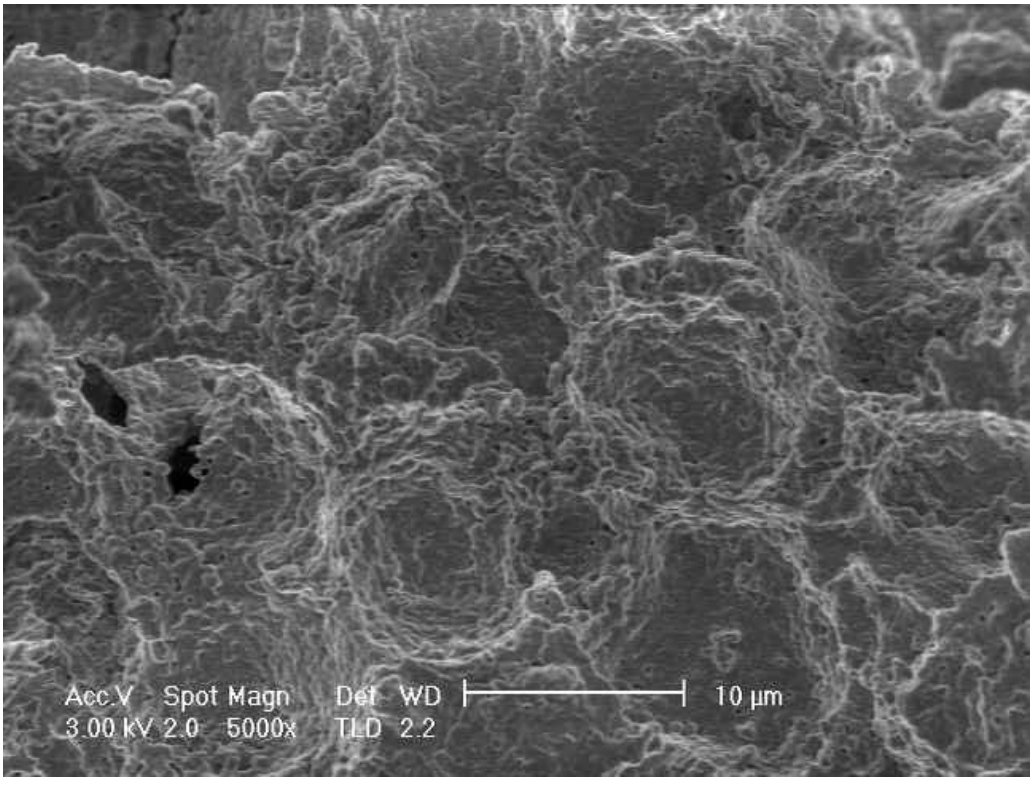

Figure5.11b) SEM of porous HA produced by dough method, PD2.

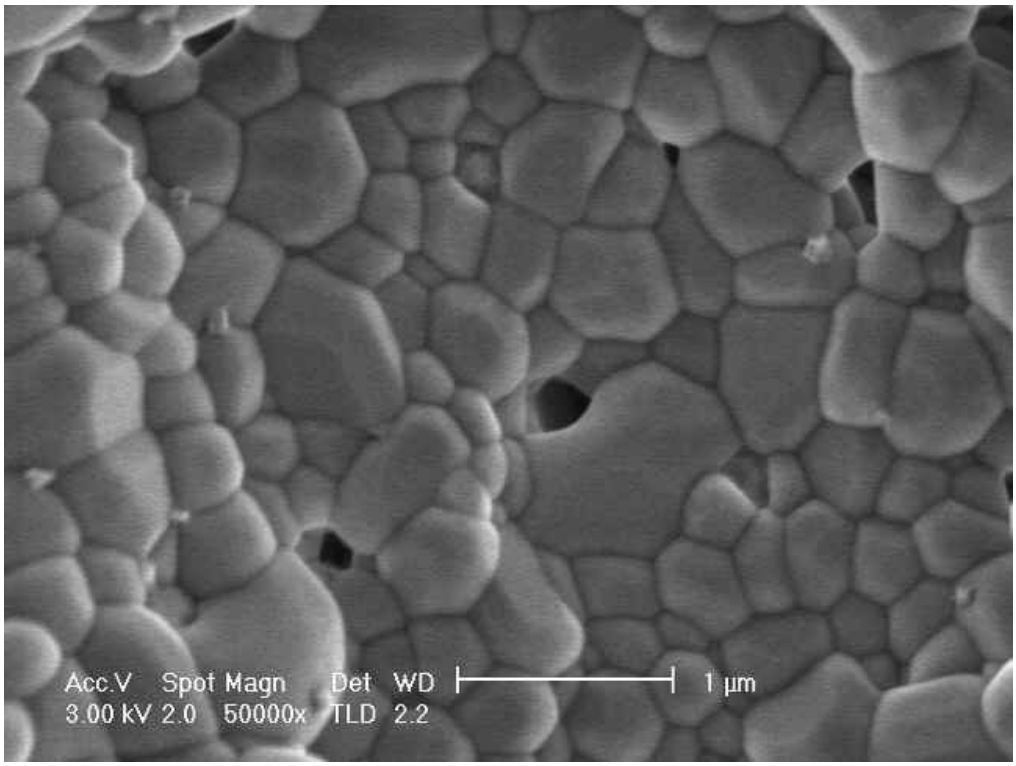

Figure5.11c) SEM of porous HA produced by dough method, PD2.

By changing ceramic type and weight percent physical, chemical, microstructural and mechanical properties of chitosan calcium phosphate composite biomaterials were characterized.

As can be seen in Table 5.5 and Figures 5.12a and 5.12b, when chitosan amount decreased and hydroxyapatite content increased the density of the composite increased which led to a decrease in porosity. CH10 had the lowest porosity and highest density while CH100 had the lowest density and highest porosity. When density and porosity changes were considered it was seen that at 90wt% of hydroxyapatite there was a decline in porosity and a big increase in density which exceeded the increasing trend of lower wt% samples. 90 weight% of HA seemed to be a critical point in the physical property change of the composite.

Table 5.5 Physical Properties of HA/Chitosan composites.

SAMPLE	ρ(g/cm^3)	POROSITY
CH100	0.053	96
CH80	0.076	94
CH60	0.069	96
CH50	0.090	94
CH40	0.094	94
CH35	0.116	94
CH30	0.13	93
CH20	0.14	93
CH10	0.29	88

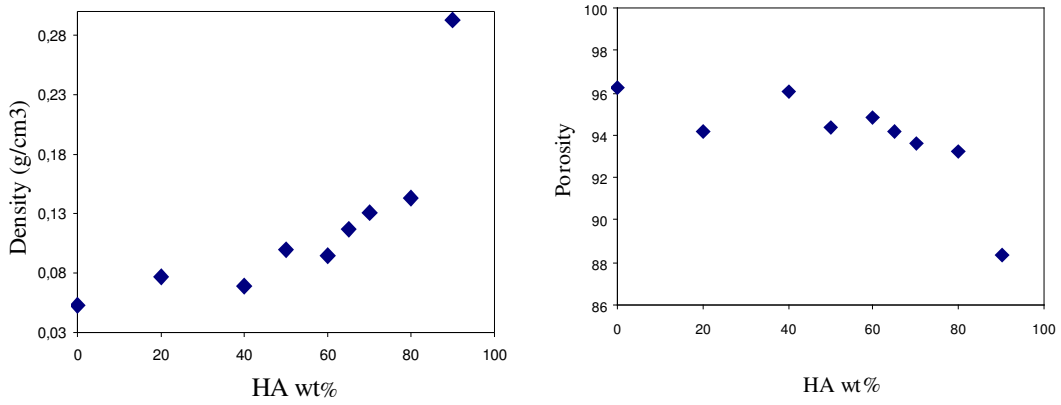

a) b)

Figure 5.12 a) Change of density due to HA wt % b) Change of porosity due to HA wt %.

As can be seen in Table 5.6 and Figures 5.13a and 5.13b, when chitosan amount decreased and β-TCP/HA content increased the density of the composite increased but a linear increase or decrease in porosity with respect to ceramic content couldnot be observed. CHT100 and CHT80 had highest porosity and CHT100 had the lowest density.

Table 5.6 Physical Properties of β-TCP/HA/Chitosan Composites.

SAMPLE	ρ(g/cm^3)	POROSITY
CHT100	0.053	96
CHT90	0.055	94
CHT80	0.056	96
CHT70	0.066	95
CHT60	0.074	95

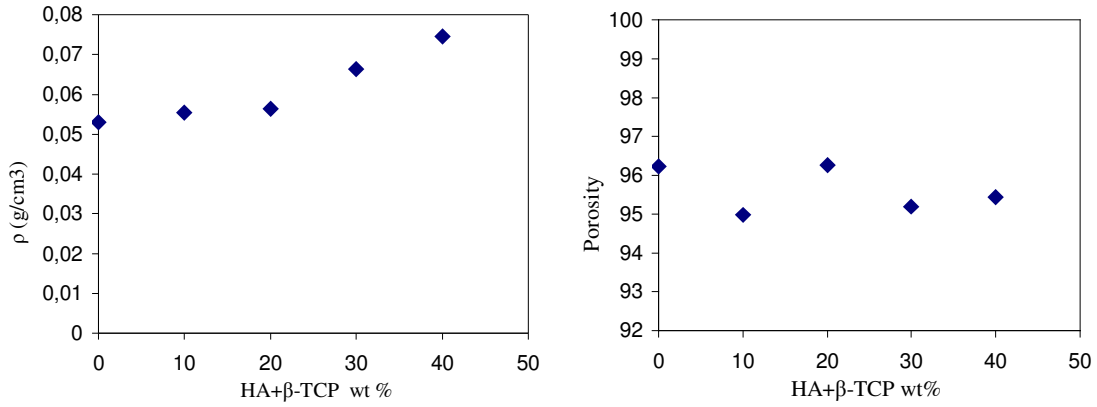

a) b)

Figure5.13a) Change of density due to HA+β-TCP wt %, b) Change of porosity due to HA+β-TCP wt %.

When hydroxyapatite whisker/chitosan composites were considered, with increasing ceramic content density increased and reached its maximum value at CW30, sample having highest whisker content. Porosity slightly decreased with increasing ceramic content

Table 5.7 Physical Properties of HA Whisker/ChitosanComposites.

SAMPLE	ρ(g/cm^3)	POROSITY
CW 100	0.053	96
CW80	0.065	95
CW60	0.066	96
CW50	0.091	94
CW40	0.093	94
CW30	0.124	94

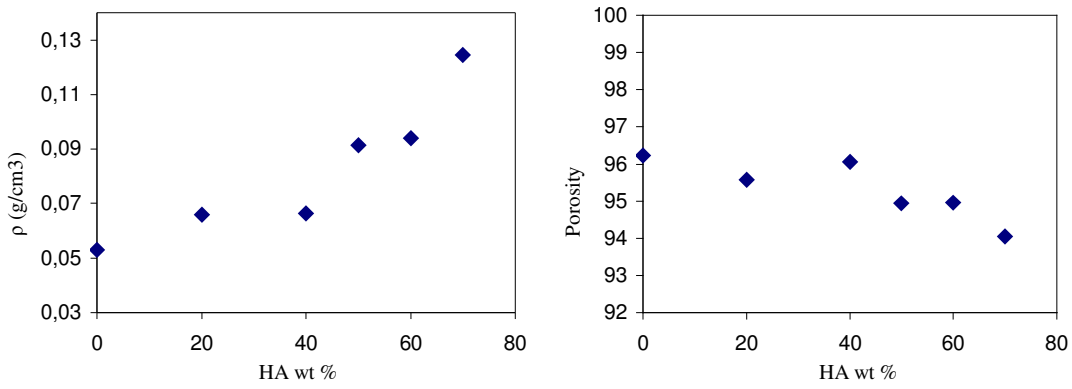

a) b)

Figure 5.14 a) Change of density due to whisker wt %, b) Change of porosity due to whisker wt %

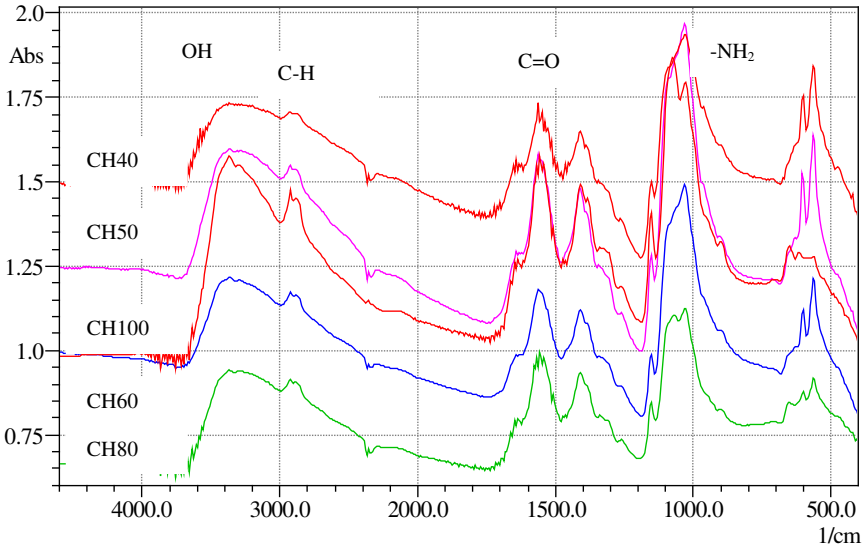

Figure 5.15 FTIR Spectra of HA/Chitosan Composites.

The FTIR spectra of the HA/Chitosan composites with chitosan weight % of 100, 80, 60, 50 and 40 can be seen in Figure 5.15. When pure chitosan (CH100) was considered the peaks at 1255 and 1040 cm^{-1} represented the free primary amino ($-NH_2$) at C_2 position of glucoseamine, a major group in chitosan [22,38]. The peaks at 1380, 1420, 2870 and 2920 cm^{-1} were due to C-H [23,38]. The bands at 280 and 2920 were

aliphatic C-H stretching [22] . There is an amide absorption band at 1565 cm^{-1} [41]. The peak at 1605 cm^{-1} was due to C=O [38]. The peak at 3420 cm^{-1} was due to -OH stretching [22]. There was an acetylated amino peak at 1650 cm^{-1} which indicated that chitosan was not fully deacetylated [22]. When the reported work in the literature was considered it was seen that the FTIR spectra corresponded to chitosan. Composites having different chitosan weight % other than 100% also seemed to have characteristic chitosan peaks and hydroxyapatite peaks previously demonstrated in Figure 5.3.

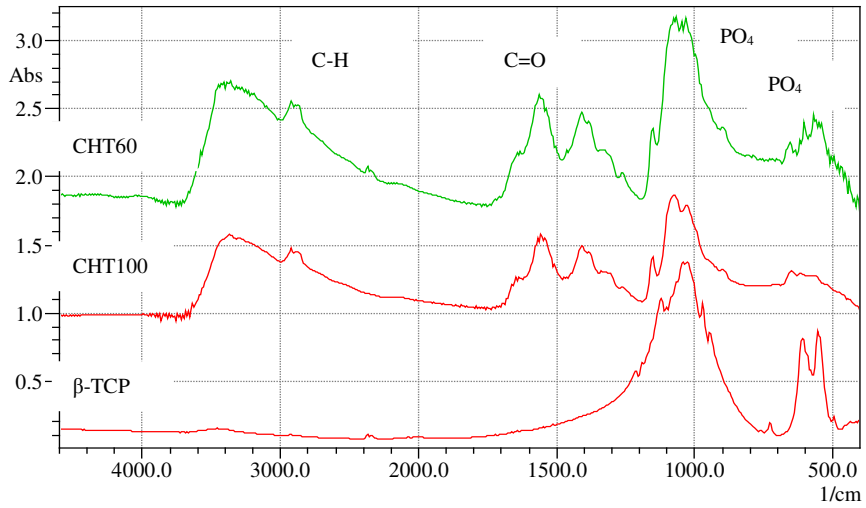

Figure5.16 FTIR Spectra of β-TCP/HA/Chitosan Composites.

The FTIR spectra of the CHT60, CHT100 and β-TCP composites can be seen in Figure 5.16. It was seen in the figure that CHT60 had the peaks of both β-TCP and chitosan.

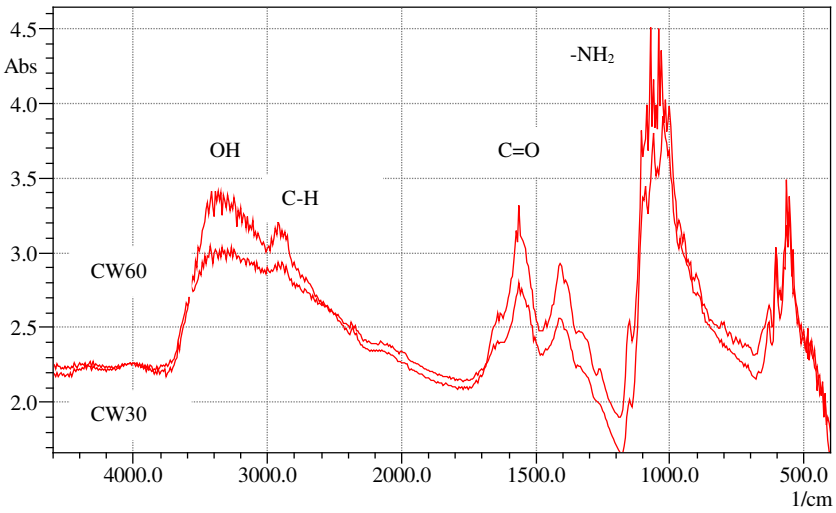

Figure 5.17 FTIR Spectra of HA Whisker/Chitosan Composites.

The FTIR spectra of the CW60, CW30 can be seen in Figure 5.17. Both samples had the original bands of whisker and chitosan and no new bands are seen. The peak at 1380 are due to C-H and amide absorption band at 1565 cm^{-1} seem to be sharper than pure chitosan.

Figure 5.18 represents the XRD patterns of the HA/Chitosan composites with different weight percents as well as pure chitosan and pure hydroxyapatite. The peak around 20^{o} was the characteristic peak of chitosan which is related to its crystallinity [8,6]. CH100 contained no HA, that is it was pure chitosan but it was dissolved in acetic acid and freeze dried. This may be the cause of widening and flattening of characteristic 20^{o} chitosan peak which showed decreasing crystallinity. When CH80 was considered chitosan peak was hardly detected while HA peaks began to be seen. When composites with lower chitosan content are considered it was seen that the peak assigned to chitosan disappeared and HA peaks became more distinguishable. In the composite with highest HA percent almost all of the HA peaks were observed. These results showed that increasing HA decreased the crystallinity of chitosan while chitosan had no preventing effect on the crystallinity of hydroxyapatite. This could be explained by the weakening of the intermolecular interactions of chitosan by HA [8,6]. There were no new peaks seen on the XRD patterns of the composites.

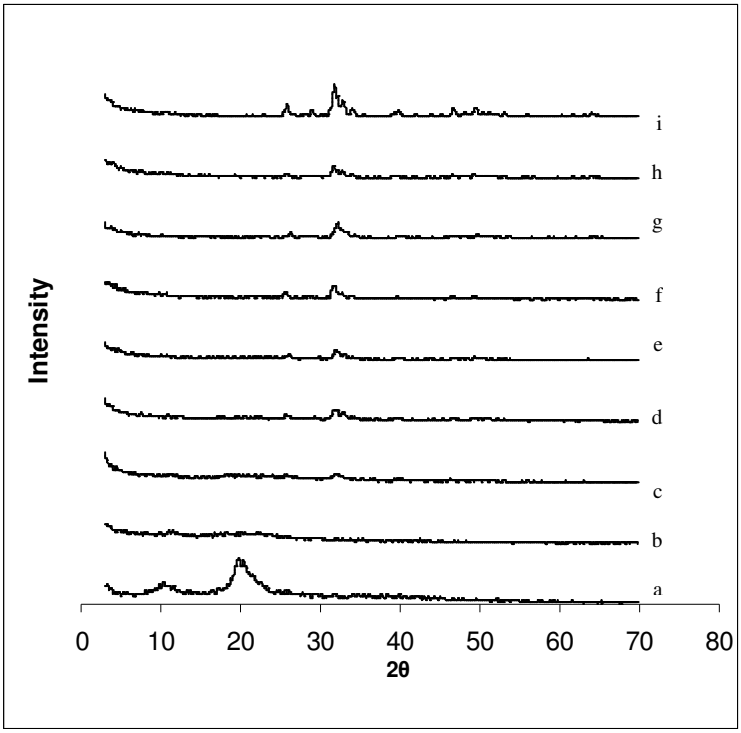

Figure5.18 XRD Spectra of HA/Chitosan Composites a) chitosan, b)CH100 c)CH80, d)CH60, e)CH50, f)CH40, g)CH20, h)CH10 and i)HA.

Figure 5.19 represents the XRD patterns of the HA Whisker/Chitosan composites with different weight percents as well as pure chitosan and pure hydroxyapatite whisker. When CW80 was considered peaks assigned to HA whisker were hardly detectable and chitosan peak disappeared. Due to increasing amount of HA whisker content, peaks assigned to it seemed to be more distinguishable. There were no new peaks other than original HA peaks.

Figure 5.20 represents the XRD patterns of the β-TCP/HA/Chitosan composites with different weight percents as well as pure chitosan, pure hydroxyapatite and pure TCP. When CHT90 and CHT80 are considered the chitosan peak is not detected anymore and no HA or TCP peaks seem to arise. When CHT70 and CHT60 are considered some peaks of HA and TCP begin to be seen but they have relatively low intensities compared with other composites mentioned before. This is not a very surprising result since CHT60 contains same wt% of HA with CH80 which also have similar XRD pattern. To have a better idea on the effect of chitosan on crystallinity of HA and TCP in the composites, samples having more ceramic ratio must be considered.

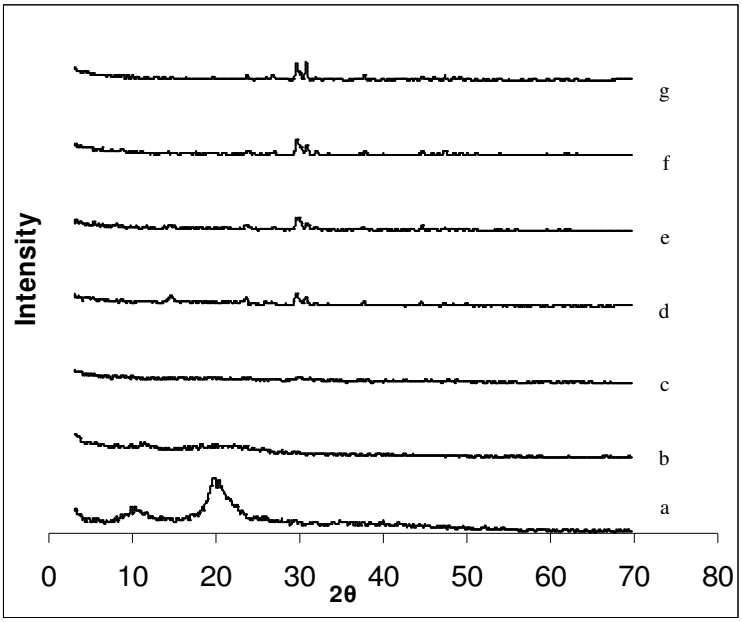

Figure5.19 XRD Spectra of HA Whisker/Chitosan Composites a)chitosan, b)CW100,c)CW80, d)CW60, e)CW50, f)CW30 and g)whisker.

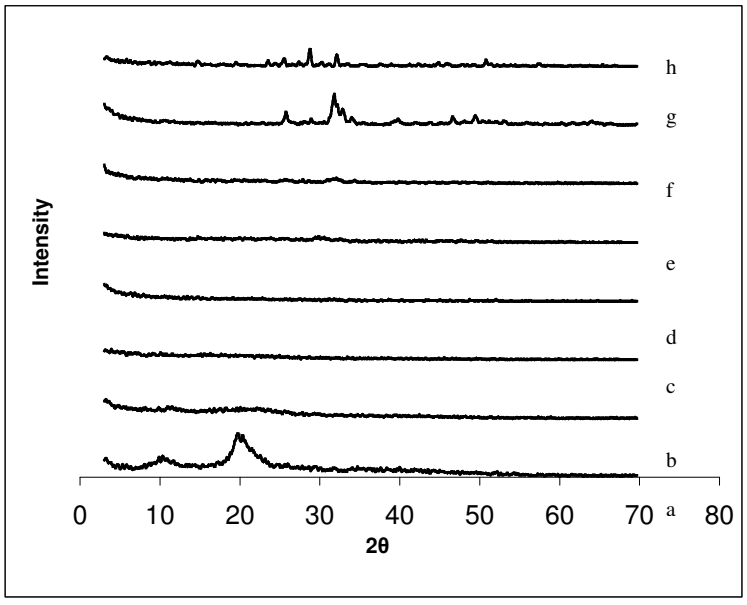

Figure 5.20 XRD Spectra of β-TCP/HA/Chiosan Composites a)chitosan, b)CHT100, c)CHT90, d)CHT80, e)CHT70, f)CHT60, g)HA and h) β-TCP.

Figure 5.21 shows the SEM images of hydroxyapatite/chitosan composites. When all the SEM images of composites are considered highly porous structure was common in all these materials. The smoothest surface at pure chitosan began to be disturbed with incorporation of hydroxyapatite gradually resulting in a rough surface which was not smooth anymore. The HA particles were embedded well in the chitosan matrix. The pore sizes were around 100-250 μ and this did not seem to change much until the critical value of 80wt% and 90wt% of HA at CH20 and CH10 respectively which can be seen in Figure 5.21.

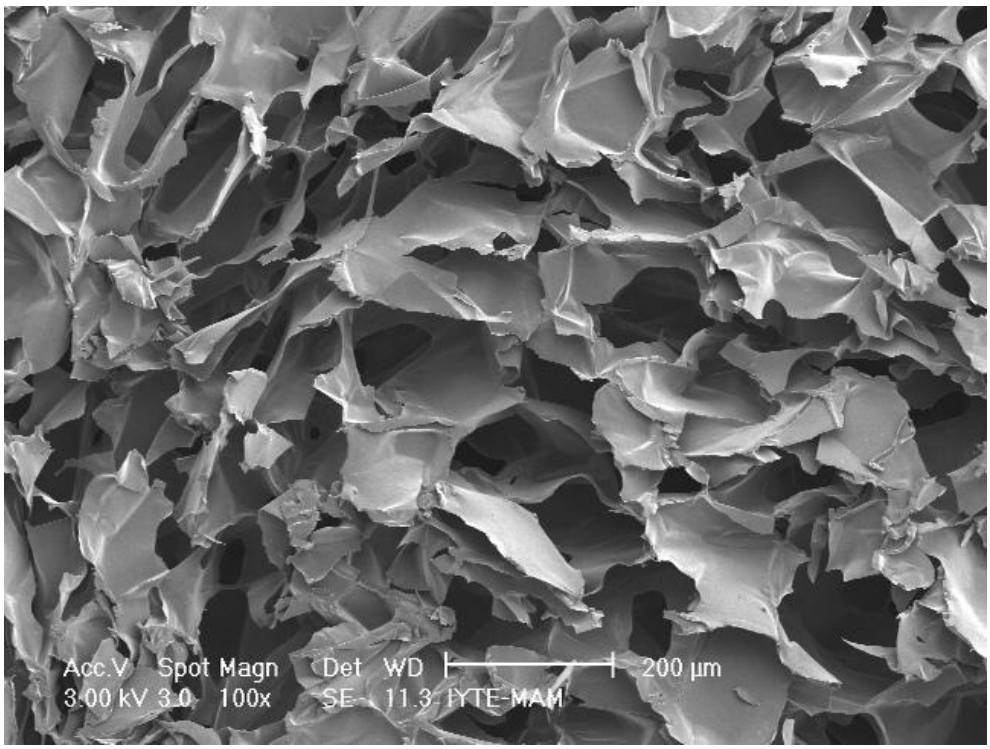

Figure5.21 a) SEM of porous chitosan,CH100.

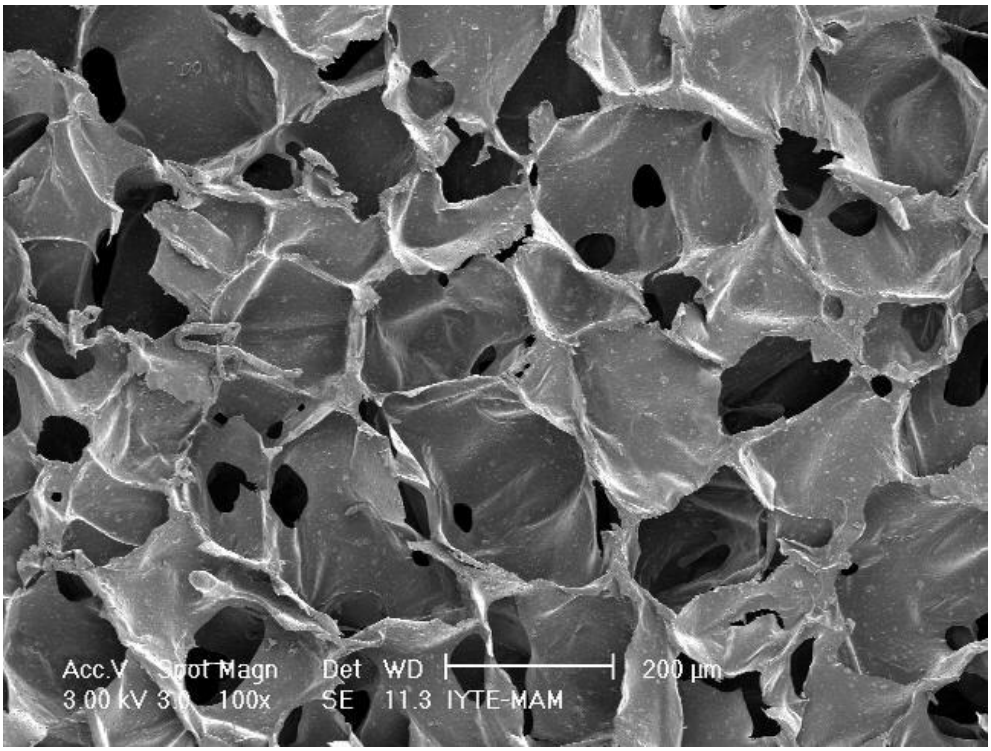

Figure5.21 b)SEM of porous HA/chitosan composite, CH80, 20wt%HA.

The uniformly distributed hydroxyapatite particles could be seen through the chitosan matrix which have interconnected cells. The pore shape seemed to change with hydroxyapatite, in pure chitosan sample pores were more flat but when HAwt% was only 20, pores became more rounded rather than flat.

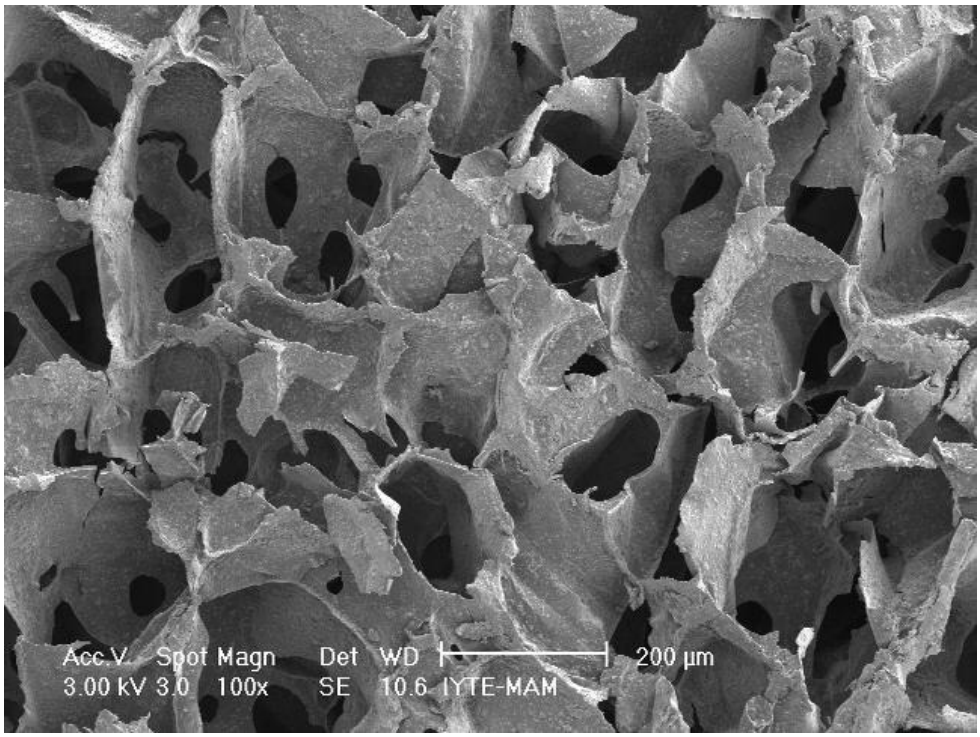

Figure5.21c) SEM of porous HA/chitosan composite, CH60, 40wt%HA.

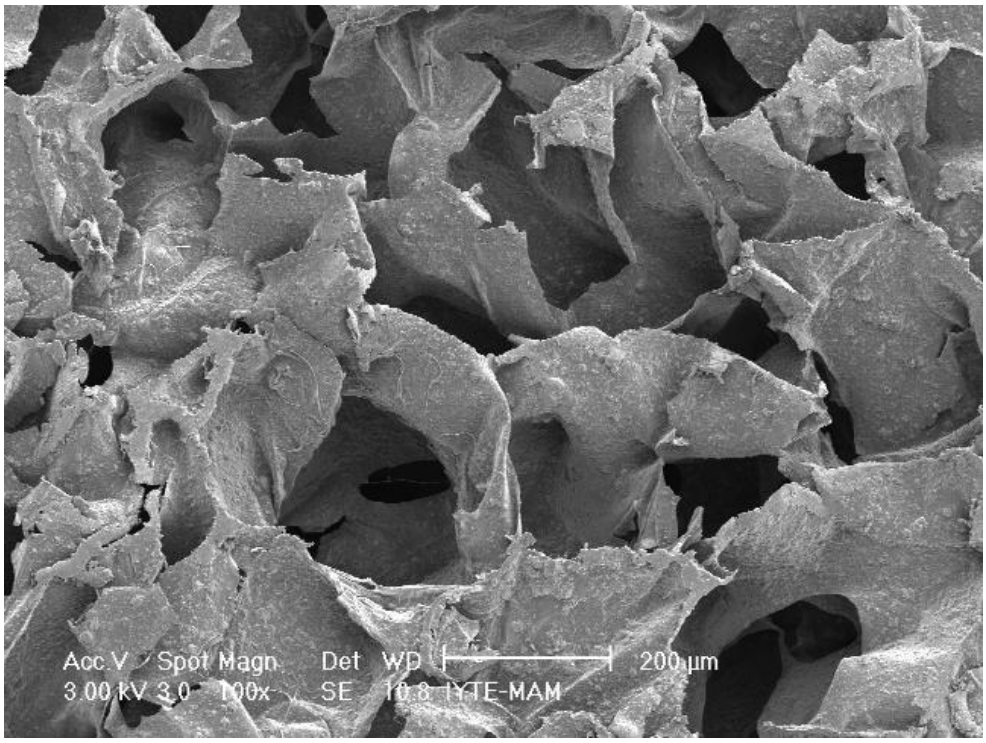

Figure5.2 d) SEM of porous HA/chitosan composite, CH50, 50wt%HA.

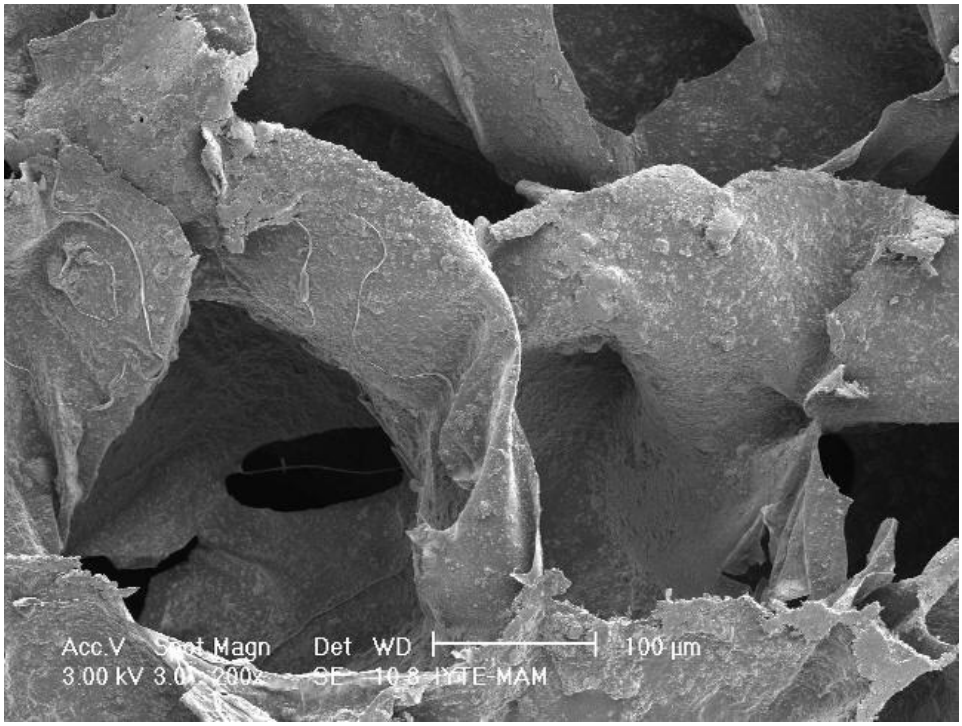

Figure5.21e) SEM of porous HA/chitosan composite, CH50, 50wt%HA.

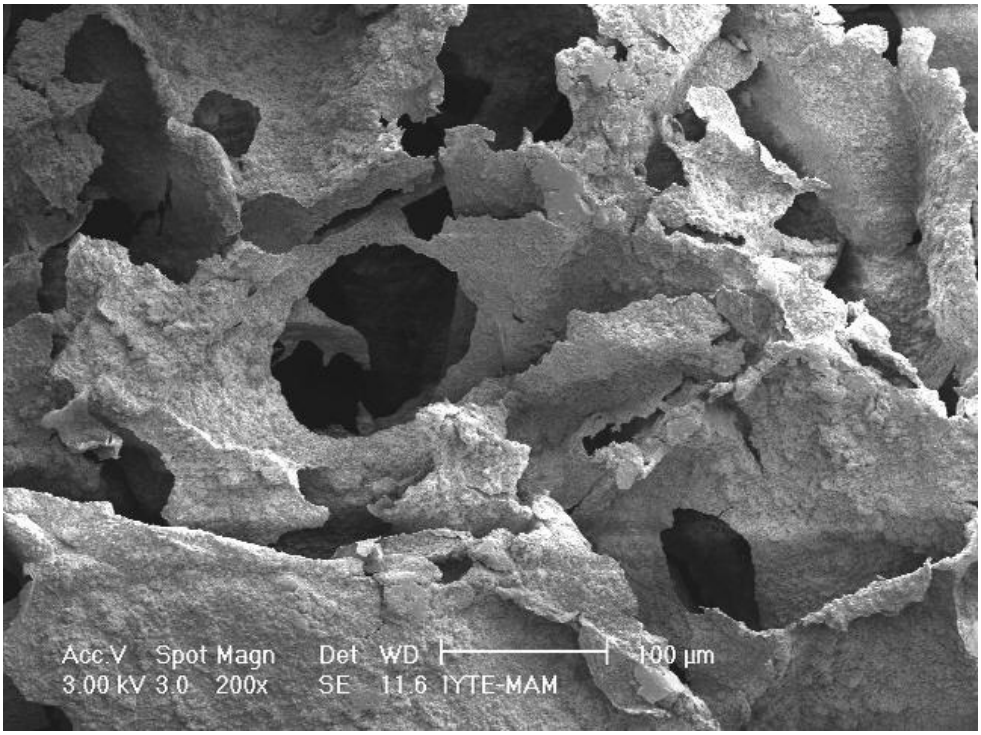

Figure5.21f) SEM of porous HA/chitosan composite, CH20, 80wt%HA.

Increasing hydroxyapatite content did not disturb the porous structure but in especially CH20 and CH10 which contained 80wt% and 90wt% HA respectively, the effect of ceramic on the morphology was significant. The pores decreased in size, cavities between cells became thin, uniformity decreased and surface became rough.

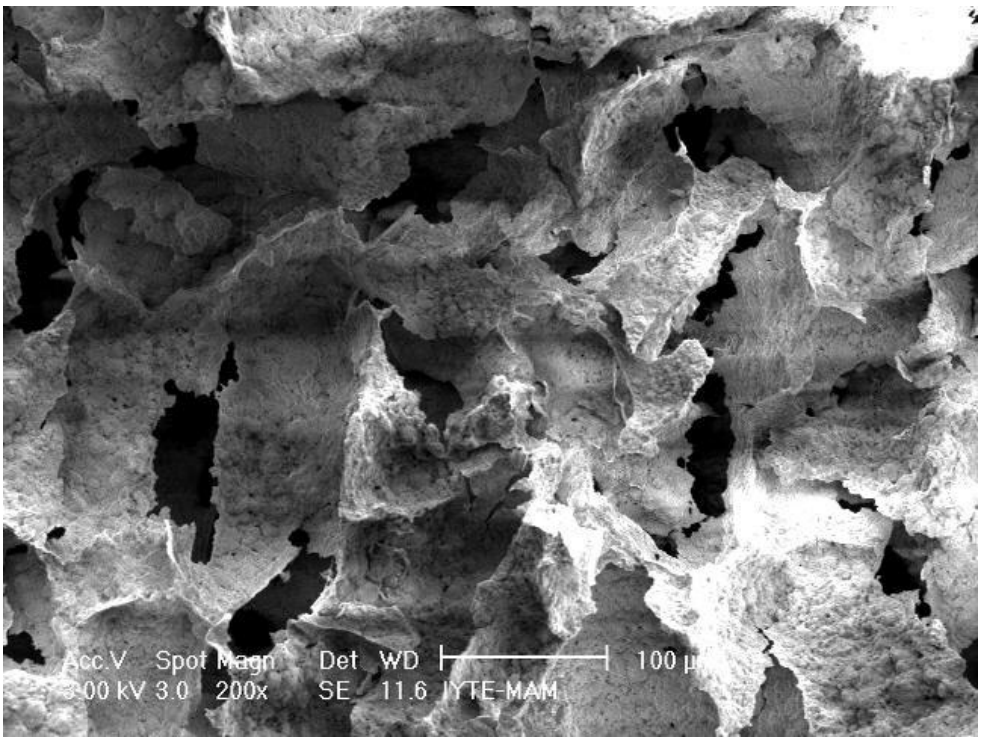

Fig5.21 g) SEM of porous HA/chitosan composite, CH10, 90wt%HA.

Figure 5.22 shows the SEM images of hydroxyapatite/chitosan composites which are horizontally cut after compression test. As can be seen from the figures the cells of the composites bent on each other but it could not be named as a fracture or collapse, moreover the structure still had pores even though they were smaller and the chitosan HA interaction did not seem to be disturbed. As a result the SEM images showed that chitosan hydroxyapatite composites formed a porous network which was formed by a chitosan matrix through which hydroxyapatite particles embedded. In Figure 5.22c partly deformed sample is seen and the difference between deformed and undeformed region can be distinguised. This image shows that deformation began in a band not in all regions at the same time. The EDX data showed that the composites contained C, Ca, P and O as expected but no N were detected which is contained by chitosan in smaller amount compared with C and O. Ca and P were thought to be

originated from hydroxyapatite, O from both of the components and C from chitosan only. The different regions of composites and different weight percent composites resulted different EDX data containing same material but with changing ratios.

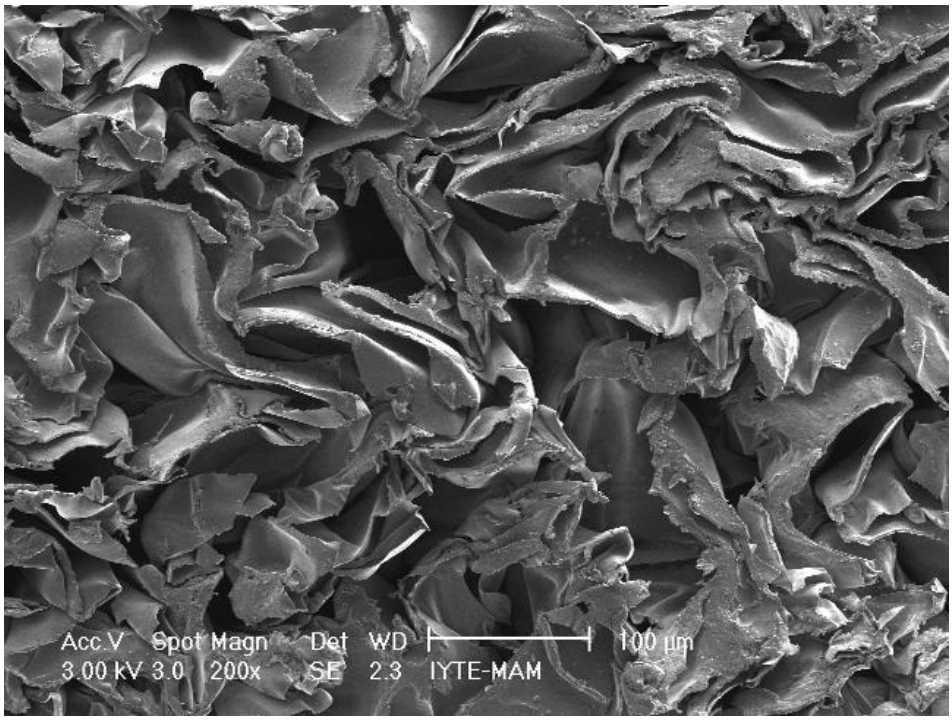

Figure 5.22 a)SEM of chitosan after compression test, CH100

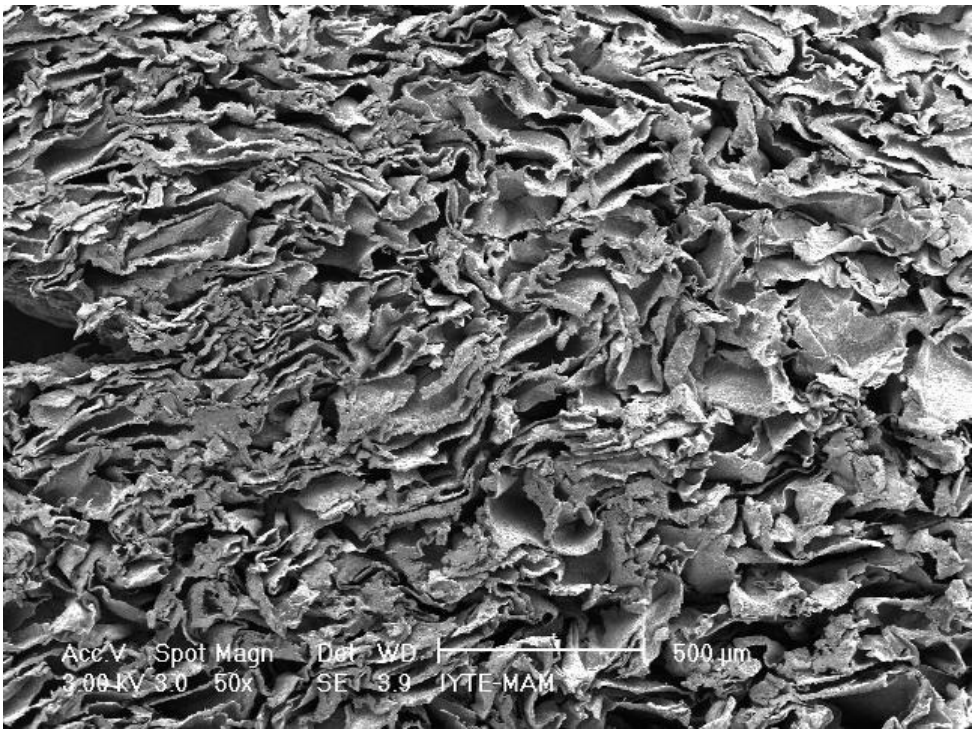

Figure 5.22 b) SEM of HA/chitosan composite after compression test CH50, 50 wt%HA.

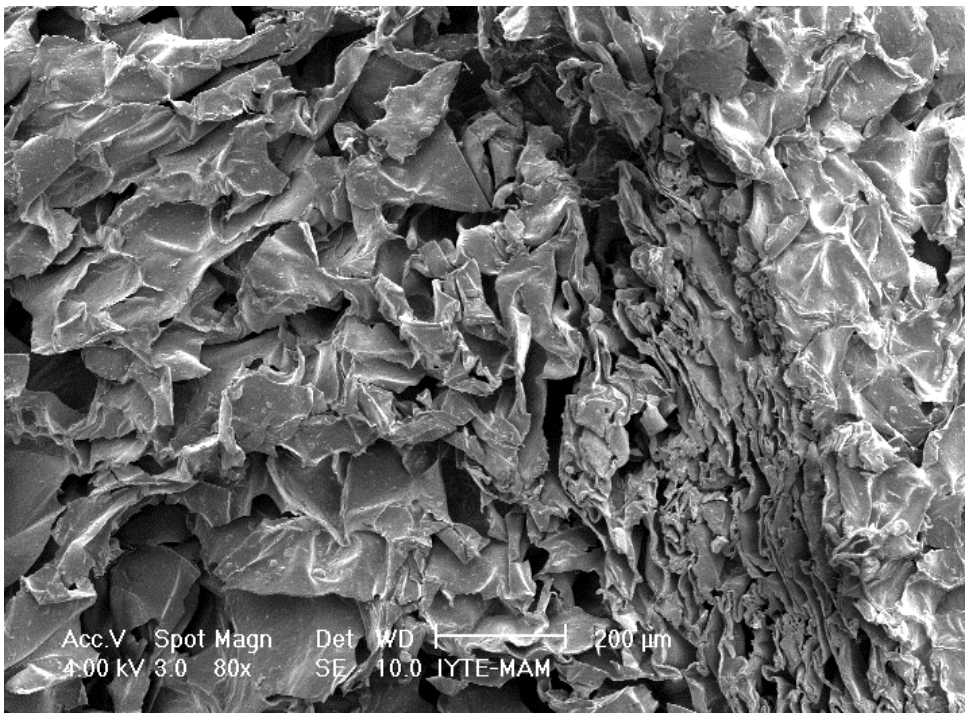

Fig.5.22 c) SEM of HA/chitosan composite after compression test CH80, 20wt%HA.

Figures 5.23a,b,c,d,e show the SEM images of β-TCP/HA/Chitosan composites at different magnifications. The pore sizes were around 100-400µ. The structure seemed to be highly porous and the pores seemed to be interconnected this was also supported by the high porosity determined by Archimedes method. Homogeneous distribution of the ceramic phase in the matrix can be seen clearly especially in Figure 5.23c. The ceramic phase was embedded in the matrix which can be seen better in Figure 5. 23d. In Figure 5.23.a and b the ceramic phase was more rare compared to 5.23 c and e due to the less ceramic content of the composite.

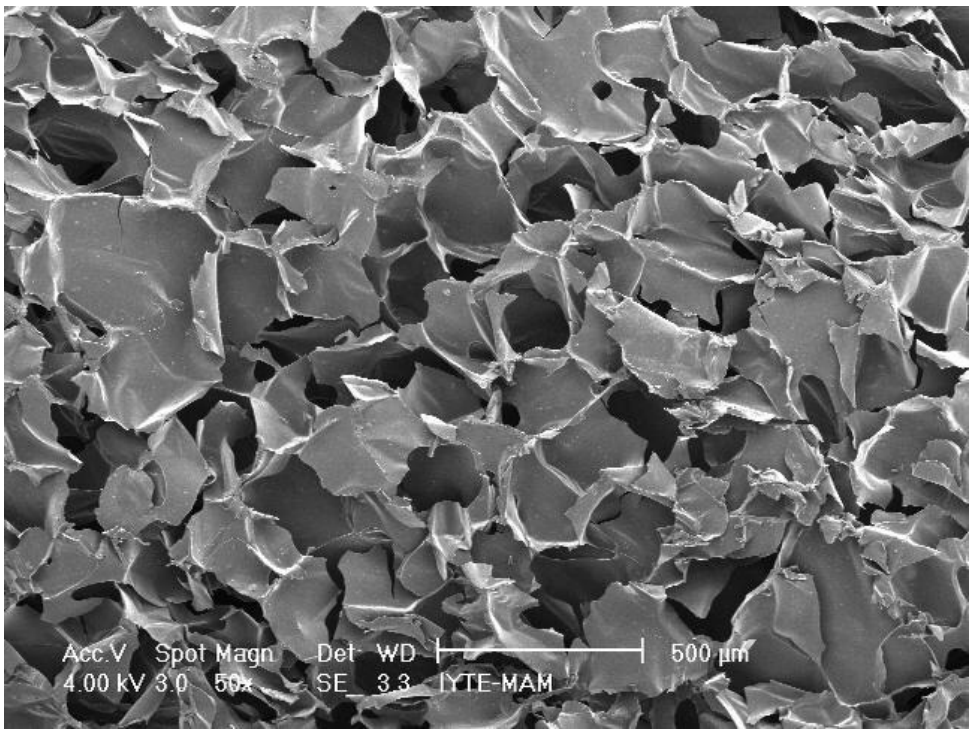

Figure 5.23 a) SEM of porous HA/ β-TCP/chitosan composite, CHT90.

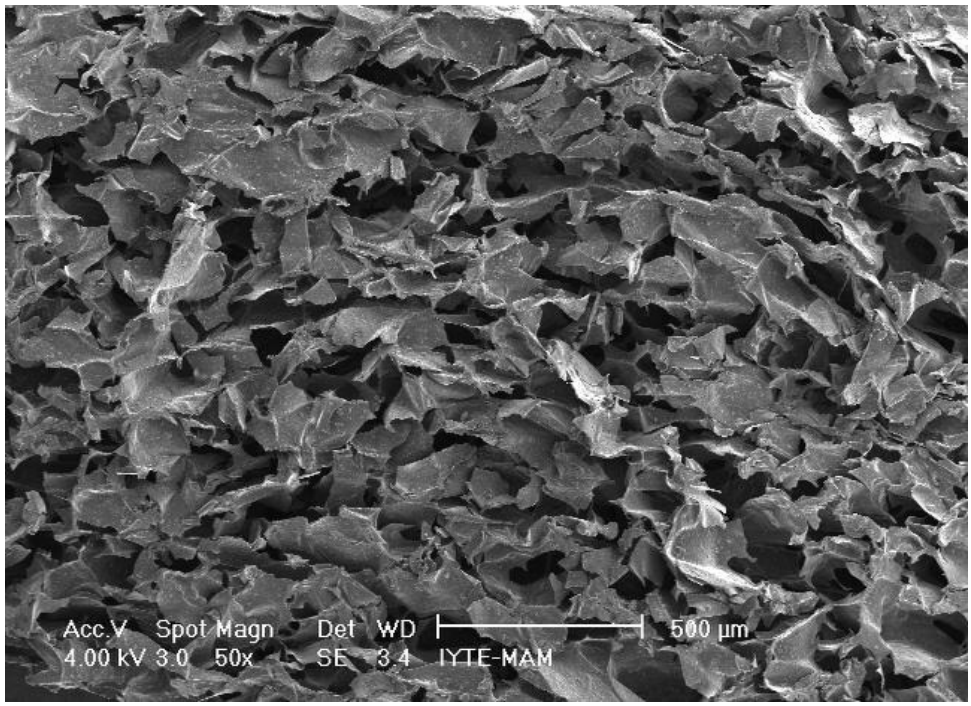

Figure 5.23 b) SEM of porous HA/ β-TCP/chitosan composite, CHT70.

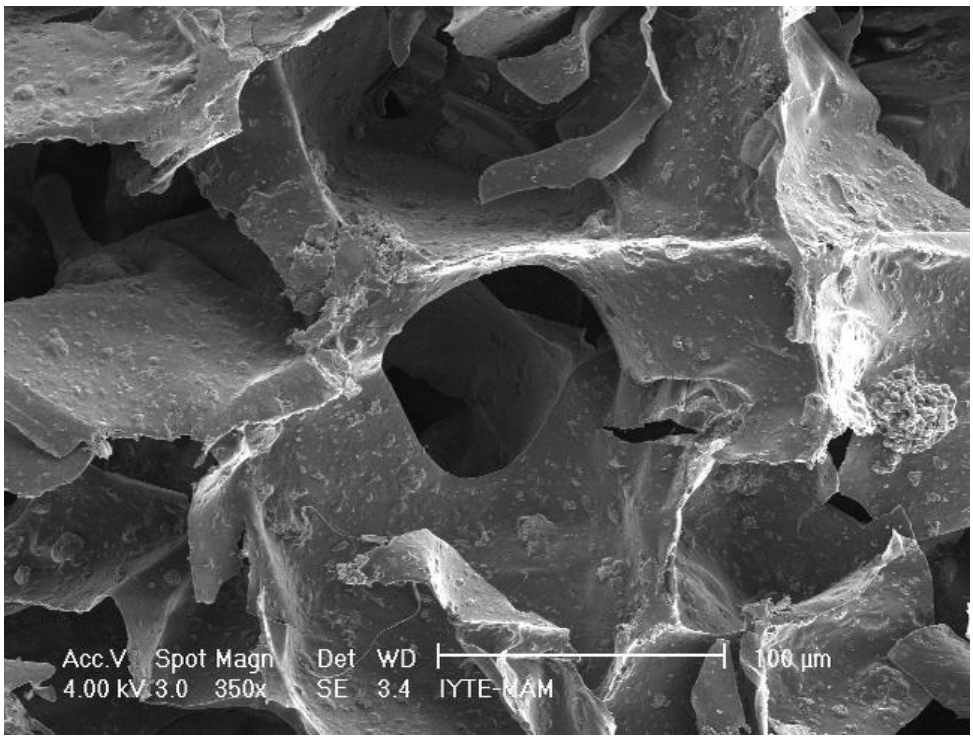

Figure 5.23 c) SEM of porous HA/ β-TCP/chitosan composite, CHT70.

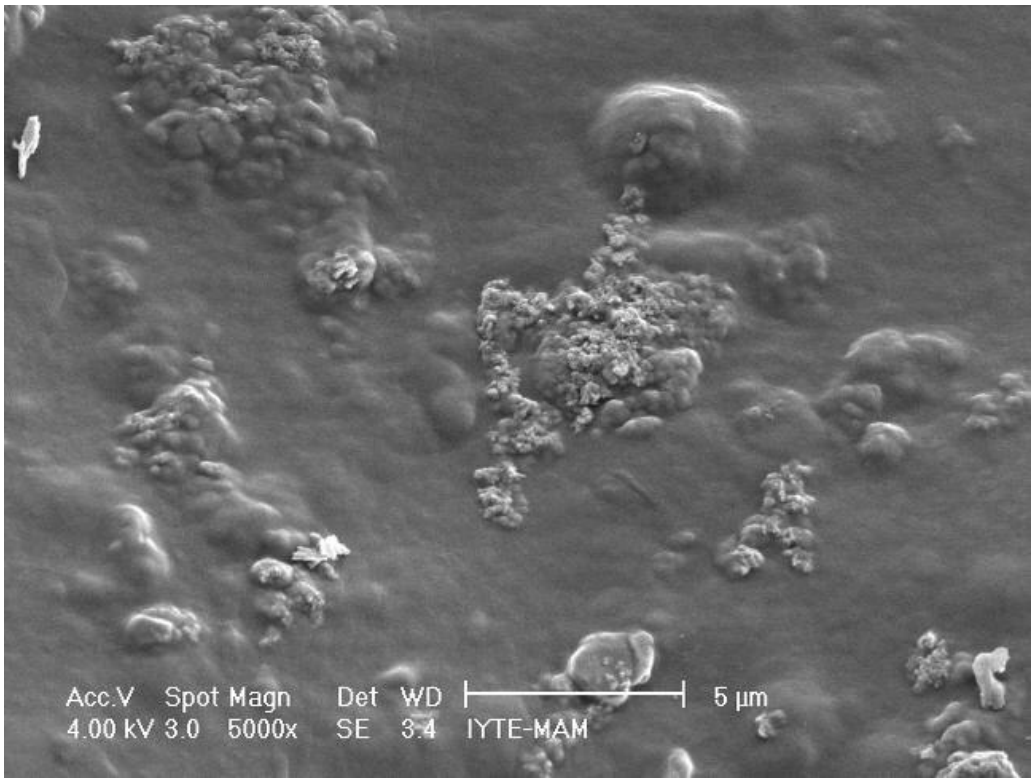

Figure 5.23 d) SEM of porous HA/ β-TCP/chitosan composite, CHT70.

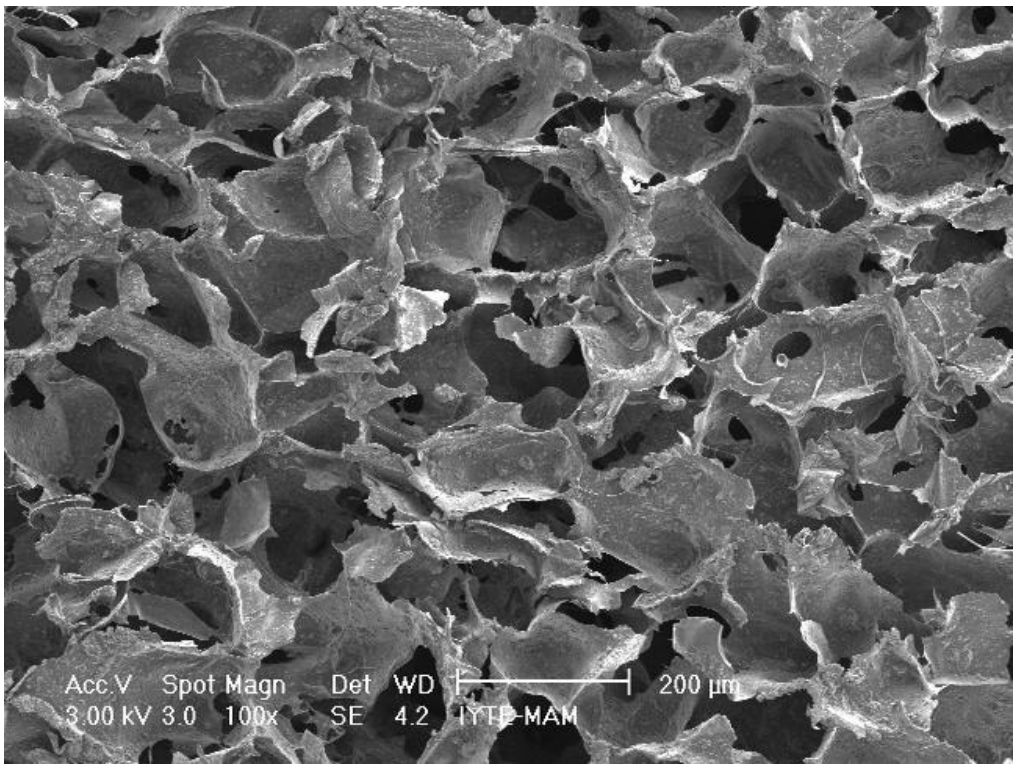

Figure 5.23 e) SEM of porous HA/ β-TCP/chitosan composite, CHT50.

Figures 5.24 show the SEM images of β-TCP/HA/Chitosan composites at different magnifications which were horizontally cut after compression test. When Figure 5.24 a,b,c and e are considered, the composite cells bent on each other without a catastrophic collapse, and this cannot be named as a brittle fracture with cracks.The polymer network seemed to continue to be porous and ceramic polymer interaction seem not to be disturbed. The bent structure can be seen more clearly in Figure 5.24b and 5.24c. In Figure 5.24d and 5.24e the ceramic phase embedded in the polymer matrix even after compression test can be seen.

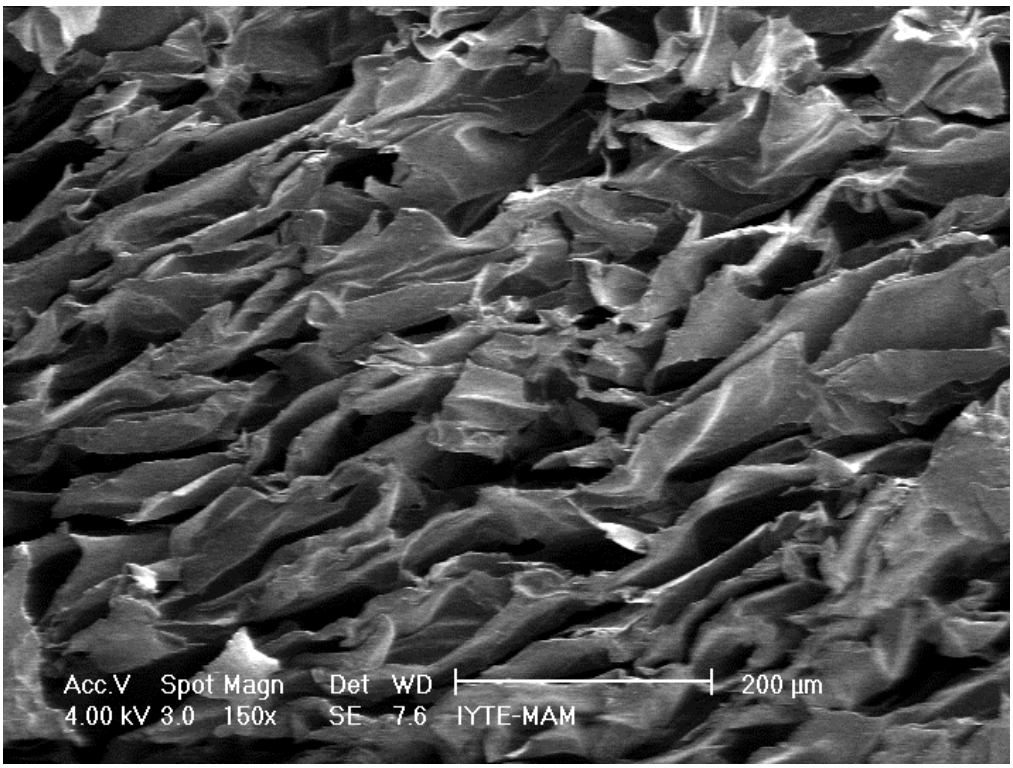

Figure 5.24 a) SEM of HA/β-TCP/chitosan composite after compression test, CHT90.

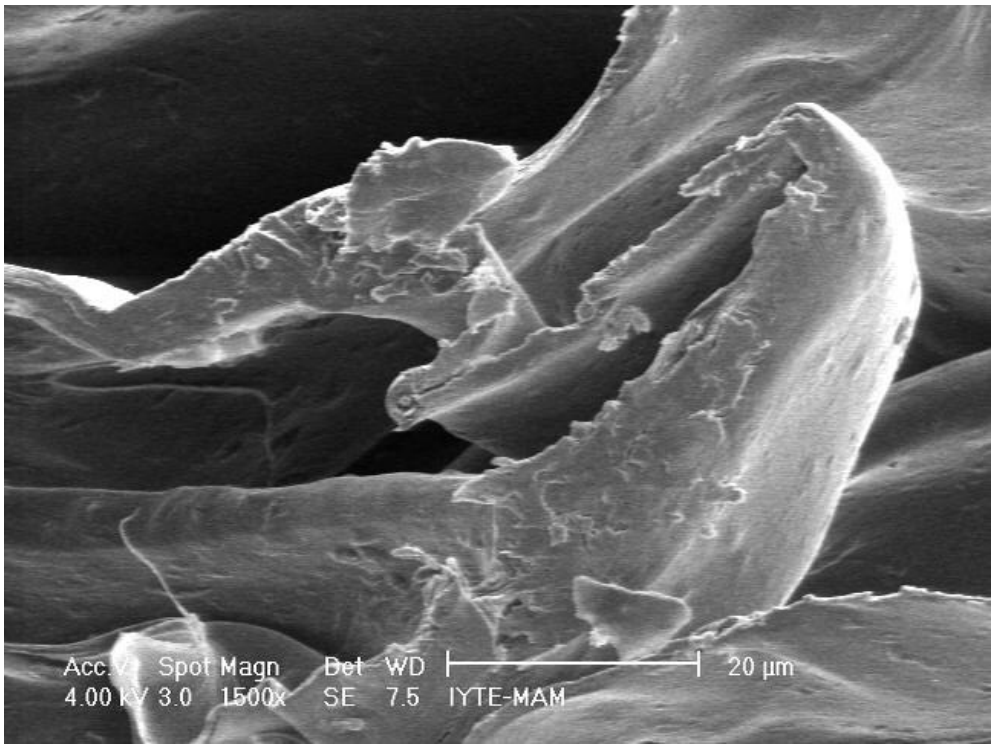

Figure 5.24 b) SEM of HA/β-TCP/chitosan composite after compression test, CHT90.

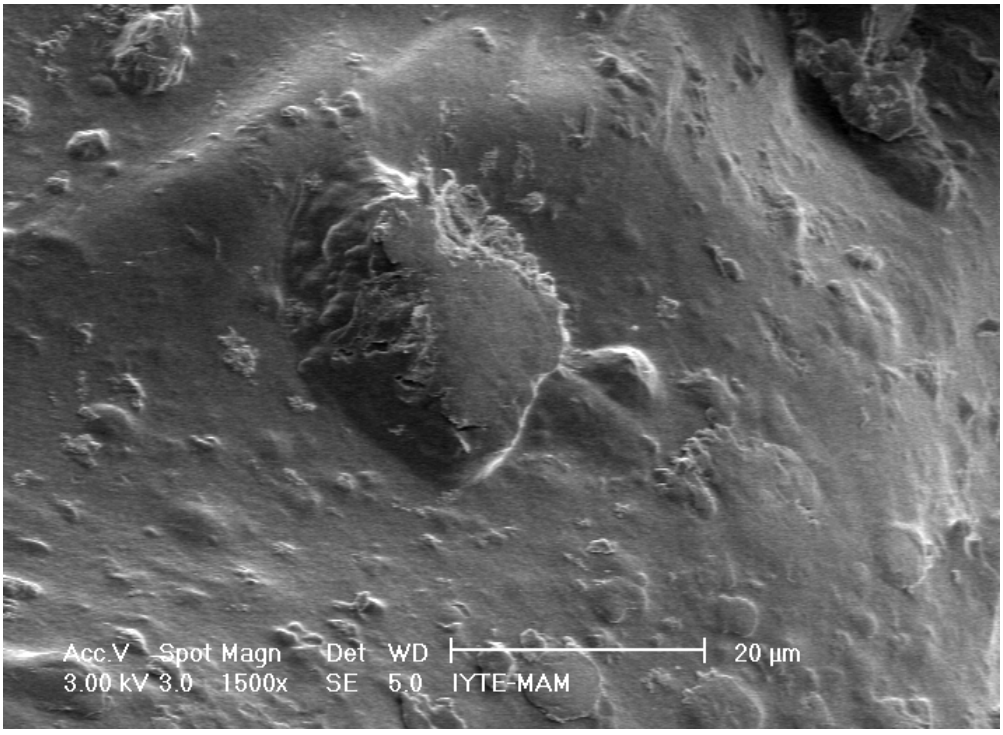

Figure 5.24 c) SEM of HA/β-TCP/chitosan composite after compression test, CHT80.

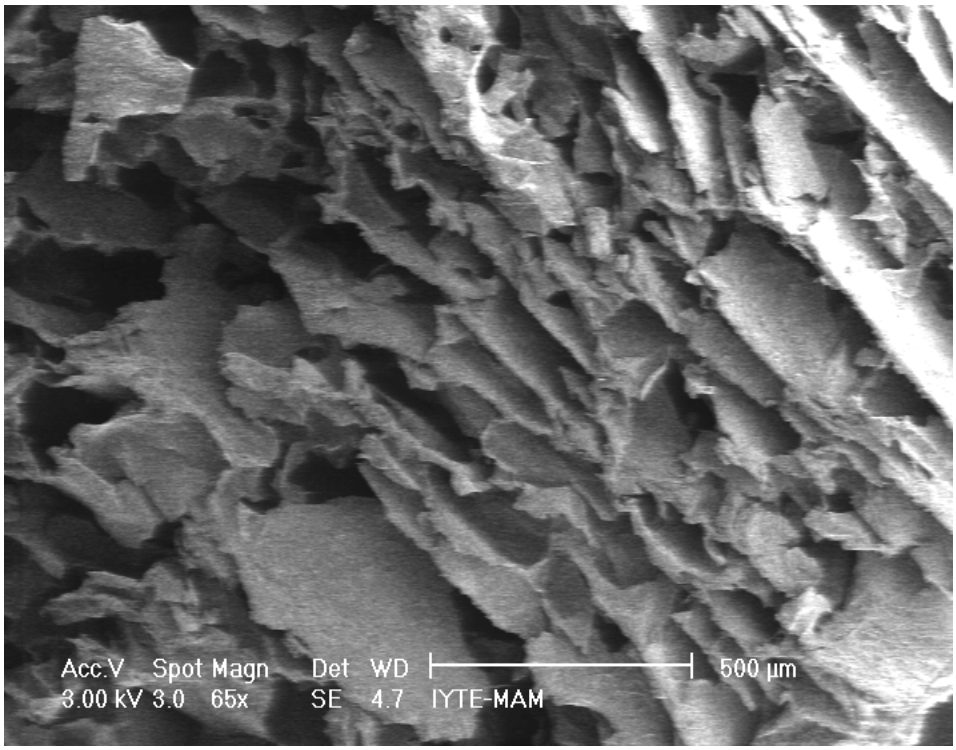

Figure 5.24 d)SEM of HA/β-TCP/chitosan composite after compression test, CHT60.

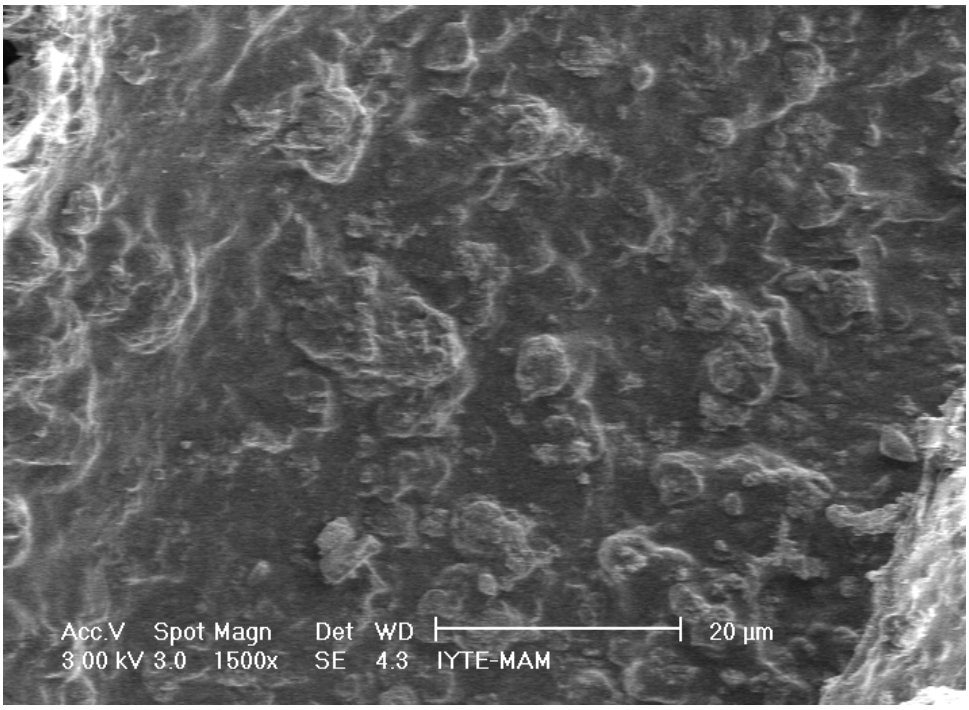

Figure 5.24 e) SEM of HA/β-TCP/chitosan composite after compression test, CHT60.

In Figure 5.25 a to c SEM images of HA Whisker/Chitosan composites can be seen. The mean pore size was around 100-200µ. The structure seemed to be highly porous containing interconnected pores this was also supported by the high porosity and determined by Archimedes method. In Figure 5.25 a and b, the homogeneous distribution of partly or wholly embedded whisker through the chitosan matrix is seen.

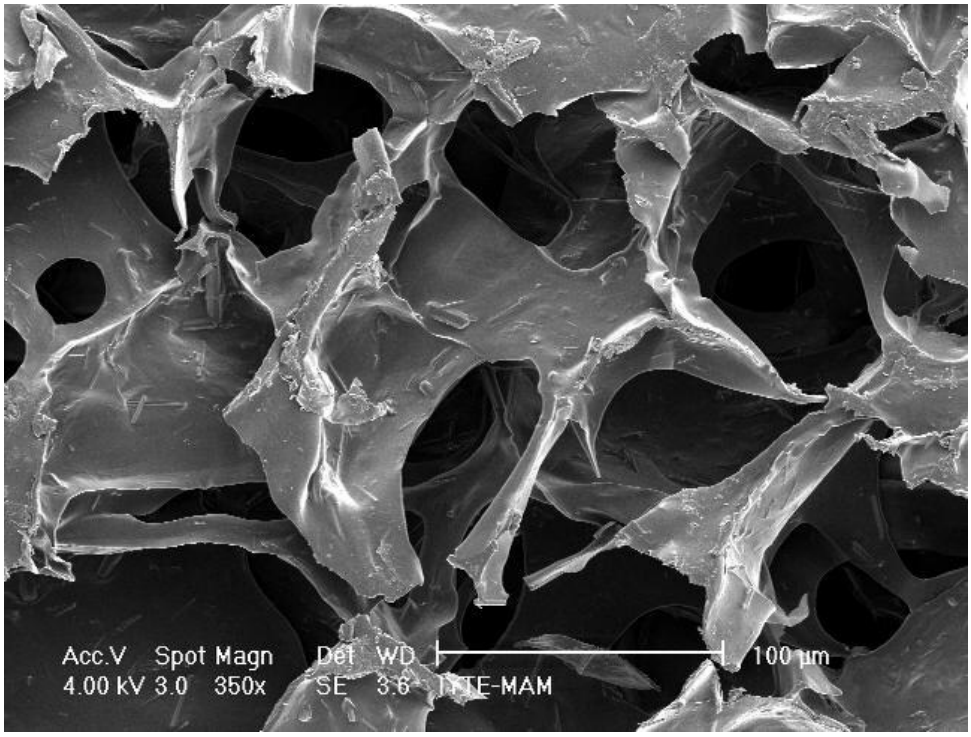

Figure 5.25 a) SEM of porous HA whisker/chitosan composite, CW80, 20 wt%HA.

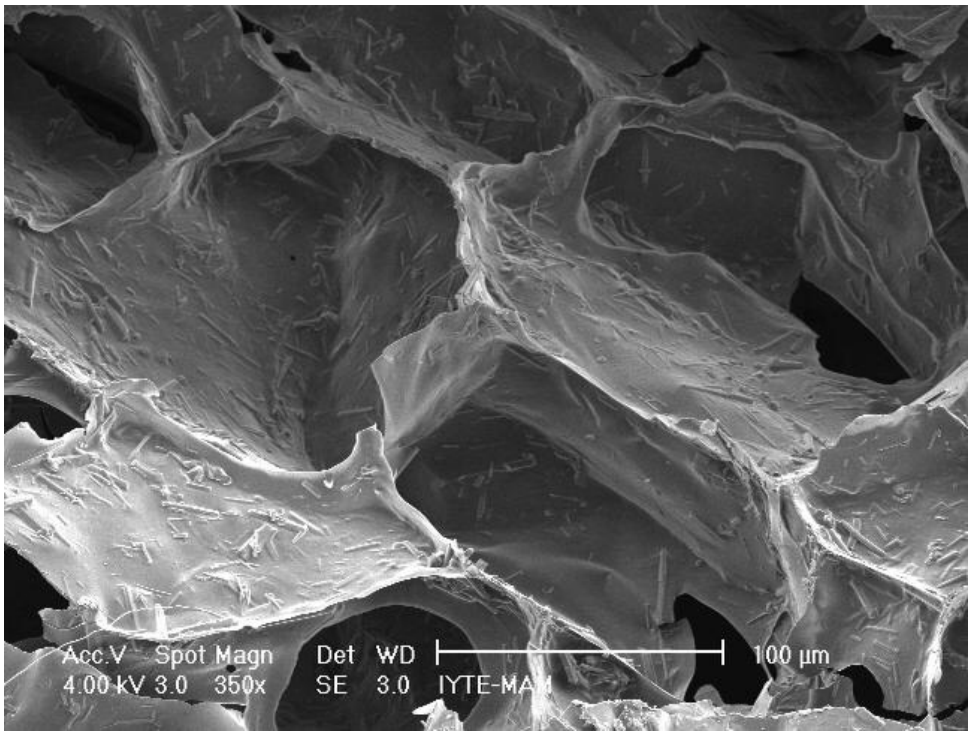

Figure 5.25b) SEM of porous HA whisker/chitosan composite, CW60, 40 wt%HA.

The whiskers seemed to disperse through the chitosan matrix uniformly both through the walls and at the edges of the cells as shown in Figure 5.25b.

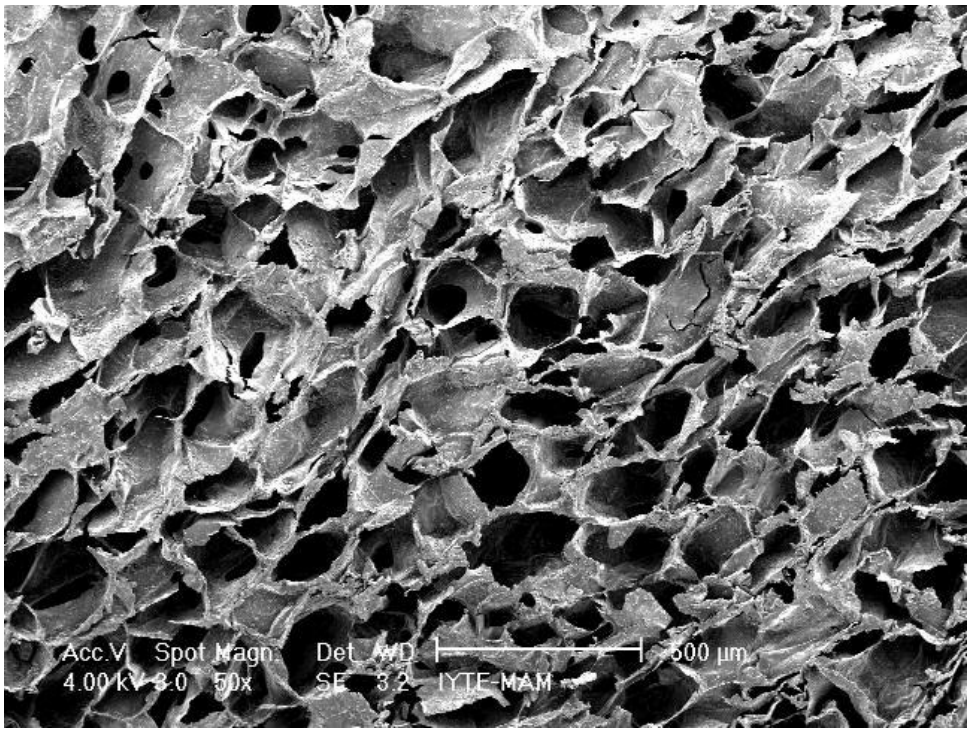

Figure 5.25c) SEM of porous HA whisker/chitosan composite, CW50, 50 wt%HA.

In Figure 5.26 SEM images of HA Whisker/Chitosan composites after compression are shown. In Figure 5.26a,b and e, the bending of the cells can be seen. The whisker/polymer interaction did not seem to be disturbed much and tearing in the

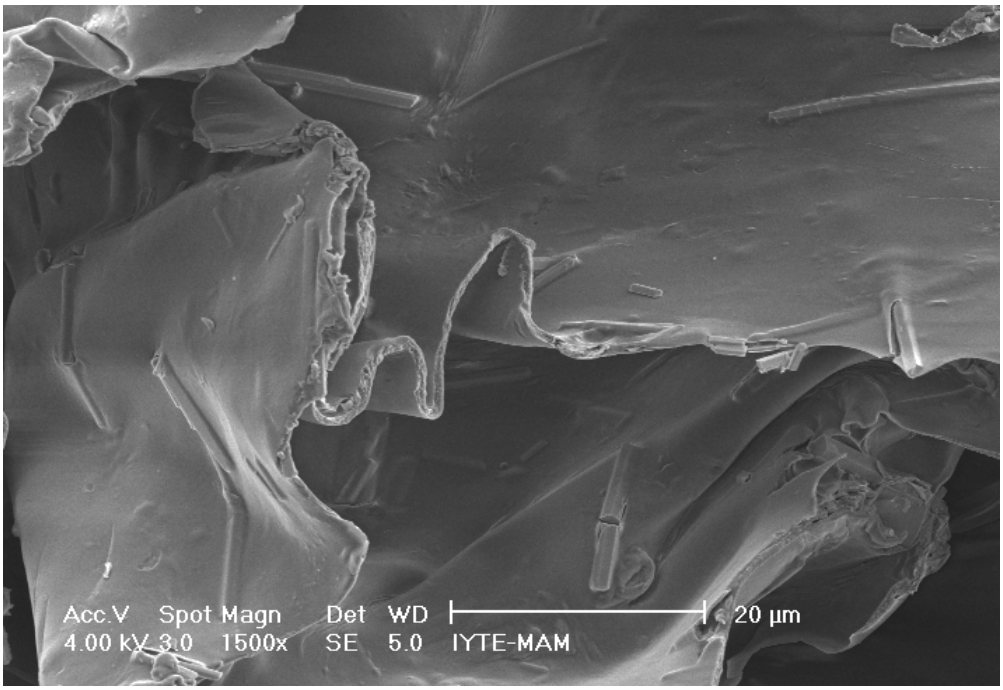

Figure 5.26 a) SEM of HA whisker /chitosan composite after compression test, CW80.

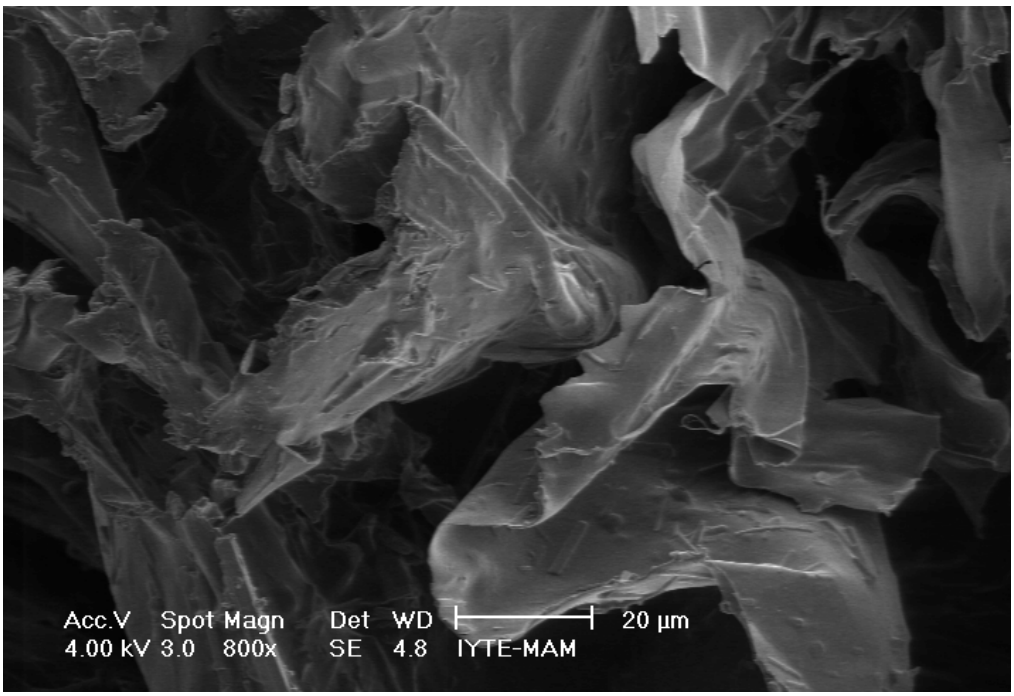

Figure 5.26 b) SEM of HA whisker /chitosan composite after compression test, CW60.

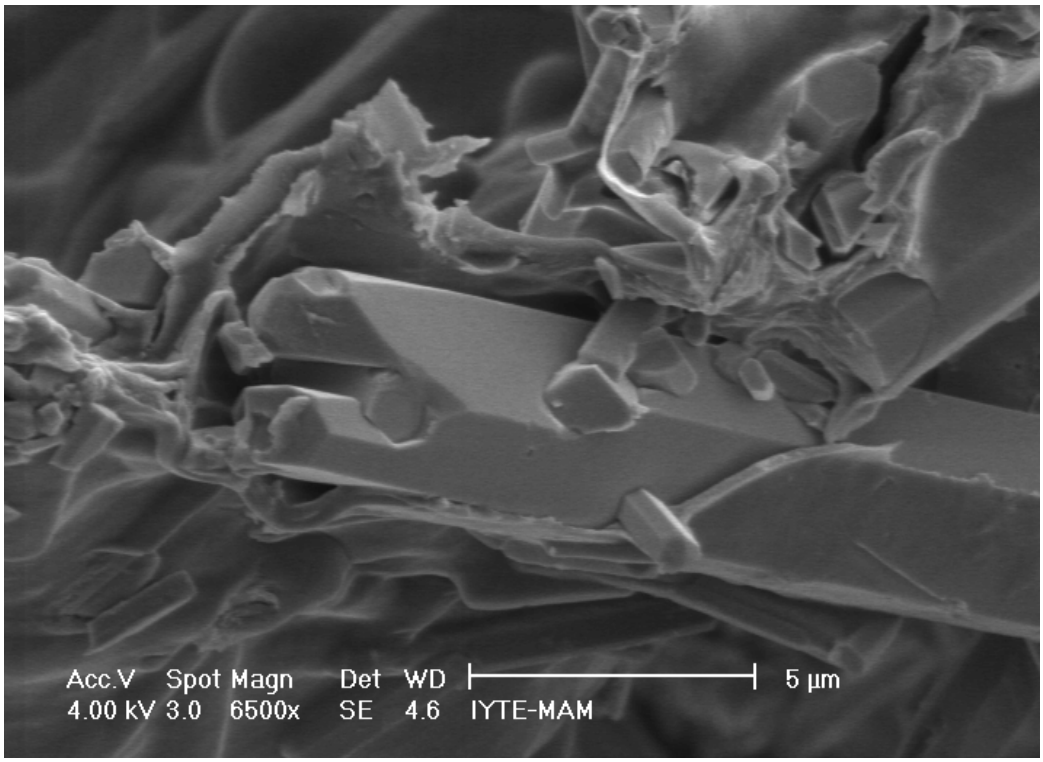

Figure 5.26c) SEM of HA whisker /chitosan composite after compression test, CW30.

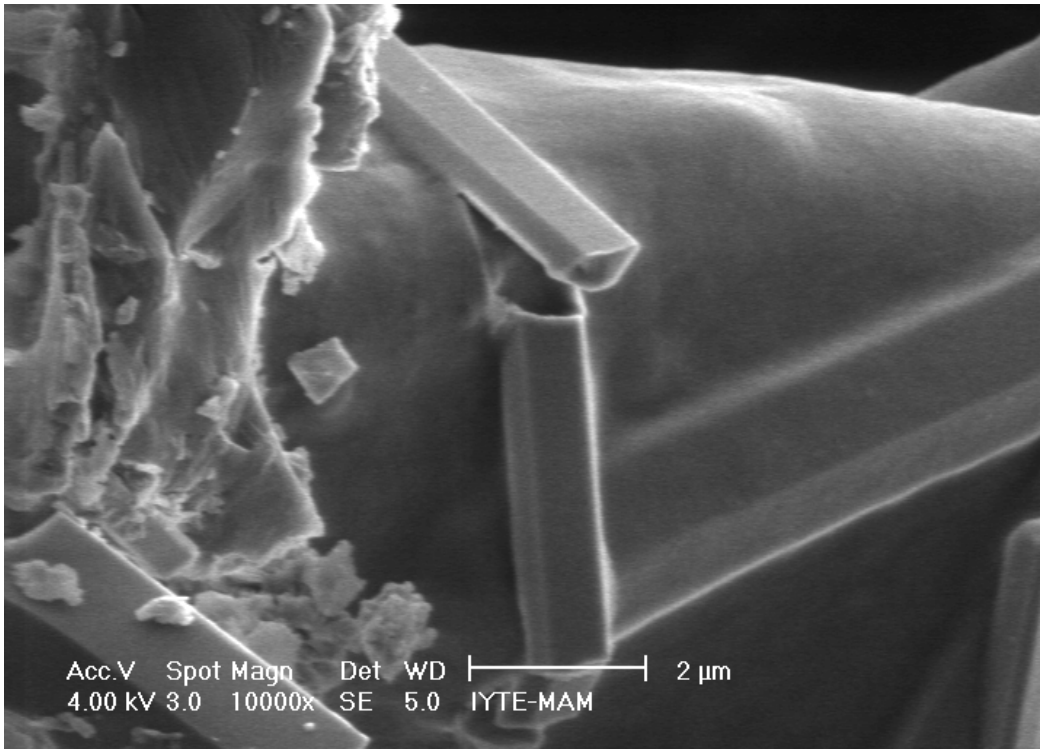

Figure 5.26 d) SEM of HA whisker /chitosan composite after compression test, CW50.

polymer was very rare. In Figure 5.26 c and d the whisker chitosan interface was seen in more details.. The whiskers seem to be covered by the polymer well and they are embedded in the matrix.

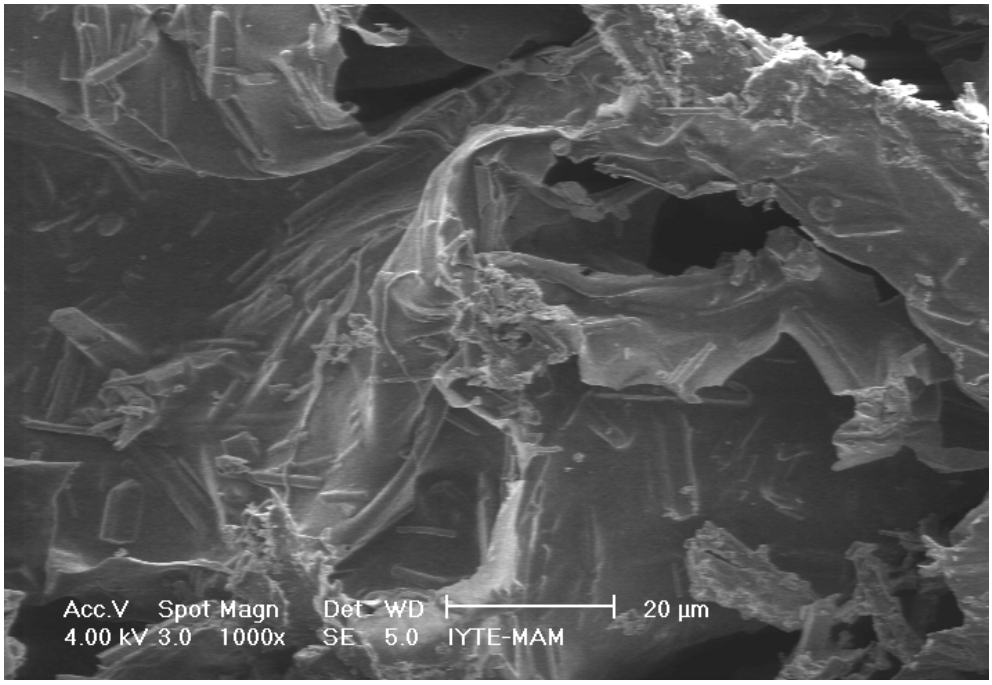

Figure 5.26e) SEM of HA whisker /chitosan composite after compression test, CW50.

In Figure 5.28 a typical stress strain graph of a sample can bee seen. The modulus was calculated from the slope of the linear elastic part of the graph. After the plateau, stress increases linearly. Except for the sample with 90 % HA content the other samples did not show brittle behaviour and no catastrophic fracture occured due the nature of the foam structure. The characteristic of the curve was consistent with a similar work reported in literature [23].

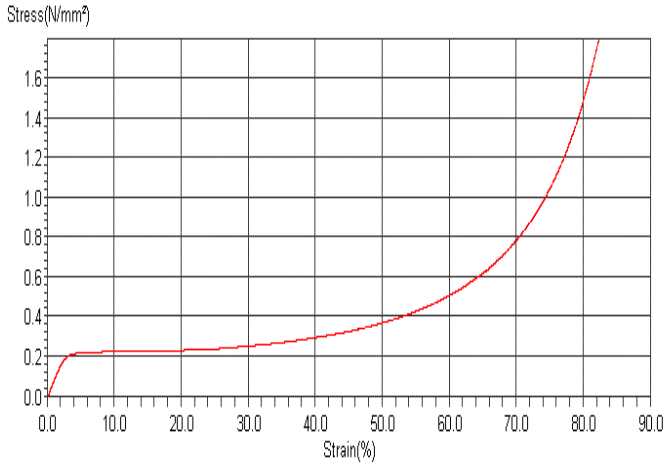

Figure 5.28 Stress Strain Graph of chitosan/HA composite,CH40, 60wt%HA.

In Table 5.8 density, porosity elastic modulus and collapse stress and in Figure 5.27 some phsical and mechanical properties of HA/Chitosan composites can be seen. As can be seen from the table, increasing HA content led to an increase in density and decreasing porosity which increased modulus and stress since hydroxyapatite has a much higher modulus than chitosan. CH30 and CH20 seemed to have closest composition to bone which contain 69% HA and 21% collagen. B20 had the best values of E and σ but these values were still far from those of bone. CH10 with 90% HA content failed at the beginning of the test. The relations between weight percent of the ceramic, density, modulus and collapse stress and also the modulus and stress values were consistent with similar work in the literature [23,7].

Table 5.8 Mechanical Properties of HA/Chitosan Composites.

SAMPLE	**HA%**	**ρ(g/cm^3)**	**POROSITY**	**E (MPa)**	**σ(Mpa)**
CH100	0	0.053	96	4.45	0.14
CH80	20	0.076	94	8.84	0.15
CH60	40	0.069	96	6.68	0.18
CH50	50	0.090	94	9.52	0.18
CH40	60	0.094	94	8.79	0.24
CH35	65	0.116	94	11.09	0.17
CH30	70	0.130	93	8.30	0.21
CH20	80	0.14	93	10.09	0.34
CH10	90	0.29	88	------	-------

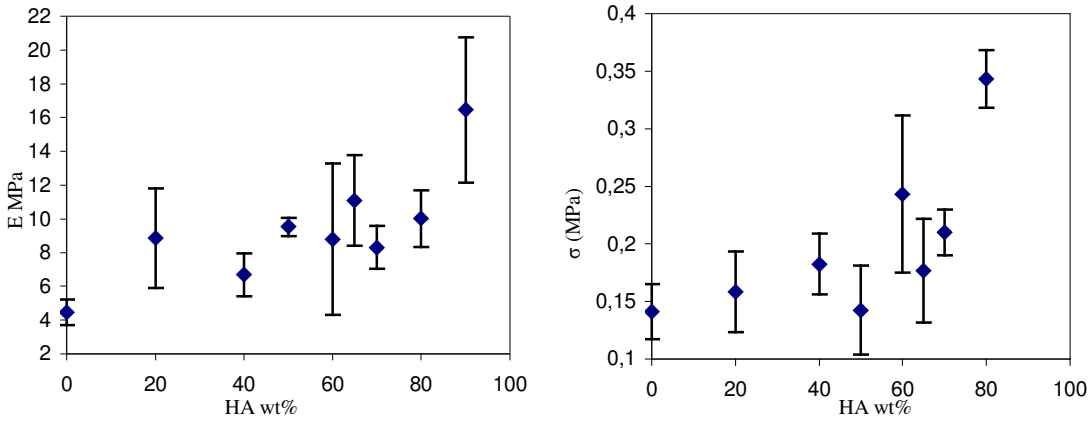

a) b)

Figure 5.27 Mechanical properties of HA/chitosan composites a)Modulus vs HA wt%, b) σ vs HA wt%.

In Table 5.9 density, porosity modulus and compressive yield stress and in Figure 5.29 mechanical properties of HA Whisker/Chitosan composites can be seen. Decreasing chitosan content led to an increase in density and slight decrease in porosity. With increasing HA whisker content modulus increased 4.45 to10.9MPa. When collapse stress was considered, increasing ceramic content made it sometimes increase and sometimes decrease but finally reached 0.23 MPa which is almost twice the starting value. CW30 seemed to have closest composition to bone which contain 69% HA and 21% collagen and has highest modulus and stress values but which were still far from those of bone. Porosity values did not change much so it was not possible to make a correlation between any parameter with changing porosity.

Table 5.9 Mechanical Properties of HA Whisker/Chitosan Composites.

SAMPLE	**ρ(g/cm^3)**	**POROSITY**	**E (MPa)**	**σ(Mpa)**
CW 100	0.053	96	4.45	0.14
CW80	0.065	95	7.92	0.11
CW60	0.066	96	8.60	0.08
CW50	0.091	94	10.76	0.17
CW40	0.093	94	9.2	0.12
CW30	0.124	94	10.9	0.23

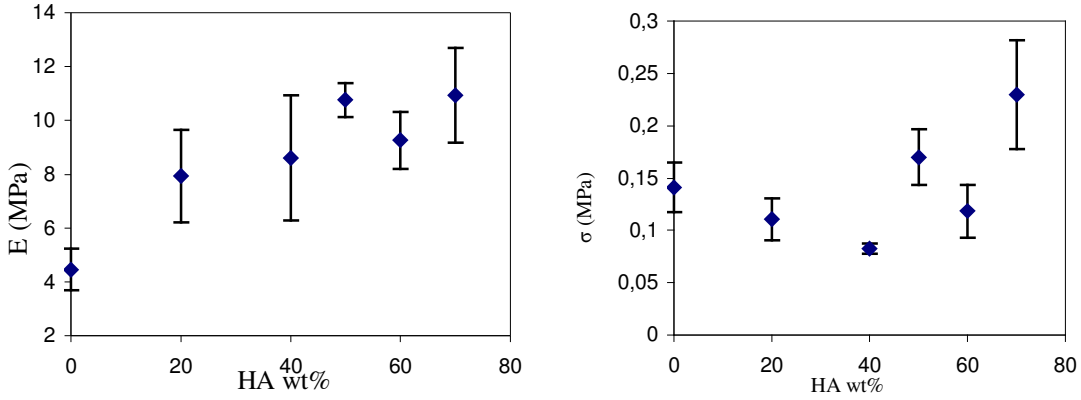

a) b)

Figure 5.29 Mechanical properties of HA Whisker/Chitosan composites a)Modulus vs HA wt%, b) Yield Stress vs HA wt%.

Table 5.9 shows density, porosity modulus and collapse stress and Figure 5.30 shows mechanical properties of β-TCP/HA/Chitosan composites. Increasing ceramic content led to an increase in density but porosity was not affected much. With increasing β-TCP/HA whisker content modulus slightly increased after a decrease at first. Yield Stress decreased with increasing ceramic content. This may be caused because of effect of HA to TCP.

Table 5.10 Mechanical Properties of β-TCP/HA/Chitosan Composites.

SAMPLE	**ρ(g/cm^3)**	**POROSITY**	**E (MPa)**	**σ(Mpa)**
CHT100	0.053	96	4.45	0.14
CHT90	0.055	94	2.68	0.073
CHT80	0.056	96	4.08	0.053
CHT70	0.066	95	3.99	0.061
CHT60	0.074	95	4.61	0.066

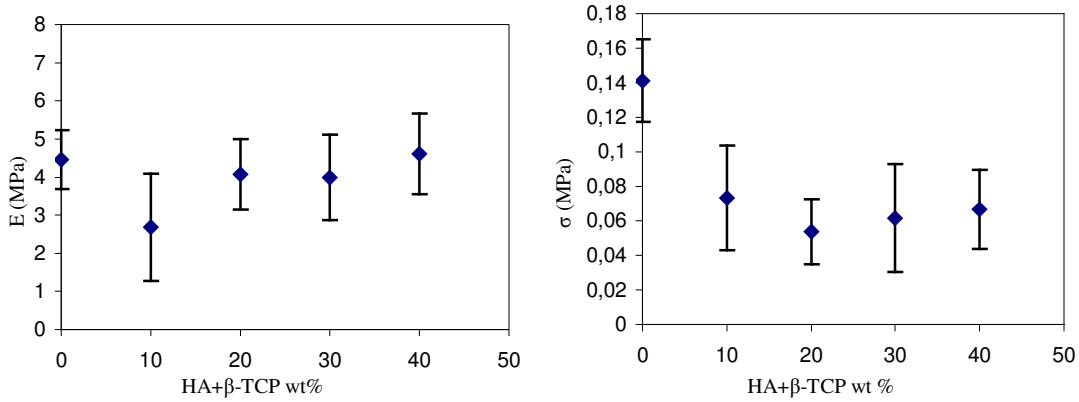

a) b)

Figure 5.30 Mechanical Properties of β-TCP/HA/Chitosan Composites, a)Modulus vs HA+ β-TCP wt%, b) Yield Stress vs HA+ β-TCP wt%.

When mechanical properties of calcium phosphate/chitosan composites are considered, they werevery low and far from the mechanical properties of bone. These low mechanical properties may be explained by the high porosities. The hierarchical structure of bone which gives it superior mechanical properties and difficult to imitate was discussed in previous chapters. The HA in the bone is in nanoscale while the ceramics in this study were in micro scale and the composites have a totally different microstructure when compared to natural bone. These are additional causes of low mechanical properties of the composites. More over these values were comparable with the values discussed in literature which were about similar composites produced by similar materials with similar methods [7,23]. The composite materials produced were suitable to be used as scaffolds for bone growth. There are several works in the literature which produced similar composites to be used as scaffolds [3,4,7,23]. Mechanical properties of the scaffolds may be improved by introducing a chemical which may help formation of a strong chemical bonding between polymer phase and ceramic phase would increase modulus and yield stress. Glutaraldehyde was discussed to cause cross-linking between chitosan and gelatin [3,30]. Citric acid was found to enhance bonding strength between chitosan/hydroxyapatite precipitates [10]. If the mechanical properies of porous composites can be improved in some way, they may be used for load bearing applications in the body.

CHAPTER 6

CONCLUSIONS

In this study the preparation and characterization of porous hydroxyapatite and biopolymer bioceramic composites by using chitosan as polymer and hydroxyapatite, hydroxyapatite whisker, β-tricalciumphosphate as ceramic is done. The effects of slurry concentration, thermal cycle, preparation method and porosifier content on the density, porosity and open pore content of the porous hydrxyapatite ceramic were investigated. The effects of ceramic type and changing weight percents of ceramic powders on the morphology, porosity, chemical composition and mechanical properties of the composites were also investigated.

Using starch as a porosifier resulted a higher open pore content and higher porosity values compared to the polymer sponge method. Control on the parameters was much more propable at dry pressing and dough method compared to polymer sponge method in which impregnation is very important and hard to control. Dough method resulted higher porosity than dry pressing since there was no pressure applied to starch-hydroxyapatite dough. By using three different methods, samples having porosities up to 73% were achieved.

The FTIR and XRD analysis of the hydroxyapatite chitosan composites showed that both of the components existed in the composite. The solvent and chitosan content did not effect crystallinity of HA in the composites. According to XRD patterns of the composites, increasing HA percent decreased chitosan crystallinity but since characteristic peaks of chitosan were observed at FTIR spectra, chitosan did not go into a total decomposition. No peaks of any new substance other than chitosan, HA or β-TCP were detected in both XRD and FTIR results.

The SEM images showed that the composites have a homogeneous and porous microstructure with pore sizes around 250μ. Hydroxyapatite particles were dispersed uniformly and were embedded in the chitosan matrix. The study showed that the feasibility of freeze drying method which resulted this three dimensional porous network structure. Porosity was calculated using Archimedes method and 96% porosity

was found to be reached. The porosity decreased due to increasing density caused by increasing ceramic content.

The mechanical test showed that the composites have typical foam deformation with an elastic region followed by a plateau but the modulus and stress values were far from those of bone's. Increasing hydroxyapatite content resulted increase both in modulus and collapse stress.

When the mechanical properties of the composites are considered it was seen that they were suitable only for low load bearing applications and when the properties of the constituents are considered they make the composites suitable to be used as scaffold for bone growth. To improve mechanical properties which would lead the usage for higher load bearing applications, the reinforcement-polymer interface may be strengthened and some ways to make chitosan regain its crystallinity may be observed..

The composite scaffolds can be studied in situ to investigate bone growth process and change in the microstructral, chemical and mechanical properties.

The mechanical characterization of porous HA may be done and methods to cover the structure with chitosan or any other degradable polymers can be investigated.

REFERENCES

[1] Hench, L.L., "Biomaterials: a forecast for the future", pp.1429-1423, Vol.19, *Biomaterials*, 2002.

[2] Ramakrishna, S., Mayer, J., Wintermantel, E., Leong, K.W., "Biomedical applications of polymer-composite materials: a review", pp.1189-1224,Vol.61, *Composites Science and Technology*, 2001.

[3] Zhao, F., Yin, Y., Lu, W.W., Leong, J.C., W. Zhang, Zhang, J., Zhang, M., Yao, K., "Preparation and histological evaluation of biomimetic three dimensional HA/chitosan-gelatin network composite scaffolds" in press *Biomaterials*

[4] Ang, T.H., Sultana, F.S.A., Hutmacher, D.W., Wong, Y.S., Fuh, J.Y.H., Mo, X.M., Loh, H.T., Burdet, E., Teoh, S.H., "Fabrication of 3D chitosan-hydroxyapatite scaffolds using a robotic dispensing system", pp.35-42, Vol. 20, *Materials Science and Engineering*, 2002.

[5] Ito, M., Hidaka, Y., Nakajima, M., Yagasaki, H.,. Kafrawy, A.H., "Effect of HA content on physical properties and connective tissue reactions to a chitosan-HA composite membrane", pp.204-208, Vol.45, *Journal of Biomedical Material Research*, 1999.

[6] Yin, Y.J., Zhao, F., Song, X.F., Yao, K.D., Lu, W.W., Leong, C., " Preparation and Characterization of Hydroxyapatite/Chitosan-Gelatin Network Composite", pp.2929-2938, Vol.77, *Journal of Applied Polymer Science*,2000.

[7] Zhang, Y., Zhang, M., "Synthesis and characterization of macroporous chitosan/calcium phosphate composite scaffolds for tissue engineering", pp.304-312, Vol.55, *Journal of Biomedical Material Research*, 2001.

[8] Yamaguchi, I., Tokuchi, K., Fukuzaki, H., Koyama, Y., Takakuda, K., Monma, J.Tanaka, H., "Preparation and microstructure analysis of chitosan/HA nanocomposites", pp.20-27, Vol.55, *Journal of Biomedical Material Research*, 2001.

[9] Muzzarelli, C., Muzzarelli, R., "Natural and artificial chitosan-inorganic composites", pp.89-94,Vol.92, *Journal of Inorganic Biochemistry*, 2002.

[10] Yamaguchi, I., Iizuka, S., Osaka, A., Monma, H., Tanaka, J., "The effect of citric acid addition on chitosan/hydroxyapatite composites", pp.111-118, Vol.214, *Colloids and Surfaces A: Physicochem. Eng. Aspects*, 2003.

[11] Hu, Q., Li, B., Wang, M., Shen, J., "Preparation and characterization of biodegradable chitosan/hydroxyapatite nanocomposite rods via in situ hybridization: a potential material as internal fixation of bone fracture", in press *Biomaterials*, 2003.

[12] Takagi, S., Chow, L.C., Hirayama, S., Eichmiller, F.C., "properties of elastomeric calcium phosphate cement-chitosan composites", pp.797-804, Vol.19, *Dental Materials*, 2003.

[13] Xu, H.H.K., Quinn, J.B., Takagi, S., Chow, L.C., " Synergistic reinforcement in situ hardening calium phosphate composite scaffold for bone tissue engineering", in press *Biomaterials*, 2003.

[14] Park, J., and. Lakes, R.S, "Biomaterials: An introduction" Plenum Press, 1992.

[15] Hench, LL., "Bioceramics", pp.1705-1728, Vol.81, *J. Am. Ceram. Soc.*, 1998.

[16] Bonfield, W.,"Composites for bone replacement", pp. 522-526, Vol. 10, *J.Biomed. Eng.*,1988.

[17] Shikinami, Y., Okuno, M., "Bioresorbable devices made of forged composites of hydroxyapatite (HA) particles and poly-L-Lactide (PLLA):Part I. Basic characteristics"pp.859-877, Vol.20, *Biomaterials*,1999.

[18] Zhang, R., Ma, P.X., "Porous poly(L-lactic acid)/apatite composites created by biomimetic process", pp.285-293, Vol.45, *J. Biomed. Mater. Res.*,1999.

[19] Suchanek, W., Yoshimura, M., "Processing and properties of hydroxyapatite-based biomaterials for use as hard tissue replacement implants", pp.94-117, Vol.13, *Journal of Materials Research*, 1998.

[20] Wang, X., Ma, J., Wang, Y., He, B., "Structural characterization of phosphorylated chitosan and their applications as effective additives of calcium phosphate cements", pp.2247-2255. Vol22, *Biomaterials,* 2001.

[21] Hench, L.L., and Wilson, J., (eds.), *An Introduction to Bioceramic*s, World Scientific, 1993.

[22] Saraswathy, G., Pal, S.C., Rose, T.P., "A novel bio-inorganic bone implant containing deglued bone, chitosan and gelatin", pp.415-420, Vol.24, *Bulletin of Material Science*, 2000.

[23] Zhang, Y., Zhang, M., "Microstructural and mechanical characterization of chitosan scaffolds reinforced by calcium phosphates", pp.159-164, Vol.282, *Journal of Non-Crystalline Solids*, 2001.

[24] Engin, N.O., Tas, A.C., “Manufacture of macroporous calcium hydroxyapatite bioceramics”, pp.2569-2572, Vol.19, *Journal of European Ceramic Society*, 1999.

[25] Montanaro, L., Jorand, Y., Fantozzi, G., Negro, A., “Ceramic foams by powder processing”, pp.1339-1350, Vol.18, *Journal of European Ceramic Society*, 1998.

[26] Callcut, S., Knowles, J.C., “Correlation between structure and compressive strength in a reticulated glass-reinforced hydroxyapatite foam”, pp.485-489, Vol.13, *Journal of Materials Science:Materials in Medicine*, 2002.

[27] Tampieri, A., Celotti, G., Sprio, S., Delcogliano, A., Franzese, S., “Porosity graded hydroxyapatite ceramics to replace natural bone”, pp.1365-1370, Vol.22, *Biomaterials*, 2001.

[28] Liu, D.M., “Fabrication of hydroxyapatite ceramic with controlled porosity”, pp.227-232, Vol.8, *Journal of Materials Science:Materials in Medicine*, 1997.

[29] Liu, D.M., “Influence of porosity and pore size on the compressive strength of porous hydroxyapatite ceramic”, pp.135-139, Vol.23, *Ceramics International*, 1997.

[30] Majeti, N.V., Kumar, R., “A review of chitin and chitosan applications” pp.1-27,Vol.46, *Reactive & Functional Polymers*, 2000.

[31] Zhang, Y., Zhang, M., “Calcium phosphate/chitosan composite scaffolds for controlled *in vitro* antibiotic drug release”, pp.378-386, Vol.62, *Journal of Biomedical Materials Research*, 2002.

[32] Yokoyama, A., Yamamoto, S., Kawasaki, T., Kohgo, T., Nakasu, M., “Development of calcium phosphate cement using chitosan and citric acid for bone substitute materials”, pp.1091-1101. Vol.23, *Biomaterials*, 2002.

[33] Xu, H.H.K., Quinn, J.B., Takagi, S., Chow, L.C., "Processing and Properties of Strong and No-rigid Calcium Phosphate Cement ", pp. 219-224, Vol. 81(3), *J Dent Res* , 2002.

[34] Varma, H.K., Yokogawa, Y., Espinosa F.F., Kawamoto, Y., Nishizawa, K., Nagata, F., Kameyama, T., “Porous calcium phosphate coating over phosphorylated chitosan film by a biomimetic method”, pp.879-884,Vol.20, *Biomaterials*,1999.

[35] Şimşek, D., “The Preparation and Characterization of HA Powders, Dense and Porous HA Based Ceramic Composites”, MS Thesis, İzmir Institute of Technology, 2002.

[36] Sivakumar, M., Panduranga, R.K., "Preparation, characterization and in vitro release of gentamicin from coralline hydroxyapatite-gelatin composite microspheres" *Biomaterials* ,in press

[37] Paul, W., Sharma, C.P., " Development of porous spherical hydroxyapatite granules: application towards protein delivery", pp.383-388, Vol.10, *Journal of Materials Science*, Materials in Medicine, 1999.

[38] Chen, F., Wang, Z.C., Lin, C.J, "Preparation and characterization of nano-sized hydroxyapatite particles and hydroxyapatite/chitosan nano-composite for use in biomedical materials", pp.858-861, Vol.57, *Materials Letters*, 2002.

[39] Gedde, Ulf. W., *Polymer Physics*, Chapman & Hall,1995.

[40] Pen, J., Regy, M.V., "hydroxyapatite, tricalcium phosphate and biphasic materials prepared by a liquid mix technique", pp.1687-1696, Vol.23, *Journal of the European Ceramic Society*,2003.

[41] Varma, H.K., Yokogawa, Y., Espinosa, F.F., Kawamoto, Y., Nishizawa, K., Nagata, F., Kameyama, T., "Porous calcium phosphate coating over phosphorylated chitosan film by a biomimetic method", pp.879-884,Vol.20, *Biomaterials*,1999.

[42] Lin, F.H., Liao, C.J., Chen, K.S., Sun, J.S., "Preparation of high-temperature stabilized ß-tricalcium phosphate by heating deficient hydroxyapatite with $Na_4P_2O_7.10H_2O$", pp.1101-1107, Vol.19, *Biomaterials*,1998.